BCG vaccination induces TCR-dependent effector functions among Vδ1/3 T cells that are associated with protection against tuberculosis

Megan D. Maerz

A dissertation

submitted in partial fulfillment of the

requirements for the degree of

Doctor of Philosophy

University of Washington

2025

Reading Committee:

Chetan Seshadri, Chair

Jane H. Buckner

Evan W. Newell

Program Authorized to Offer Degree:

Laboratory Medicine and Pathology

© Copyright 2025

Megan D. Maerz

University of Washington

ABSTRACT

BCG vaccination induces TCR-dependent effector functions among Vδ1/3 T cells that are associated with protection against tuberculosis

Megan D. Maerz

Chair of the Supervisory Committee:

Chetan Seshadri, MD. Professor.

Department of Medicine, Division of Allergy and Infectious Diseases

Intravenous vaccination with *Mycobacterium bovis* strain bacillus Calmette-Guérin (IV-BCG) protects macaques against *Mycobacterium tuberculosis* (Mtb) challenge and intradermal BCG protects human infants from disseminated tuberculosis. γδ T cells expressing a Vδ1+ or Vδ3+ T cell receptor (TCR) are enriched at mucosal surfaces and recognize mycobacterial antigens, but their role in protection against Mtb is largely unknown. We used multimodal single-cell RNA sequencing, mass cytometry, and flow cytometry to profile γδ T cells from human infants and macaques after protective BCG vaccination. A subset of Vδ1/3 T cells in BCG-vaccinated human infants shows evidence of clonal expansion and differentiation into pro-inflammatory and cytotoxic effector cells that respond to Mtb. In macaques, IV-BCG induced pro-inflammatory and

cytotoxic responses to Mtb among Vδ1/3 T cells that were enriched in the airway compared to the blood. Notably, these responses were dependent on signaling through the TCR, and clonal expansion was most prominent among cytotoxic Vδ1/3 T cells. Finally, the total frequency of Vδ1/3 T cells in the lung and frequency of cytokine-expressing Vδ1/3 T cells in the airway were associated with protection against Mtb challenge. Thus, Vδ1/3 T cells are activated by BCG in a TCR-dependent manner and accumulate in the lung, where they upregulate cytotoxic and pro-inflammatory functions that may contribute to protective immunity against Mtb.

TABLE OF CONTENTS

LIST OF ABBREVIATIONS

5-OP-RU:	5-(2-oxopropylideneamino)-6-D-ribitylaminouracil
BAL:	Bronchoalveolar lavage
BCG:	Bacillus Calmette-Guérin vaccine
BTN:	Butyrophilin
BTNL:	Butyrophilin-like
CD1:	Cluster of differentiation 1
CDR:	Complementarity-determining region
CFU:	Colony-forming units
CMV:	Cytomegalovirus
DURT:	Donor-unrestricted T cell
HLA:	Human leukocyte antigen
IFN-γ:	Interferon gamma
iNKT:	Invariant natural killer T
IV-BCG:	Intravenous BCG
MAIT:	Mucosal-associated invariant T
MHC:	Major histocompatibility complex
MR1:	MHC-related protein 1
MR1T:	MR1-restricted T
Mtb:	Mycobacterium tuberculosis
NHP:	Non-human primate
NK:	Natural killer
PBMC:	Peripheral blood mononuclear cells
PHA:	Phytohemagglutinin
TB:	Tuberculosis
TCR:	T cell receptor
TNF:	Tumor necrosis factor
α-GalCer:	α-Galactosylceramide
γδ:	Gamma delta

ACKNOWLEDGEMENTS

This work would not have been possible without the hard work and generosity of our collaborators across the USA and Cape Town, South Africa.

I would first like to thank the past and present members of the Seshadri Lab, all of whom provided insightful feedback, technical help, and expertise that contributed to this work, with special thanks to Emma Bishop, Erik Layton, and Steven Makatsa. Emma Bishop established our customized computational pipelines that annotate γδ T cell receptors from humans and rhesus macaques, facilitated my use of the CoNGA tool, and provided coding support on countless occasions. Our flow cytometry wizard Erik Layton provided ongoing assistance in developing and troubleshooting flow cytometry panels. Early in my training, Steven agreed to share a pilot cohort of precious non-human primate samples so we could analyze them jointly. The results of this analysis spurred an ongoing collaboration between Steven, me, and the IMPAc-TB consortium which resulted in most of the work shown here.

I would also like to thank our collaborators outside of Seattle who made vital contributions to this work. Thank you to Thomas J. Scriba, who supervised the clinical studies that generated the human infant and cord blood samples, and to Allison Bucsan, Matthew S. Sutton, and Patricia A. Darrah for their work generating our non-human primate samples. Thank you to Mike Vilme for performing the next-generation sequencing on our single-cell libraries. I would also like to thank Mario Roederer, Alex K. Shalek, and Robert A. Seder for providing funding and oversight. I would also like to acknowledge Benjamin Bimber for providing us with the custom primer sequences we used to generate our non-human primate γδ TCR libraries.

I would also like to thank the wonderful people at the UW core facilities that provided the instruments, technical support, and training that made this work possible: Delphina Walker-Phelan and Thane Mittelstaedt at the UW Cell Analysis facility and Inah Golez and Michael Gale at Seattle Genomics.

Thank you to my committee members, Philip H. Bradley, Jane H. Buckner, Aude G. Chapuis, Jennifer M. Lund, and Evan W. Newell for their incisive feedback and guidance throughout my doctoral training which improved the quality and scope of this work.

Finally, I would like to thank my advisor, Chetan Seshadri, for welcoming me into his lab and allowing me the privilege of learning from him and his team of brilliant and talented scientists. For all his trainees, Chetan places a distinct emphasis on rigorous scientific methods, meticulous data analysis and interpretation, and precise scientific communication, all of which I am grateful to carry with me through my career. Chetan is not only a model of an exceptional scientist, but also a truly thoughtful mentor. He has set the standard for mentorship that I hope to achieve.

CHAPTER 1: INTRODUCTION

***Note**: This chapter has been adapted from the review article published in Immunology & Cell Biology* (PMID: 38659280).

Functional and biological implications of clonotypic diversity among human donor-unrestricted T cells

Megan D Maerz [1 2], Deborah L Cross [1], Chetan Seshadri [1]

[1] Department of Medicine, University of Washington School of Medicine, Seattle, WA, USA.
[2] Molecular Medicine and Mechanisms of Disease Program, Department of Laboratory Medicine and Pathology, University of Washington, Seattle, WA, USA.

1.1 Global impact of tuberculosis and the BCG vaccine

Tuberculosis (TB) has been a leading infectious cause of death worldwide for thousands of years (Kim & Swaminathan, 2021). In 2023, an estimated 8.2 million people were newly diagnosed with TB, the highest number since 1995 (Geneva: World Health Organization, 2023, 2024). TB is an infection caused by *Mycobacterium tuberculosis* (Mtb) bacilli, which is typically established through inhalation of airborne droplets containing as few as three bacilli (Donald et al., 2018). Once Mtb bacteria reach the lower respiratory tract, a spectrum of outcomes is possible. The majority of exposures do not produce symptoms, with Mtb bacilli either remaining dormant or establishing varying degrees of subclinical active infection (Pai et al., 2016). In approximately 10% of cases, Mtb bacteria are thought to be completely cleared by the immune system (Seshadri et al., 2017; Stein et al., 2008; Sun et al., 2024). In an estimated 5% of cases, Mtb bacteria rapidly establish disease that can disseminate to extrapulmonary tissues and cause a range of symptoms, including coughing, fever, fatigue, and weight loss (Miller et al., 2000; Young et al., 2009). Without

treatment, the mortality rate of active tuberculosis is approximately 50% (Geneva: World Health Organization, 2023). One quarter of the global population is estimated to have been infected with TB, with the highest number of new cases occurring across Asia (India, Indonesia, Pakistan, Philippines, China, and Bangladesh) and in some parts of Africa (Nigeria and Democratic Republic of the Congo) (Geneva: World Health Organization, 2024).

The only licensed TB vaccine, the live-attenuated bacillus Calmette-Guérin (BCG), was developed over a century ago ("BCG Vaccines," 2018). BCG shows only partial efficacy against pulmonary disease in adults, which is responsible for most transmission (Fine, 1995). However, BCG is approximately 80% effective in preventing severe TB in children and is therefore widely used in TB endemic countries (A. Roy et al., 2014). Despite its widespread use, the mechanisms of immune protection offered by the BCG vaccine are incompletely understood (Bhatt et al., 2015). Understanding the protective immune response induced by BCG vaccination will be critical in developing more effective vaccines.

1.2 CD4 and CD8 T cell responses to tuberculosis

The adaptive immune system evolved to respond to pathogens, in part, through the recognition of non–self-proteins by T cells. These proteins are processed into linear peptide antigens that are loaded onto polymorphic major histocompatibility complex (MHC) molecules expressed on the surface of professional antigen-presenting cells. T cells specific for the foreign peptide antigen are selectively activated through their T-cell receptor (TCR), which directly binds to the peptide–MHC

complex. Conventionally, T cells express a TCR heterodimer comprising an α-chain and a β-chain and are further characterized through their expression of either a CD4 or CD8 coreceptor.

Approximately 7-11 days after Mtb exposure in the lungs, antigen-specific CD4 T cells are activated in the draining lymph nodes, where they rapidly expand before trafficking to the site of infection (Gallegos et al., 2008; Reiley et al., 2008; Wolf et al., 2008). A requirement for CD4 T cells in Mtb control has been demonstrated in both humans and in mouse models. In mice, depletion of CD4 T cells using antibodies leads to increased bacterial burden after Mtb infection, while adoptive transfer of CD4 T cells is protective (Müller et al., 1987; Orme & Collins, 1983, 1984). HIV-infected humans with depleted CD4 T cell counts show increased susceptibility to TB (Selwyn et al., 1989). Once localized to the lungs, the critical CD4 T cell functions are the production of pro-inflammatory cytokines such as interferon gamma (IFN-γ) and tumor necrosis factor (TNF) (Alcaïs et al., 2005; Flynn et al., 1995; Keane et al., 2001). IFN-γ knockout mice and humans with genetic deficiencies in IFN-γ show increased susceptibility to TB (Cooper et al., 1993; Flynn et al., 1993; Ottenhoff et al., 2000). In mice, the absence of TNF signaling results in more severe TB disease, and humans receiving TNF-neutralizing drugs are at greater risk of developing TB (Flynn et al., 1995; Keane et al., 2001). However, in human infants who received BCG at birth, antigen-specific CD4 T cells expressing IFN-γ or TNF did not correlate with protection against childhood TB (Kagina et al., 2010). Additionally, the TB vaccine candidate MVA85A successfully promoted pro-inflammatory CD4 T cell responses in human infants but failed to provide protection against Mtb infection (Tameris et al., 2013). These results suggest that pro-

inflammatory CD4 T cells are necessary, but not sufficient for immune protection against TB in humans.

While CD8 T cells produce pro-inflammatory cytokines such as IFN-γ and TNF, they also express cytolytic molecules including granzymes, granulysin, and perforin that are capable of killing Mtb-infected cells or directly targeting Mtb bacilli (Stenger et al., 1998). Analysis in mouse models suggests that CD8 T cells respond to Mtb infection and traffic to the lungs at approximately the same time as CD4 T cells (Serbina & Flynn, 1999). In mice, CD8 T cell depletion did not increase bacterial burden during acute Mtb infection, but led to a 10-fold increase in bacterial burden during late, chronic infection (van Pinxteren et al., 2000). Additionally, CD8 T cells are present in TB granulomas in non-human primates (NHPs) and humans, and depletion of CD8 T cells diminishes the protection conferred by the BCG vaccine in NHP models (Chen et al., 2009; Lin et al., 2006; McCaffrey et al., 2022). The cytolytic activity of CD8 T cells has been shown to reduce Mtb colony-forming units (CFU) in *in-vitro* systems (Cho et al., 2000; Stenger et al., 1997). In sum, these observations suggest that cytotoxic T cells, including CD8 T cells, are a critical element of the protective immune response against TB.

1.3 Donor-unrestricted T cells

In addition to recognizing MHC-presented peptides, T cells have evolved to recognize non-peptide antigens through MHC-independent systems. The cluster of differentiation 1 (CD1) family of antigen-presenting molecules mediate presentation of lipids, MHC-like related protein 1 (MR1) mediates presentation of riboflavin or folate derivatives, and butyrophilins (BTNs) mediate

activation of γδ T cells by phosphoantigens (Godfrey et al., 2015). Unlike MHC molecules which are highly polymorphic, these alternative antigen-presenting and antigen-sensing systems are virtually non-polymorphic, allowing for shared T cell responses across unrelated individuals (Van Rhijn & Moody, 2015). Accordingly, T cells expressing TCRs that recognize conserved ligands such as CD1, MR1, or BTNs have been termed 'donor-unrestricted T cells' (DURTs) (Van Rhijn & Moody, 2015).

DURTs share many characteristics with MHC-restricted T cells, such as expression of a clonotypic TCR at the cell surface, antigen specificity, and ability to perform helper or cytotoxic immune functions (Godfrey et al., 2015). In addition, DURTs also display many innate-like features including enrichment in the skin and mucosa, the ability to respond to cytokines in the absence of TCR signaling, and the capacity to respond to pathogens without prior antigen priming (Ismail et al., 2011; Nel et al., 2021; Wencker et al., 2014). Consequently, DURT TCRs have been described as unspecialized receptors responding *en masse* to microbial antigens (Kulicke et al., 2020; C. T. Morita et al., 2000). Human DURTs may be categorized into several groups that are defined according to their TCR gene usage and TCR restriction (**Table 1**). These subsets exhibit distinct tissue homing patterns, transcriptional profiles, and effector functions (Godfrey et al., 2015; Gutierrez-Arcelus et al., 2019). All DURT subsets are thought to mediate rapid immune responses to infectious microorganisms, but they may also play a role in tumor recognition and the maintenance of tissue homeostasis (de Jong & Ogg, 2021; Godfrey et al., 2015; Nielsen et al., 2017).

MR1-restricted T cells (MR1T cells) comprise roughly 3% of circulating T cells and are defined by their recognition of MR1, an MHC-like molecule capable of presenting riboflavin derivatives, folate derivatives, and potentially other ligands (Gherardin et al., 2018; Kjer-Nielsen et al., 2012; Kulicke et al., 2020; Lepore et al., 2017; Meermeier et al., 2016). MR1T cells are found in circulation and are enriched in tissues including the liver, intestinal mucosa and lungs, where they are believed to play a critical role in the early immune response to microbial pathogens (Hinks & Zhang, 2020; López-Sagaseta et al., 2013; Magalhaes et al., 2020; Salou et al., 2019). Most MR1T cells are mucosal-associated invariant T (MAIT) cells recognizing intermediates of the bacterial riboflavin biosynthesis pathways in a TCR-dependent manner (Reantragoon et al., 2013). Since mammals lack the capacity to synthesize B vitamins, these small molecules act as an indicator of microbial infection (Kulicke et al., 2020). In addition to their role in recognizing bacterial metabolites, MR1T cells have been implicated in several other settings including inflammatory bowel disease, psoriasis, rheumatoid arthritis, multiple sclerosis and cancer (Ussher et al., 2014).

T cells are also capable of recognizing the CD1 family of proteins, which evolved to present microbial- and self-derived lipids to T cells (Beckman et al., 1994; Eckhardt & Bastian, 2021; Porcelli et al., 1992). Humans express four CD1 isoforms (CD1a, CD1b, CD1c, and CD1d) which vary in the configuration of their lipid-binding grooves, patterns of cellular expression, and subcellular trafficking (Van Rhijn et al., 2013). CD1-restricted T cells are present in the healthy immune system and can be detected at low frequencies in the peripheral blood, lungs, gut, and skin, where they exert diverse immune functions including cytotoxic activity and the production of type 1, type 2, and type 3 cytokines (Bagchi et al., 2018; Cotton et al., 2021; de Jong et al., 2010; Layton et al., 2021; Lopez et al., 2020; Sáez de Guinoa et al., 2018; Siddiqui et al., 2015). A

polymorphism in CD1a leading to low surface expression and diminished activation of CD1a-restricted T cells was associated with tuberculosis risk, supporting an important role for CD1 and CD1-restricted T cells in protection against bacterial infections (Seshadri et al., 2013, 2014). Other studies have begun to elucidate a role for CD1-restricted T cells in the anti-tumor response, allergic skin mediated diseases, and autoimmunity (Cheung et al., 2016; Fu et al., 2020; Nicolai et al., 2020).

Gamma delta (γδ) T cells are characterized by their expression of a TCR-γ chain and TCR-δ chain instead of the TCR-α and TCR-β chains expressed by most T cells. γδ T cells arose over 400 million years ago and are conserved in most vertebrates, supporting a key role for γδ T cells in the healthy immune system (Hayday, 2000). γδ T cells compose approximately 3-9% of T cells in the circulating blood, but their frequency can be highly variable across individuals and may be affected by environmental factors such as exposure to *Plasmodium falciparum* or cytomegalovirus (CMV) (Hviid et al., 2000; Sanz et al., 2023; von Borstel et al., 2021). Additionally, γδ T cells are enriched in barrier tissues such as the skin, gut epithelium, and lungs, where they may represent more than 30% of T cells and are hypothesized to perform immune surveillance to detect early signs of infection or tumorigenesis (Chien et al., 2014; Deusch et al., 1991).

1.4 TCR diversity in γδ T cells

Although they are frequently considered as a single immune compartment, γδ T cells are composed of two major subsets that are defined by the gene usage of their TCR. In human adults, most circulating γδ T cells express a γ-chain using a Variable-9 gene and a δ-chain using a Variable-

2 gene and are thus termed Vγ9Vδ2 T cells (Parker et al., 1990). T cells expressing a Vδ2 chain are overwhelmingly likely to also express a Vγ9 chain (Davey et al., 2018). The other subset expresses a TCR that does not pair a Vγ9 chain with a Vδ2 chain and primarily express either a Vδ1 or Vδ3 chain. As a result of their distinct TCR structures, Vγ9Vδ2 T cells and Vδ1/3 T cells display fundamental differences in their immunobiology, including their tissue homing profiles, modes of antigen recognition and activation, and hypothesized immune roles (Maerz et al., 2024). Further, single-cell RNA sequencing experiments have failed to reveal non-TCR-encoding genes capable of differentiating γδ T cells from cytotoxic αβ T cells or NK cells (Gideon et al., 2020; Pizzolato et al., 2019; Song et al., 2023). However, the conservation of γδ T cells in nearly all vertebrates is consistent with a distinct and critical immune role (Rast et al., 1997). This suggests that the γδ TCR is uniquely responsible for the distinct immune functions exerted by γδ T cells, warranting a thorough understanding of γδ TCR diversity and ligands.

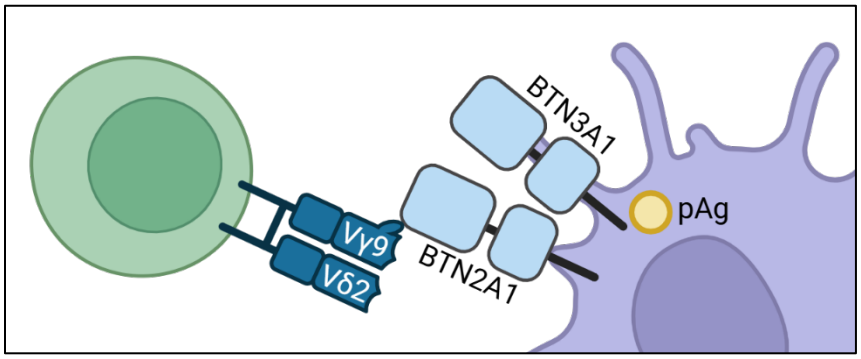

Figure 1.1. Antigen recognition by Vγ9Vδ2 T cells. Vγ9Vδ2 T cells sense the presence of phosphoantigens (pAgs) through a unique, 'inside-out' mechanism wherein pAgs bind to an intracellular domain of butyrophilin 3A1 (BTN3A1). This triggers an association with BTN2A1 which binds directly to a framework region of the Vγ9 chain.

The Vγ9Vδ2 TCR is responsive to small phosphorylated molecules called phosphoantigens (Sandstrom et al., 2014). Notably, how Vγ9Vδ2 TCRs sense these antigens is not though direct presentation, but rather through a unique 'inside-out' mechanism (**Figure 1.1**). Intracellular phosphoantigens bind to the cytosolic B30.2 domain of BTN3A1, triggering an association with BTN2A1 which engages extracellularly with a germline-encoded region of the Vγ9 chain (Karunakaran et al., 2020; Rigau et al., 2020; Sandstrom et al., 2014). Mutational analyses and the limited clonal diversity of Vγ9Vδ2 T cells support requirements for the γ-chain complementarity-determining region 3 (CDR3γ) and CDR3δ in the response to phosphoantigens, but the molecular consequences of Vγ9Vδ2 clonotypic variation remain poorly understood (Karunakaran et al., 2020; Rigau et al., 2020). Throughout the human lifespan, the invariant Vγ9 clonotype CALWEVQELGKKIKVF, which is generated through simple recombination of the germline-encoded Vγ9 and JγP genes, is observed at a high frequency (Davey et al., 2018). Between 4-45% of adult Vγ9Vδ2 T cells use the CALWEVQELGKKIKVF clonotype and frequencies are even higher in cord blood (Willcox et al., 2018). In both cord blood and adult peripheral blood, several other shared Vγ9 clonotypes were found that are conserved across populations (Willcox et al., 2018). Overall, roughly 80% of adult Vγ9 clonotypes are shared (Willcox et al., 2018).

By contrast, the TCR repertoire of non-Vγ9Vδ2 γδ T cells, which mostly use Vδ1 or Vδ3 segments, is highly diverse, with few clonotypes shared between individuals (Davey et al., 2017). In human cord blood, the Vδ1 and Vδ3 TCR repertoire uses a wide range of CDR3s each constituting less than 1-2% of the total repertoire (Davey et al., 2017). Accordingly, Vδ1/3 T cells have a wide range of antigen specificities and mixed modes of antigen recognition (**Figure 1.2**). TCR sequencing and

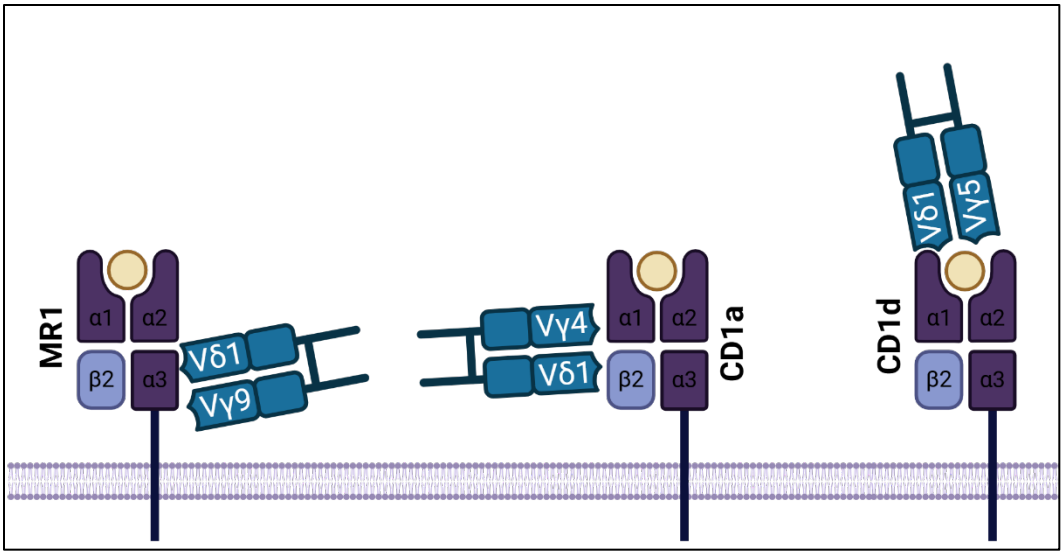

Figure 1.2. Diverse TCRs and binding modes by Vδ1 T cells. Simplified schematics illustrating the variable docking modes and gamma chain genes used by Vδ1 TCRs to bind MHC-like molecules. From left to right: The G7 TCR in complex with MR1-5-OP-RU (Le Nours et al., 2019); The CO3 TCR in complex with CD1a-sulfatide (Uldrich et al., 2013); The 9C2 TCR in complex with CD1d-αGalCer (Wegrecki et al., 2022).

crystal structures were used to describe γδ T cells recognizing MR1-5-(2-oxopropylideneamino)-6-D-ribitylaminouracil (5-OP-RU) (Le Nours et al., 2019). Most clonotypes used a Vδ1 or Vδ3 segment in combination with a Vγ8 segment, but use of all six functional Vγ genes were observed. In total, 75 unique MR1-restricted clonotypes were identified (Le Nours et al., 2019). Although fewer CD1-restricted γδ TCRs have been sequenced, the existing data suggest that they may be equally varied. Two γδ T cell clonotypes with distinct CDR3 sequences were shown to recognize CD1a, one using a Vγ4Vδ1 TCR and the other using a Vγ2Vδ1 TCR (Wegrecki et al., 2022). Additionally, the TCRs of γδ T cells recognizing CD1d-α-galactosylceramide (α-GalCer) were characterized, revealing eight unique clonotypes with diverse Vγ segments (Uldrich et al., 2013). Mutational analysis of the CD1b antigen-presentation platform demonstrated dramatically different molecular footprints among three unique, CD1b-restricted Vδ1 TCRs (Reijneveld et al.,

2020). These studies uncover a high level of Vδ1/3 TCR diversity which influences antigen and ligand reactivity. γδ TCRs also appear variable in their degree of antigen selectivity or promiscuity, with some clonotypes showing entirely antigen-independent recognition and others showing more restricted specificity and direct antigen contact (Le Nours et al., 2019; Reijneveld et al., 2020; Uldrich et al., 2013). Although few crystal structures have been solved, the existing evidence suggests that Vδ1/3 TCRs use diverse rather than conserved docking modes to bind CD1 and MR1 (Le Nours et al., 2019; Luoma et al., 2013; Rice et al., 2021; Uldrich et al., 2013; Wegrecki et al., 2022).

Though Vδ1/3 TCRs appear to display a greater degree of TCR and ligand diversity compared to Vγ9Vδ2 T cells, shared Vδ1 clonotypes have also been described. Semi-invariant clonotypes among human Vδ1 T cells include Vγ4Vδ1 T cells, which dominate the γδ T cells in the gut, and Vγ8 T cells, which arise in response to in-utero CMV infection (Eggesbø et al., 2020; Fichtner et al., 2020; Vermijlen et al., 2010). The enrichment of semi-invariant Vγ4+ TCRs in the human gut epithelium is thought to be driven by the expression of butyrophilin-like (BTNL) molecules on enterocytes, which bind to a germline-encoded region of the Vγ4 chain (Di Marco Barros et al., 2016; Willcox et al., 2019). TCR sequencing of clonotypes expanded during fetal CMV infection revealed a shared Vγ8Vδ1 TCR using germline-encoded CDR3γ and CDR3δ sequences (Vermijlen et al., 2010). The expanded Vγ8Vδ1 cells showed antiviral activity mediated by IFN-γ and direct lysis of infected cells, consistent with a role in protection against viral infections occurring during gestation (Vermijlen et al., 2010).

1.5 The immune role of γδ T cells

γδ T cells express a T cell receptor with variable degrees of diversity and antigen specificity, and thus have been described as lying at the intersection of innate and adaptive immunity. The 'lymphoid stress surveillance' hypothesis proposed a molecular mechanism for this blurring between innate and adaptive immune roles (Hayday, 2009). Conventionally, myelocytes mount rapid, generalized immune responses to pathogens, while lymphocytes respond to highly specific antigens in a slower process requiring the priming and expansion of rare clonotypes (Iwasaki & Medzhitov, 2015). However, some lymphocytes, including γδ T cells, are also capable of responding rapidly to general signals of cellular stress, an immune function termed lymphoid stress surveillance (Hayday, 2009). In part, lymphoid stress surveillance is thought to be mediated by TCR recognition of endogenous proteins expressed on the surface of unhealthy cells (Adams et al., 2005, 2008; Groh et al., 1998). In contrast to MHC-I molecules, which are constitutively expressed, the expression of these proteins is tightly regulated and increased in settings of cellular stress, tissue damage, or inflammation (Groh et al., 1996, 1998). Thus, γδ TCRs may act as "stress sensors" in addition to their role as "antigen sensors".

Lymphoid stress surveillance can be exemplified by Vγ9Vδ2 T cells, which recognize endogenous BTN complexes that assemble in the presence of microbially derived phosphoantigens, such as (E)-4-hydroxy-3-methyl-but-2-enyl pyrophosphate, or phosphoantigens accumulating in tumors, such as isopentenyl pyrophosphate (Karunakaran et al., 2020). Vγ9Vδ2 T cells are present at high frequencies in circulating blood and respond polyclonally to BTN–phosphoantigen complexes, allowing rapid, innate-like deployment of antimicrobial or antitumor effector programs without

clonal expansion (Hayday, 2009). More recently, the concept of lymphoid stress surveillance has expanded to include immune responses requiring the expansion of rare clonotypes, yet still directed against stress-induced endogenous proteins (Davey et al., 2017). This adaptive form of surveillance may be a central function of Vδ1/3 T cells, which are activated through their TCR by stress-regulated proteins such as CD1, MR1, MHC class I chain–related proteins A and B, endothelial cell protein C receptor, and annexin A2 (Chancellor et al., 2022; Groh et al., 1999; Le Nours et al., 2019; Marlin et al., 2017; D. Morita et al., 2013; Rice et al., 2021; Willcox et al., 2012). Unlike Vγ9Vδ2 T cells, which have a highly restricted TCR repertoire at birth, the Vδ1 TCR repertoire is clonally diverse in infancy but becomes more focused by adulthood, perhaps as a result of clonal expansion in response to stress signals (Davey et al., 2017). Indeed, Vδ1/3 T cell clonotypes that were highly expanded during CMV infection were found to recognize endothelial cell protein C receptor and HLA-DR, which are upregulated in response to inflammatory cues (Deseke et al., 2022; Willcox et al., 2012). In sum, γδ TCRs are well positioned to fulfill both adaptive and innate immune roles during infection. However, the relative contribution of innate- and adaptive-like γδ T cell functions during Mtb infection and their respective roles in mediating protection remain poorly understood.

1.6 Central question

Increasing evidence suggests that γδ T cells are important for TB immunity. To date, most research has focused on the Vγ9Vδ2 subset. Although this subset is formally defined through its paired expression of Vγ9 and Vδ2 chains, as these chains are overwhelmingly paired together in humans, identification through individual use of Vδ2- or Vγ9-directed antibodies is common (Hu et al.,

2023). Vγ9Vδ2 T cells display primary responses to intradermal BCG vaccination and an amplified response to BCG re-vaccination that persists for up to 7 months, hallmarks of an adaptive immune response (Y. Shen et al., 2002). A vaccine specifically targeting the activation and expansion of Vγ9Vδ2 T cells was sufficient to control pulmonary TB in macaques, and adoptive transfer of phosphoantigen-specific Vγ9Vδ2 T cells was sufficient to attenuate Mtb infection in macaques (Qaqish et al., 2017; L. Shen et al., 2019). In human infants, intradermal BCG vaccination is associated with an expansion of IFN-γ-expressing γδ T cells in the blood (Gela et al., 2022). Further, NK-like CD8+ γδ T cells are expanded in the blood of Mtb-infected South African adolescents who do not progress to active TB (Chowdhury et al., 2023). Finally, deep-sequencing revealed clonal expansions of γδ TCRs in lung explants from TB patients (Ogongo et al., 2020). However, very little is known about the role of Vδ1/3 T cells in Mtb control, including how their transcriptomes, immune functions, and TCR repertoires are modulated by protective BCG vaccination.

Here, we sought to understand how Vδ1/3+ T cells respond to BCG vaccination in two contexts where BCG confers protective immunity against Mtb. The first aim of this work is to define the effect of protective BCG vaccination on the transcriptomes and functional profiles of Vδ1/3 T cells. We first used single-cell RNA sequencing, single-cell TCR sequencing, and cell-based functional assays to analyze γδ T cells from BCG-vaccinated human infants as well as a cohort of cord blood controls. This work revealed a subset of Vδ1/3 T cells enriched in BCG-vaccinated infants that displayed an activated cytotoxic effector phenotype and exerted cytotoxic and pro-inflammatory activity in response to stimulation with Mtb antigens. Next, we applied the same multimodal

analysis method to γδ T cells from rhesus macaques who received an intravenous BCG (IV-BCG) vaccine. Concordantly, we found that Vδ1/3 T cells upregulate cytotoxic and pro-inflammatory effector functions following vaccination that are enriched in the lung compared to the blood. Further, the frequency of Vδ1/3 T cells producing pro-inflammatory cytokines in the lung correlated with protection against Mtb challenge. The second aim of this work is to determine to what extent the Vδ1/3 T cell response to BCG is mediated through the TCR. In BCG-vaccinated human infants, we observed that the same population of Vδ1/3 T cells that appeared activated and cytotoxic also expressed clonally expanded TCRs, consistent with a TCR-dependent response to the BCG vaccine. In IV-BCG-vaccinated rhesus macaques, Vδ1/3 T cells underwent clonal expansion in response to vaccination. We also showed that the antimicrobial effector functions exerted by Vδ1/3 T cells following IV-BCG are mediated through the TCR. Taken together, these results highlight a potentially important role for Vδ1/3 T cells in BCG-mediated protective immunity to Mtb.

CHAPTER 2: THE γδ T CELL FUNCTIONAL RESPONSE TO BCG VACCINATION

2.1 Introduction

Studies in BCG-vaccinated human infants have begun to elucidate the role of specific T cell subsets and functions in immune protection against Mtb. Although pro-inflammatory CD4 T cells are required for Mtb control in adults, they did not correlate with protection against TB disease in infants who received the BCG vaccine or infants who received the TB vaccine candidate MVA85A (Kagina et al., 2010; Tameris et al., 2013). Additionally, CD4 T cells expressing the activation marker HLA-DR were associated with increased TB risk in BCG-vaccinated South African infants, but it is unclear whether HLA-DR+ CD4 T cells indicate impaired immunity against mycobacteria or are a marker of subclinical TB (Fletcher et al., 2016). Notably, a study of 10-week-old, BCG-vaccinated Australian infants revealed that γδ T cells and natural killer (NK) cells are the primary producers of IFN-γ after stimulation with BCG *in vitro* (Zufferey et al., 2013). A targeted analysis of DURTs in 10-week-old South African infants found increased frequency of circulating γδ T cells, but not other DURT subsets, in infants who received BCG at birth compared to BCG-unvaccinated infants (Gela et al., 2022). Intriguingly, no difference in γδ T cell frequency was observed after BCG revaccination during adulthood, which does not provide protection against TB (Gela et al., 2022). Considered together, these observations suggest that pro-inflammatory CD4 T cell responses alone may be insufficient for protection against Mtb and that a coordinated immune response between several immune cell subsets is required. Further, the contribution of DURTs, including γδ T cells, may be underappreciated.

The IV-BCG rhesus macaque model was first established over 50 years ago in experiments comparing alternative routes of BCG immunization, which revealed no evidence of gross lung disease after Mtb aerosol challenge in roughly half of the study animals who received IV-BCG (Barclay et al., 1970). These results were recapitulated in 2020 in a similar study comparing BCG doses and routes in rhesus macaques, in which the authors observed complete sterilizing protection against Mtb challenge in six of ten study animals who received IV-BCG (Darrah et al., 2020). The same study revealed dramatic expansion of several T cell populations, including CD4 T cells, CD8 T cells, Vγ9+ T cells, and Vγ9-negative T cells, in the lungs of animals who received IV-BCG but not aerosol or intradermal BCG (Darrah et al., 2020). The authors hypothesized that the high magnitude of mycobacteria-specific T cells in the lungs may have been responsible for the superior protection offered by the IV route, but were unable to determine correlates of protection due to an insufficient range of lung CFU burden after challenge (Darrah et al., 2020).

A follow-up study employed varying doses of IV-BCG and reported several immune correlates of protection in bronchoalveolar lavage (BAL) samples, including pro-inflammatory CD4 T cells, pro-inflammatory CD8 T cells, NK cells, and Vγ9+ T cells (Darrah et al., 2023). Importantly, analysis of peripheral blood mononuclear cells (PBMC) found less extensive correlations compared to analysis of BAL, underlining the importance of analyzing immune responses in the airway (Darrah et al., 2023). However, cytotoxic CD107a+ Vγ9+ T cells in PBMC were correlated with protection against Mtb challenge (Darrah et al., 2023). Another follow-up study depleted specific T cell populations after IV-BCG but before Mtb challenge, and discovered a requirement for CD4 T cells

and CD8α-expressing T cells in protection against TB (Simonson et al., 2024). In sum, these results underline the critical role of pro-inflammatory CD4 T cells in the lungs, but also emphasize the importance of CD8 T cells, NK cells, and Vγ9+ T cells in Mtb control.

Despite these advances, several questions remain unaddressed. First, the role of γδ T cells in BCG-vaccinated human infants remains unclear, including how their transcriptional and functional profiles might be modulated by BCG vaccination. Second, prior studies demonstrated that Vγ9-negative γδ T cells are expanded in the airway after IV-BCG, suggesting that Vδ1/3 T cells may also respond to IV-BCG. However, it remains unknown how IV-BCG modulates the functions of Vδ1/3 T cells or whether Vδ1/3 T cells correlate with protection against Mtb challenge (Darrah et al., 2020). Here, we seek to address these gaps in our knowledge, with the overall goal of understanding the role of Vδ1/3 T cells in BCG-mediated protection against Mtb.

2.2 Analysis of γδ T cells reveals antibacterial transcriptional and functional programs in BCG-vaccinated human infants

We first used single-cell RNA sequencing (scRNA-seq) and TCR sequencing to characterize unstimulated peripheral γδ T cells from ten-week-old South African infants (n=6) who received intradermal BCG at birth (Hawkridge et al., 2008). As the BCG vaccine is routinely administered to all infants born in South Africa, we were unable to obtain age-matched samples from BCG-unvaccinated South African infants for this analysis. However, the peak CD4 T cell response to BCG occurs at ten weeks and γδ T cells are expanded at this time point compared to unvaccinated

infants (Gela et al., 2021; Soares et al., 2013). We hypothesized that Vδ1/3 T cells would display an effector memory phenotype in BCG-vaccinated infants (Chowdhury et al., 2023; Ogongo et al., 2020).

After quality control filtering and data integration, a total of 14,302 unstimulated γδ T cells were analyzed with an average of 2,033 cells per sample (**Appendix A.I**). Nine distinct clusters of γδ T cells were defined based on their gene expression (**Figure 2.1A**). 43% of cells expressed a Vδ1+ TCR, 8% expressed a Vδ3+ TCR, and 43% expressed a Vγ9Vδ2 TCR (**Figure 2.1B and Appendix A.II**). Paired chain TCRs isolated from 2,329 cells bearing a Vγ9-negative γδ TCR revealed that 73% expressed a Vδ1+ TCR, 13% expressed a Vδ3+ TCR, and 14% expressed a Vδ2+ TCR (**Appendix A.II**). As expected, Vδ1+ and Vδ3+ γδ T cells were strongly overlapping and were enriched in clusters 0, 6, 8, and 3, whereas Vγ9Vδ2+ γδ T cells were enriched in clusters 1, 2, and 7 (**Figure 2.1B**).

Cell clusters enriched for Vγ9Vδ2+ cells typically expressed low levels of genes associated with a naïve-like phenotype (*SELL*, *CCR7* and *TCF7*) together with higher levels of cytotoxicity-associated genes (*GZMK*, *GZMA*, *CST7*, *PRF1*, and *GZMM*) (**Figure 2.1B and 2.1C**). In contrast, clusters that were enriched for Vδ1+ and Vδ3+ T cells typically expressed higher levels of naïve-associated genes and lower levels of cytotoxicity-associated genes (**Figure 2.1B and 2.1C**). These results align with previous reports that Vγ9Vδ2+ cells express a pre-programmed cytotoxic effector phenotype, while Vδ1 T cells express a naïve-like phenotype at birth (Davey et al., 2017). Cluster 3 was uniquely enriched in Vδ1/3 expressing low levels of naïve-like genes, high levels of

cytotoxicity genes, high levels of genes associated with T cell activation (*HLA-DPA1*, *HLA-DPB1*, *HLA-DRB1*, and *TIGIT*), and high expression of *TXB21*, which encodes a master regulator of pro-inflammatory function in T cells (**Figure 2.1C**). In sum, these results suggest that Vδ1/3 T cells express an activated cytotoxic effector phenotype in BCG-vaccinated infants.

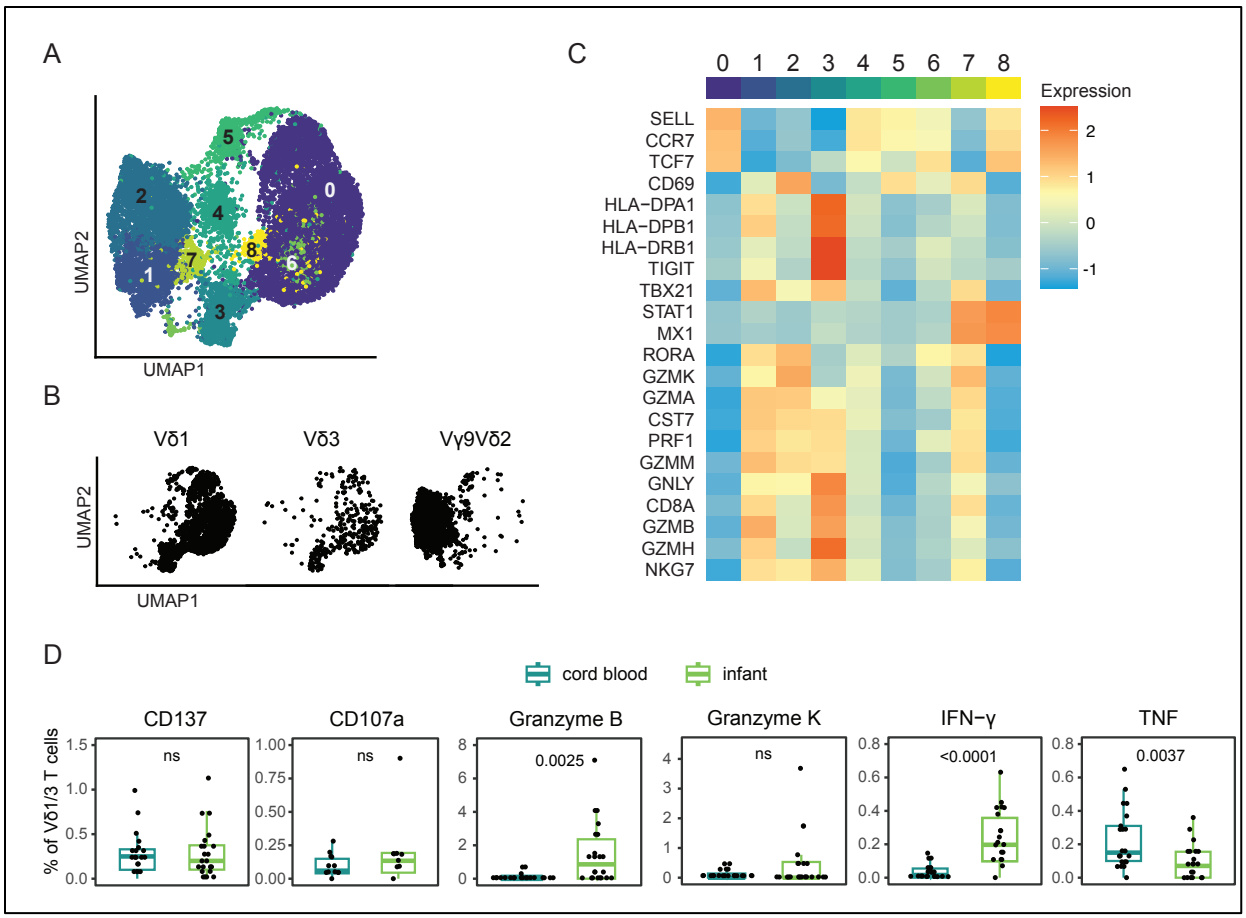

Figure 2.1. Single cell analysis of γδ T cells in BCG-vaccinated human infants reveals evidence of antibacterial effector functions. (A) UMAP displaying 14,302 γδ T cells from 10-week-old South African infants who were vaccinated with BCG at birth (n=6). Cells are clustered according to their gene expression. Each cell is color-coded according to its cluster assignment. **(B)** Cluster positions of cells expressing Vδ1+, Vδ3+, or Vγ9Vδ2 TCRs. **(C)** Heat map displaying the average expression of key genes within each γδ T cell cluster. **(D)** Background-subtracted frequency of Vδ1/3 T cells expressing cell surface and intracellular proteins after stimulation with Mtb whole cell lysate. The frequency in 10-week-old, BCG-vaccinated South African infants (n=22) is compared to the frequency in unmatched cord blood from South African mothers (n=21). Boxplots indicate median and interquartile range. Statistical testing was performed using an unpaired Student's t-test. Unadjusted p-values are displayed.

To validate the cytotoxic functional programs identified by scRNA-seq, we used flow cytometry to compare γδ T cell responses to Mtb whole cell lysate in PBMC from BCG-vaccinated infants (n=22) and cord blood (n=21) (**Figure 2D and Appendix B.I**). All samples were collected from the same geographic region of Cape Town, South Africa, but were not matched by donor (Shey et al., 2014; Soares et al., 2008). γδ T cells were identified and stratified into Vγ9-positive or Vγ9-negative subsets and analyzed for markers of activation (CD137), cytotoxicity (CD107a, granzyme B, granzyme K), cytokine production (IFN-γ, TNF). We inferred that Vγ9-negative γδ T cells are mostly Vδ1/3+ on the basis of paired-chain TCR sequencing as noted above (**Appendix A.II**).

We did not observe a significant difference in the frequency of activated CD137+ Vδ1/3 T cells after Mtb lysate stimulation (**Figure 2.1D**). However, the frequency of Vδ1/3 T cells expressing Granzyme B after stimulation was approximately 1% in BCG-vaccinated infants compared to 0% in cord blood (p=0.0025) (**Figure 2.1D**). Additionally, we observed 12-fold higher expression of IFN-γ among Vδ1/3 T cells in BCG-vaccinated infants compared to cord blood (p<0.0001) (**Figure 2.1D**). Interestingly, the frequency of Vδ1/3 T cells expressing TNF was twice as high in cord blood compared to BCG-vaccinated infants (p=0.0037). The frequency of Vδ1/3 T cells expressing CD107a or Granzyme K was not significantly different between PBMC and cord blood (**Figure 2.1D**). Considered together, our results suggest that the production of Granzyme B and IFN-γ by Vδ1/3 T cells in response to Mtb whole cell lysate is elevated in BCG-vaccinated infants compared to neonates.

2.3 Single cell analysis of γδ T cells reveals antibacterial transcriptional programs following IV-BCG vaccination

We next examined γδ T cells in a discovery cohort of IV-BCG-vaccinated rhesus macaques. We performed multi-modal scRNA-seq on PBMC collected from Indian origin rhesus macaques (n=4) prior to IV-BCG as well as PBMC and bronchoalveolar lavage (BAL) collected at four weeks and eight weeks post-vaccination (**Figure 2.2A**). γδ T cells were sorted immediately after thawing in the absence of stimulation, allowing us to define the transcriptional programs expressed by γδ T cells pre- and post-IV-BCG.

After quality control filtering and data integration, a total of 12,777 γδ T cells were analyzed with an average of 3,200 cells per sample (**Appendix A.III**). Overall, 12 clusters of γδ T cells were defined which broadly separated as cells derived from PBMC or BAL, consistent with distinct transcriptional profiles across the two tissues (**Figure 2.2B and 2.2C**). γδ T cells bearing a Vδ1+ or Vδ3+ TCR were abundant and populated all 12 clusters. In contrast, Vγ9Vδ2 T cells were enriched in cluster 10 and composed less than 1% of the γδ T cells analyzed (**Figure 2.2D, Appendix A.IV**). This result was inconsistent with previously published data showing that Vγ9+ T cells constituted 25-75% of γδ T cells in PBMC and 30-85% of γδ T cells in BAL when analyzed directly ex vivo by flow cytometry (Darrah et al., 2020). We considered several technical explanations for this discrepancy including age and sex distribution, IV-BCG dose, specificity of monoclonal antibodies, and spillover spreading from fluorochromes, but ruled these out (**data not shown**). Notably, the frequency of Vγ9-negative γδ T cells among total T cells in the samples we analyzed was

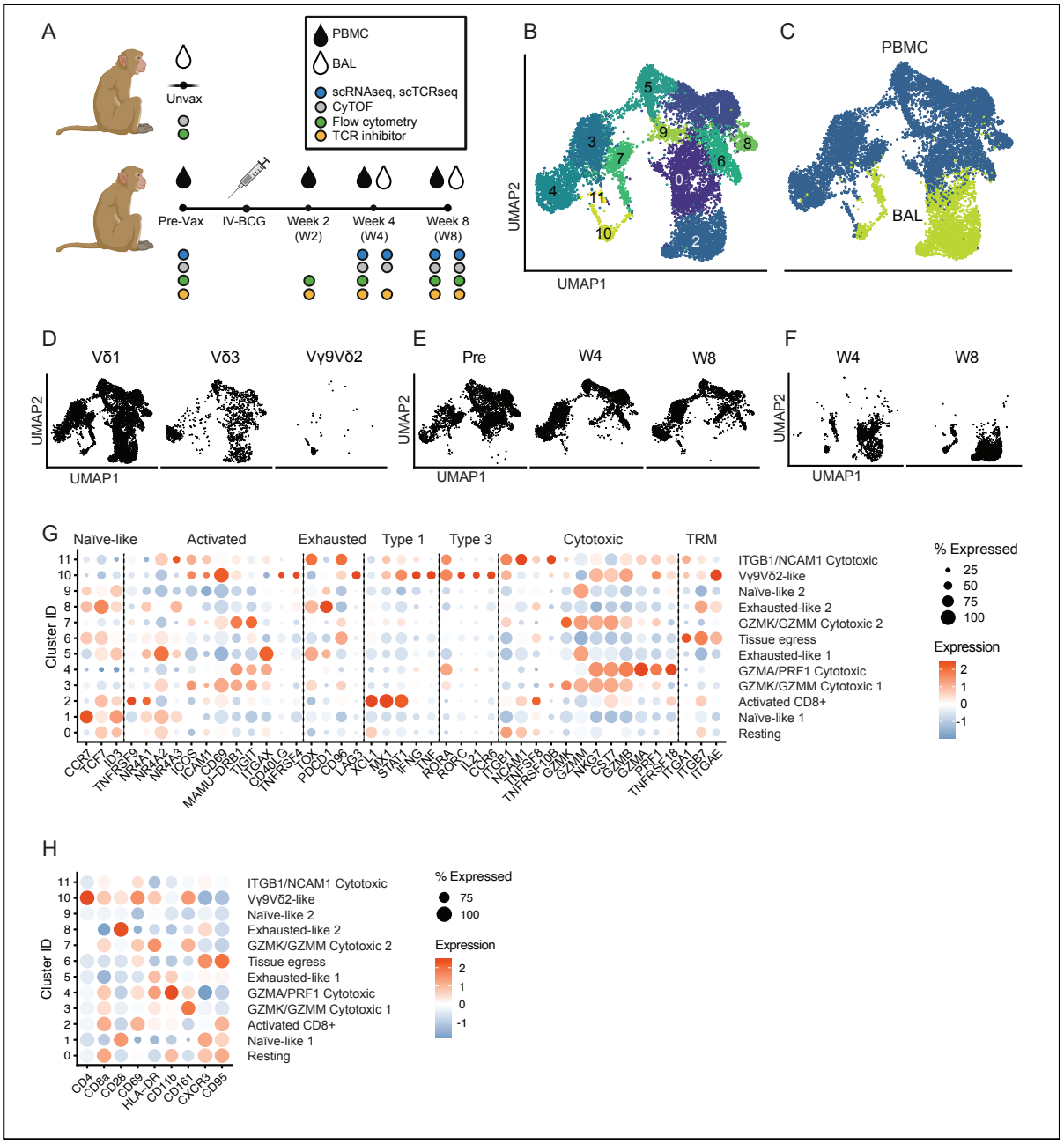

Figure 2.2. γδ T cells display diverse transcriptional profiles in IV-BCG-vaccinated rhesus macaques. (A) Study schema depicting the rhesus macaque samples used for each mode of analysis. **(B and C)** UMAPs displaying 12,777 γδ T cells from IV-BCG vaccinated rhesus macaques (n=4). Cells are clustered according to their gene expression. Each cell is color-coded according to its **(B)** cluster assignment and **(C)** tissue of origin. **(D)** Cluster positions of cells expressing Vδ1, Vδ3, or Vγ9Vδ2 TCRs. **(E)** Cluster positions of cells derived from pre-vaccination (Pre), week 4 (W4), or week 8 (W8) PBMC samples. **(F)** UMAP positions of cells derived from week 4 (W4) or week 8 (W8) BAL samples. **(G)** Heat map displaying the average expression of key genes in each γδ T cell cluster. **(H)** Heat map displaying the average expression of key cell surface proteins in each γδ T cell cluster.

approximately 2% in PBMC and 0.5% in BAL, which was similar to what was reported previously (**Appendix B.III**) (Darrah et al., 2020).

The transcriptomic profile of γδ T cells changed over time in both PBMC and BAL, suggesting that IV-BCG vaccination directly modulated gene expression (**Figure 2.2E and 2.2F**). All γδ T cell clusters were annotated manually according to their RNA and surface protein expression patterns (**Figure 2.2G, Figure 2.2H**). Cluster 0 expressed low levels of *CCR7*, low CD28 protein, and low T cell effector genes and were likely resting cells. Clusters 1 and 9 expressed high levels of *CCR7* and CD28 protein and low levels of T cell effector genes, leading to their annotation as naïve-like cells. Cluster 2 expressed *TNFRSF9* (encoding CD137), *NR4A1* (encoding Nur77), and genes associated with pro-inflammatory activity (*XCL1*, *MX1*, and *STAT1*) together with CD8 protein and were labelled as Activated CD8+ cells. Clusters 3, 4, and 7 were cytotoxic T cell subsets differentiated by expression of granzymes (*GZMA*, *GZMK*, and *GZMM*) and perforin (*PRF1*). Clusters 5 and 8 expressed high levels of *TOX*, *PDCD1*, and *ITGAX* together with low levels of T cell effector genes, suggesting an exhausted-like phenotype. Cluster 6 expressed the tissue residency markers *ITGA1* (CD49a), *ITGB7*, and *ITGAE* (CD103), but was populated by PBMC-derived cells, consistent with recent tissue egress. Cluster 10 was enriched in cells using a Vγ9Vδ2 TCR and expressed genes related to Type 1, Type 3, and cytotoxic activity, including *IFNG*, *TNF*, *RORC*, and *GZMB*. Finally, Cluster 11 expressed high levels of *ITGB1* (CD29) and *NCAM1* (CD56), two genes which have been associated with cytotoxic activity, but expressed relatively low levels of granzyme genes.

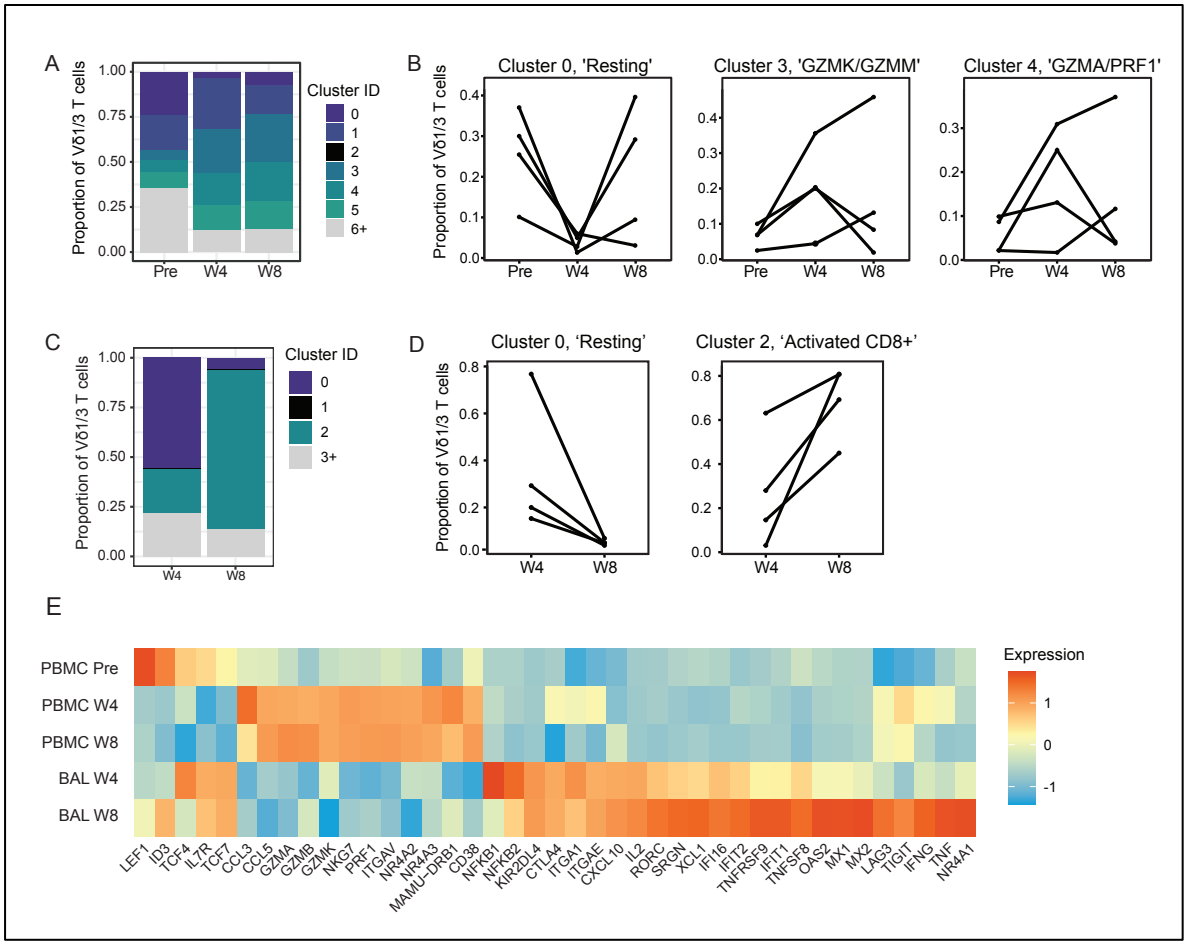

Figure 2.3. Single cell analysis of γδ T cells in rhesus macaques reveals antibacterial transcriptional programs following IV-BCG vaccination. (A) Relative proportion of the top 5 PBMC clusters at each time point. **(B)** Relative proportion of PBMC-derived cells populating Cluster 0, Cluster 3, and Cluster 4 at each time point. Each sample donor is shown in a separate line. **(C)** Relative proportion of the top 4 BAL clusters at each time point. **(D)** Relative proportion of BAL-derived cells populating Cluster 0 and Cluster 2 at each timepoint. Each sample donor is shown in a separate line. **(E)** Heat map displaying the average expression of key genes across each tissue and time point.

Among the six most abundant clusters, Naïve-like-1, GZMK/GZMM-Cytotoxic-1, GZMA/PRF1-Cytotoxic, and Exhausted-like-1 cells were mostly derived from PBMC, Activated-CD8+ cells were mostly derived from BAL, and Resting cells included both PBMC- and BAL-derived cells (**Figure 2.2B, 2.2C, and 2.2G**). Among PBMC, Resting cells were relatively enriched pre-vaccination and

Cytotoxic cells appeared to be expanded after vaccination (**Figure 2.3A and 2.3B**). Within BAL, Resting cells were relatively enriched at week 4 and Activated CD8+ cells were expanded at week 8 (**Figure 2.3C and 2.3D**). Overall, multi-modal scRNA-seq revealed cytotoxic transcriptional programs among γδ T cells that partially tracked with time after IV-BCG vaccination and tissue of origin.

Having observed changes in cluster abundance across tissues and time, we next investigated how IV-BCG vaccination and tissue of origin influenced the gene expression profiles of Vδ1/3 T cells independent of cluster assignment. Differential gene expression analysis revealed down-regulation of naïve-like genes (*LEF1*, *ID3*, *TCF4*, and *IL7R*) and up-regulation of cytotoxic effector genes (*GZMA*, *GZMB*, *GZMK*, and *PRF1*) and genes associated with activated T cells (*NR4A2*, *NR4A3*, *CD38*, and *MAMU-DRB1*) in Vδ1/3 T cells derived from PBMC at 4 weeks and 8 weeks compared to baseline (**Figure 2.3E**). At week 4, Vδ1/3 T cells in BAL expressed lower levels of cytotoxicity-associated genes (*GMZA*, *GZMB*, *GZMK*, *NKG7*, and *PRF1*) compared to PBMC. However, genes that were upregulated in BAL at week 4 relative to PBMC included signatures of response to Type I IFN (*IFI16*, *IFIT2*, and *IFIT1*) as well as *KIR2DL4*, *SRGN*, and *XCL1*, which are expressed cytotoxic cells. Other genes that were elevated in BAL compared to PBMC were associated with tissue-resident cells (*ITGA1* and *ITGAE*), recent activation through the TCR (*TNFRSF9* and *NR4A1*), and chronic stimulation (*CTLA4*, *LAG3*, and *TIGIT*). Notably, one of the most highly upregulated genes at four weeks and eight weeks in BAL compared to PBMC was *TNFSF8* (CD153), which has been associated with Mtb control in both mice and humans (Du Bruyn et al.,

2021; Sallin et al., 2018). These results show that Vδ1/3 T cells in the blood and airway acquire antibacterial and cytotoxic gene expression programs in response to IV-BCG vaccination.

2.4 IV-BCG promotes cytotoxic and pro-inflammatory responses to mycobacterial antigens among Vδ1/3 T cells in the blood and airway

To extend the results of transcriptome analysis, the same samples were analyzed using a 42-parameter mass cytometry panel measuring the surface protein expression and intracellular protein expression of CD45+ leukocytes including γδ T cells (**Figure 2.2A, Appendix C.I and C.II**) (Makatsa et al., 2024). Total PBMC and BAL samples were either left unstimulated or were stimulated for 18 hours using Mtb whole cell lysate. γδ T cells were identified and stratified into Vγ9-positive or Vγ9-negative subsets and analyzed for expression of cytotoxicity (granzyme B, granzyme K, perforin), cytokines (IFN-γ, TNF), and a marker of T cell activation (CD69) (**Appendix C.I**). Although we did not directly identify Vδ1 T cells in this experiment, we performed paired-chain TCR sequencing on γδ T cells derived from these samples. Of 5,738 γδ T cells expressing a Vγ9-negative γδ TCR, 74% expressed a Vδ1+ TCR, 22% expressed a Vδ3+ TCR, and only 4% expressed a Vδ2+ TCR, thus Vγ9-negative γδ T cells are inferred to be Vδ1/3+ (**Appendix A.IV**).

In unstimulated PBMC, the frequency of Vδ1/3 T cells expressing granzyme B, granzyme K, and perforin was higher after IV-BCG (**Figure 2.4A, Figure 2.4B, Figure 2.4C**). After stimulation with Mtb whole cell lysate, Vδ1/3 T cells showed increased upregulation of CD69, IFN-γ, and TNF in both PBMC and BAL compared to pre-vaccination (**Figure 2.4D, Figure 2.4E, Figure 2.4F**). Vδ1/3 T cells producing IFN-γ and TNF in response to Mtb lysate appeared to be enriched in the BAL

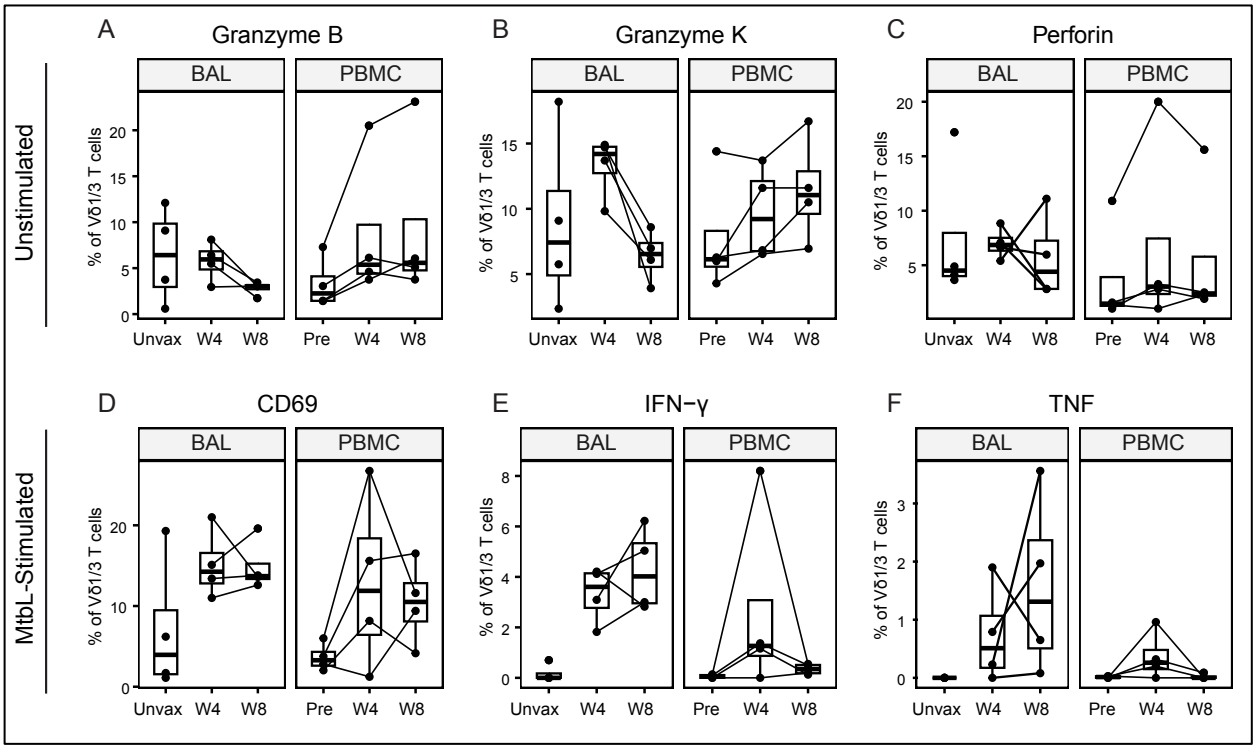

Figure 2.4. CyTOF reveals enhanced pro-inflammatory and cytotoxic effector programs in Vδ1/3 T cells after IV-BCG. (A-C) Expression of intracellular proteins in unstimulated cells at each tissue and timepoint. Matched samples are indicated by a black line. (D-F) Background-subtracted expression of cell surface protein and intracellular proteins after stimulation with Mtb whole cell lysate. Matched samples are indicated by a black line.

compared to PBMC at both 4 weeks and 8 weeks post-vaccination (**Figure 2.4E, Figure 2.4F**). In line with results obtained using scRNA-seq, these results suggest that IV-BCG promotes cytotoxic and antimicrobial activity among mycobacteria-reactive Vδ1/3 T cells.

To confirm and extend the results of scRNA-Seq and CyTOF analysis in our discovery cohort, we analyzed γδ T cell activation (CD69, CD137), pro-inflammatory cytokine production (IFN-γ, TNF), and cytotoxicity (granzyme B, granzyme K, CD107a) in the presence or absence of stimulation with Mtb whole-cell lysate for 18 hours using flow cytometry (**Appendix B.II and B.IV).**

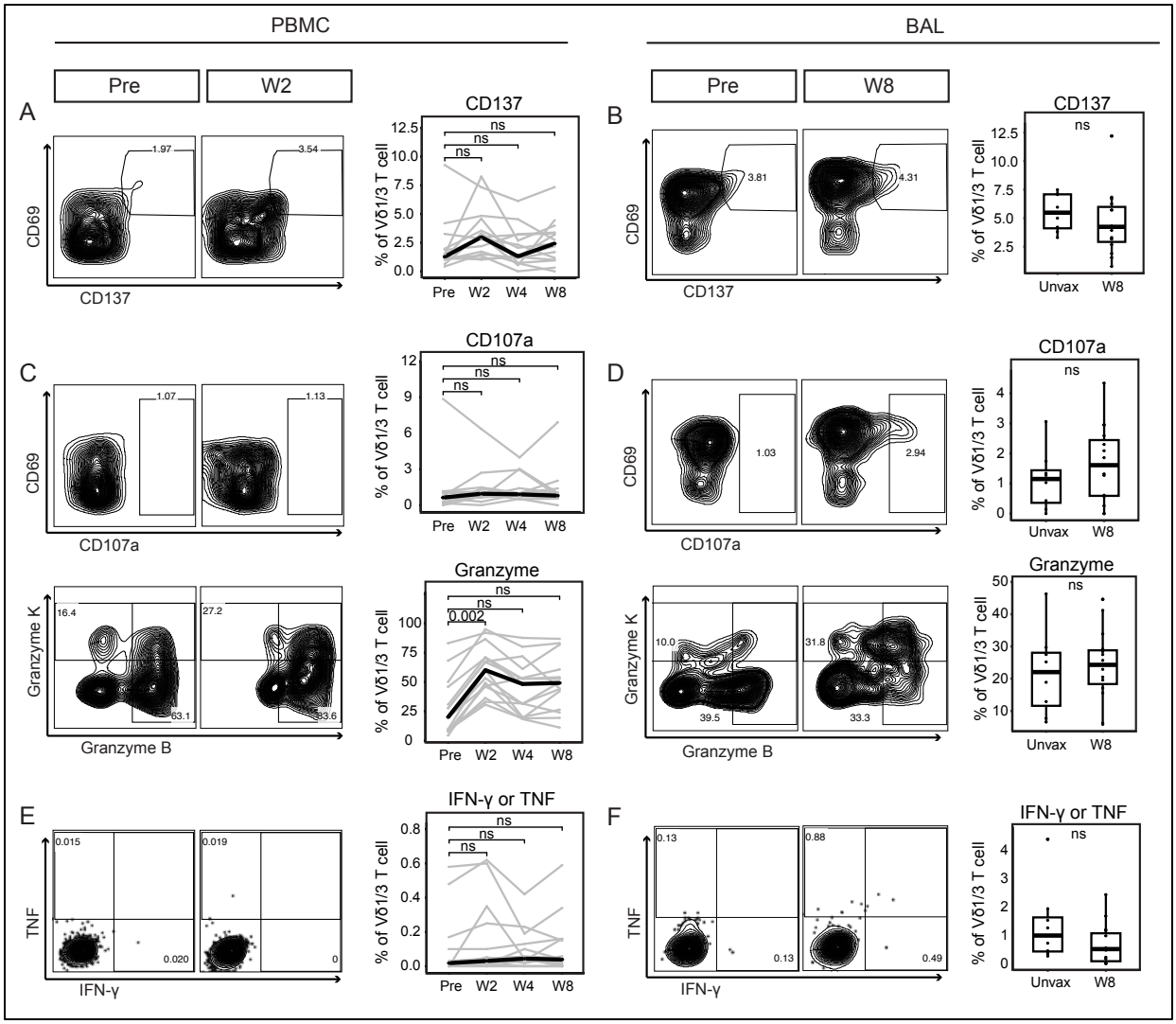

Figure 2.5. Vδ1/3 T cells display elevated cytotoxic potential after intravenous BCG. Frequency of unstimulated Vδ1/3 T cells expressing cell surface and intracellular proteins. Profiling was performed in Vδ1/3 T cells collected from IV-BCG vaccinated (n=16) and unvaccinated (n=9) rhesus macaques. **(A)** Representative flow cytometry plots illustrating gating scheme for CD137 in PBMC pre-vaccination (Pre) and week 2 (W2) post-vaccination with IV-BCG (left). Percentage of Vδ1/3 T cells in PBMC expressing CD137 over time (right). Each sample donor is shown in a separate line. Median frequencies are shown in black. **(B)** Representative flow cytometry plots illustrating gating scheme for CD137 in BAL pre-vaccination (Pre) and week 8 (W8) post-vaccination with IV-BCG (left). Percentage of Vδ1/3 T cells in BAL expressing CD137 among unvaccinated macaques (Unvax) and week 8 (W8) after IV-BCG (right). Boxplots indicate median and interquartile range. **(C)** Representative flow cytometry plots illustrating gating scheme for CD69 and CD107a in PBMC stimulated with Mtb lysate pre-vaccination (Pre) and week 2 (W2) post-vaccination with IV-BCG (left). Percentage of Vδ1/3 T cells in PBMC expressing CD107a or Granzymes (granzyme B or granzyme K) after stimulation with Mtb lysate over time (right). Each sample donor is shown in a separate line. Median frequencies are shown in black. **(D)** Representative flow cytometry plots illustrating gating scheme for CD107a, granzyme B, and

granzyme K in BAL pre-vaccination (Pre) and week 8 (W8) post-vaccination with IV-BCG (left). Percentage of Vδ1/3 T cells in BAL expressing CD107a or Granzymes (granzyme B or granzyme K) among unvaccinated macaques (Unvax) and week 8 (W8) after IV-BCG (right). Boxplots indicate median and interquartile range. **(E)** Representative flow cytometry plots illustrating gating scheme for IFN-γ and TNF in PBMC pre-vaccination (Pre) and week 2 (W2) post-vaccination with IV-BCG (left). Percentage of Vδ1/3 T cells in PBMC expressing IFN-γ or TNF over time (right). Each sample donor is shown in a separate line. Median frequencies are shown in black. **(F)** Representative flow cytometry plots illustrating gating scheme for IFN-γ and TNF in BAL pre-vaccination (Pre) and week 8 (W8) post-vaccination with IV-BCG (left). Percentage of Vδ1/3 T cells in BAL expressing IFN-γ or TNF among unvaccinated macaques (Unvax) and week 8 (W8) after IV-BCG (right). Boxplots indicate median and interquartile range.

We analyzed PBMC from a validation cohort of IV-BCG-vaccinated rhesus macaques (n=16) before vaccination and at week 4 and week 8 after IV-BCG vaccination. We also analyzed BAL obtained at week 8 after IV-BCG and compared this to BAL samples from a separate cohort of unvaccinated rhesus macaques (n=9) (**Figure 2.2A**). Consistent with our scRNA-seq analysis, the frequency of Vγ9+ γδ T cells was lower than previously reported in vaccinated and unvaccinated animals (**Appendix B.VII**) (Darrah et al., 2020). We noted greater than a two-fold increase in Vδ1/3 T cells expressing granzymes from pre-vaccination to week 2 in PBMC (p=0.002) but not BAL (**Figure 2.5C, 2.5D**). By contrast, the expression CD137, CD107a, or cytokines in unstimulated samples was not significantly increased after IV-BCG in either PBMC or BAL at any timepoint (**Figure 2.5A, 2.5B, 2.5C, 2.5D, 2.5E, 2.5F**). These results suggest that IV-BCG vaccination promotes cytotoxic potential of circulating Vδ1/3 T cells *in vivo.*

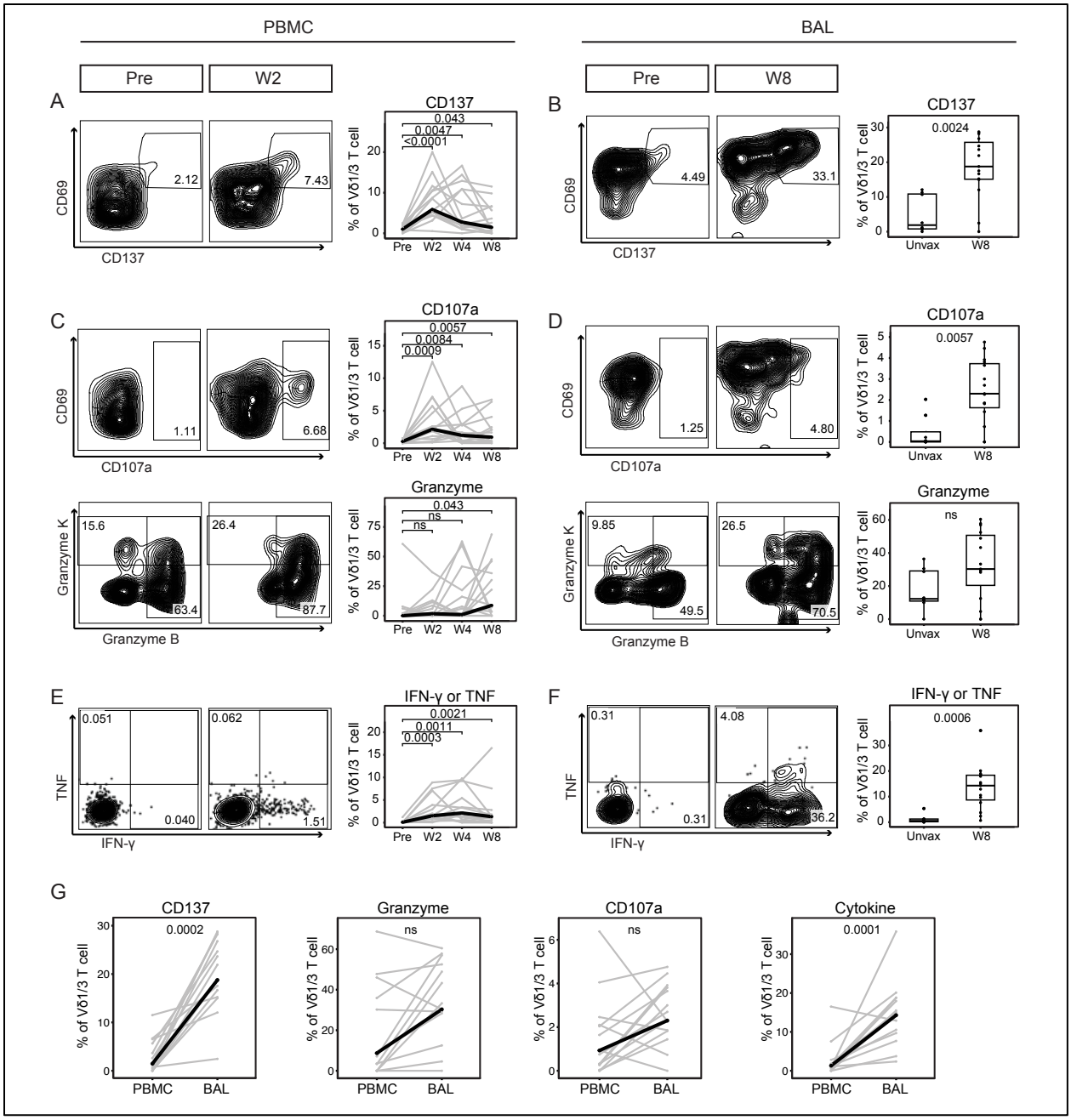

Figure 2.6. IV-BCG promotes cytotoxic and pro-inflammatory responses to mycobacterial antigens among Vγ9-negative γδ T cells in the blood and airway. Background-subtracted frequency of T cell subsets expressing cell surface and intracellular proteins after stimulation with Mtb whole cell lysate. Profiling was performed in Vδ1/3 T cells collected from IV-BCG vaccinated (n=16) and unvaccinated (n=9) rhesus macaques. **(A)** Representative flow cytometry plots illustrating gating scheme for CD137 in PBMC stimulated with Mtb lysate pre-vaccination (Pre) and week 2 (W2) post-vaccination with IV-BCG (left). Percentage of Vδ1/3 T cells in PBMC expressing CD137 after stimulation with Mtb lysate over time (right). Each sample donor is shown in a separate line. Median frequencies are shown in black. **(B)** Representative flow cytometry plots illustrating gating scheme for CD137 in BAL stimulated with Mtb lysate pre-vaccination (Pre)

and week 8 (W8) post-vaccination with IV-BCG (left). Percentage of Vδ1/3 T cells in BAL expressing CD137 after stimulation with Mtb lysate among unvaccinated macaques (Unvax) and week 8 (W8) after IV-BCG (right). Boxplots indicate median and interquartile range. **(C)** Representative flow cytometry plots illustrating gating scheme for CD107a in PBMC stimulated with Mtb lysate pre-vaccination (Pre) and week 2 (W2) post-vaccination with IV-BCG (left). Percentage of Vδ1/3 T cells in PBMC expressing CD107a or Granzymes (granzyme B or granzyme K) after stimulation with Mtb lysate over time (right). Each sample donor is shown in a separate line. Median frequencies are shown in black. **(D)** Representative flow cytometry plots illustrating gating scheme for CD107a, granzyme B, and granzyme K in BAL stimulated with Mtb lysate pre-vaccination (Pre) and week 8 (W8) post-vaccination with IV-BCG (left). Percentage of Vδ1/3 T cells in BAL expressing CD107a or Granzymes (granzyme B or granzyme K) after stimulation with Mtb lysate among unvaccinated macaques (Unvax) and week 8 (W8) after IV-BCG (right). Boxplots indicate median and interquartile range. **(E)** Representative flow cytometry plots illustrating gating scheme for IFN-γ and TNF in PBMC stimulated with Mtb lysate pre-vaccination (Pre) and week 2 (W2) post-vaccination with IV-BCG (left). Percentage of Vδ1/3 T cells in PBMC expressing IFN-γ or TNF after stimulation with Mtb lysate over time (right). Each sample donor is shown in a separate line. Median frequencies are shown in black. **(F)** Representative flow cytometry plots illustrating gating scheme for IFN-γ and TNF in BAL stimulated with Mtb lysate pre-vaccination (Pre) and week 8 (W8) post-vaccination with IV-BCG (left). Percentage of Vδ1/3 T cells in BAL expressing IFN-γ or TNF after stimulation with Mtb lysate among unvaccinated macaques (Unvax) and week 8 (W8) after IV-BCG (right). Boxplots indicate median and interquartile range. **(G)** Comparison of background-subtracted frequencies of Vδ1/3 T cells expressing CD137, Granzyme (granzyme B or granzyme K), CD107a, and Cytokine (IFN-γ or TNF) between PBMC and BAL at week 8. In Panels A, C, E, and G, statistical testing was performed using the paired Wilcoxon signed-rank test. In Panels B, D, and F, statistical testing was performed with an unpaired Wilcoxon signed-rank test. Unadjusted p-values are displayed.

Next, we explored the effect of IV-BCG on the response of Vδ1/3 T cells to Mtb whole-cell lysate. Following IV-BCG vaccination, the median frequency of Vδ1/3 T cells expressing CD137 in response to stimulation with Mtb lysate (Mtb-reactive) increased by up to six-fold in PBMC ($p<0.0001$) and ten-fold in the BAL ($p=0.0024$), consistent with recognition of Mtb antigens through the TCR (**Figure 2.6A and 2.6B**) (Ji et al., 2024; Pei et al., 2020). Further, Mtb-reactive Vδ1/3 T cells were enriched 13-fold in the BAL compared to PBMC after IV-BCG ($p=0.0002$) while

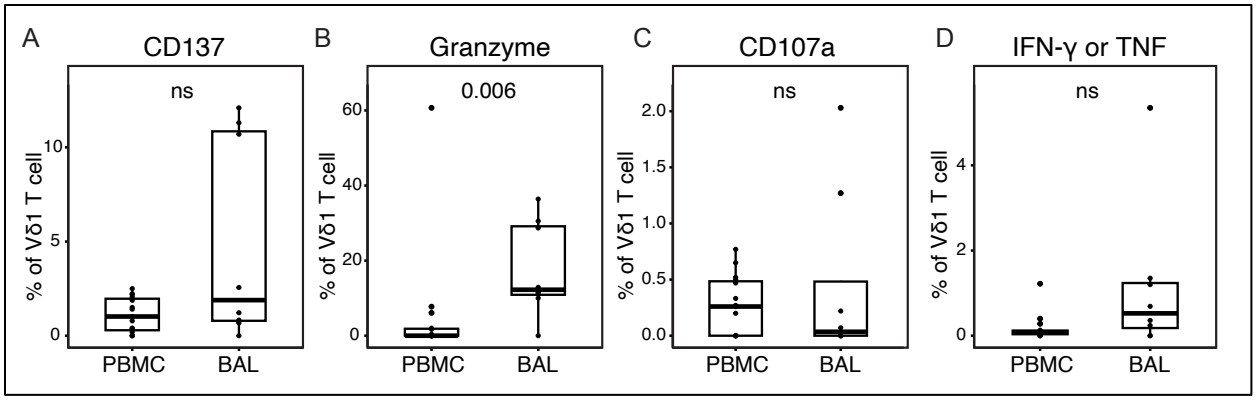

Figure 2.7. PBMC and BAL responses to Mtb lysate in unvaccinated animals. (A) Frequency of Vδ1/3 T cells expressing CD137 in response to stimulation with Mtb whole cell lysate. The frequency in unpaired PBMC and BAL samples is shown. Unpaired Wilcoxon signed-rank test. (B) Frequency of Vδ1/3 T cells expressing granzyme B or granzyme K in response to stimulation with Mtb whole cell lysate. The frequency in unpaired PBMC and BAL samples is shown. Unpaired Wilcoxon signed-rank test. (C) Frequency of Vδ1/3 T cells expressing CD107a in response to stimulation with Mtb whole cell lysate. The frequency in unpaired PBMC and BAL samples is shown. Unpaired Wilcoxon signed-rank test. (D) Frequency of Vδ1/3 T cells expressing IFN-γ or TNF in response to stimulation with Mtb whole cell lysate. The frequency in unpaired PBMC and BAL samples is shown. Unpaired Wilcoxon signed-rank test.

there was no significant difference seen before vaccination (**Figure 2.6G, Figure 2.7A**). The median frequency of Vδ1/3 T cells expressing granzymes in response to stimulation was not significantly altered after IV-BCG in BAL, but in PBMC increased from 0% at baseline to 8.7% by week 8 (p=0.043) (**Figure 2.6C and 2.6D**). The median frequency of Vδ1/3 T cells expressing CD107a increased up to eight-fold in PBMC (p=0.0009) and 50-fold in BAL (p=0.0057) after IV BCG, compared to baseline (**Figure 2.6C and 2.6D**). The median expression of granzymes and CD107a in response to stimulation did not significantly differ between PBMC and BAL in vaccinated animals, but the median expression of granzymes in response to stimulation in unvaccinated animals was 16.6% in BAL compared to 0.1% in PBMC (p=0.006) (**Figure 2.6G, Figure 2.7B, Figure 2.7C**). The frequency of Vδ1/3 T cells producing IFN-γ or TNF in response to stimulation with Mtb lysate was markedly increased after IV-BCG, rising over 20-fold in PBMC

(p=0.0003) and over 40-fold in the BAL (p=0.0006) (**Figure 2.6E and 2.6F**). Finally, cytokine-producing Vδ1/3 T cells were on average enriched over ten-fold in BAL compared to PBMC after IV-BCG (p=0.0001), which was not observed in unvaccinated animals (**Figure 2.6G, Figure 2.7D**). These results suggest that IV-BCG augments Vδ1/3 T cell responses to Mtb antigens in the blood and airway, where they may be activated through their TCR and exert cytotoxic and pro-inflammatory immune functions.

2.5 Vδ1/3 T cells respond to IV-BCG earlier than conventional T cells

The peak functional response to IV-BCG in conventional T cells occurs at 8 weeks after vaccination in the BAL and 4 weeks after vaccination in PBMC (Darrah et al., 2020). Additionally, the peak functional response of Vγ9+ T cells in PBMC appeared to occur between 2 and 4 weeks after vaccination (Darrah et al., 2023). However, the timepoint of peak functional response among Vδ1/3 T cells remains uncharacterized. Among peripheral blood Vδ1/3 T cells stimulated with Mtb lysate, we found that peak expression of CD137 and CD107a occurred on average at week 2, earlier than in CD8 T cells (**Figure 2.8A and 2.8C, Appendix B.V**). Similarly, peak expression of cytokines in Vδ1/3 T cells occurred at 2-4 weeks after vaccination, while peak expression of cytokines in CD8 T cells occurred at 4-8 weeks, on average (**Figure 2.8D, Appendix B.V**). Despite showing a peak functional response earlier than CD8 T cells, Vδ1/3 T cells did not have significantly lower functional responses to Mtb lysate compared to CD8 T cells at week 8, except

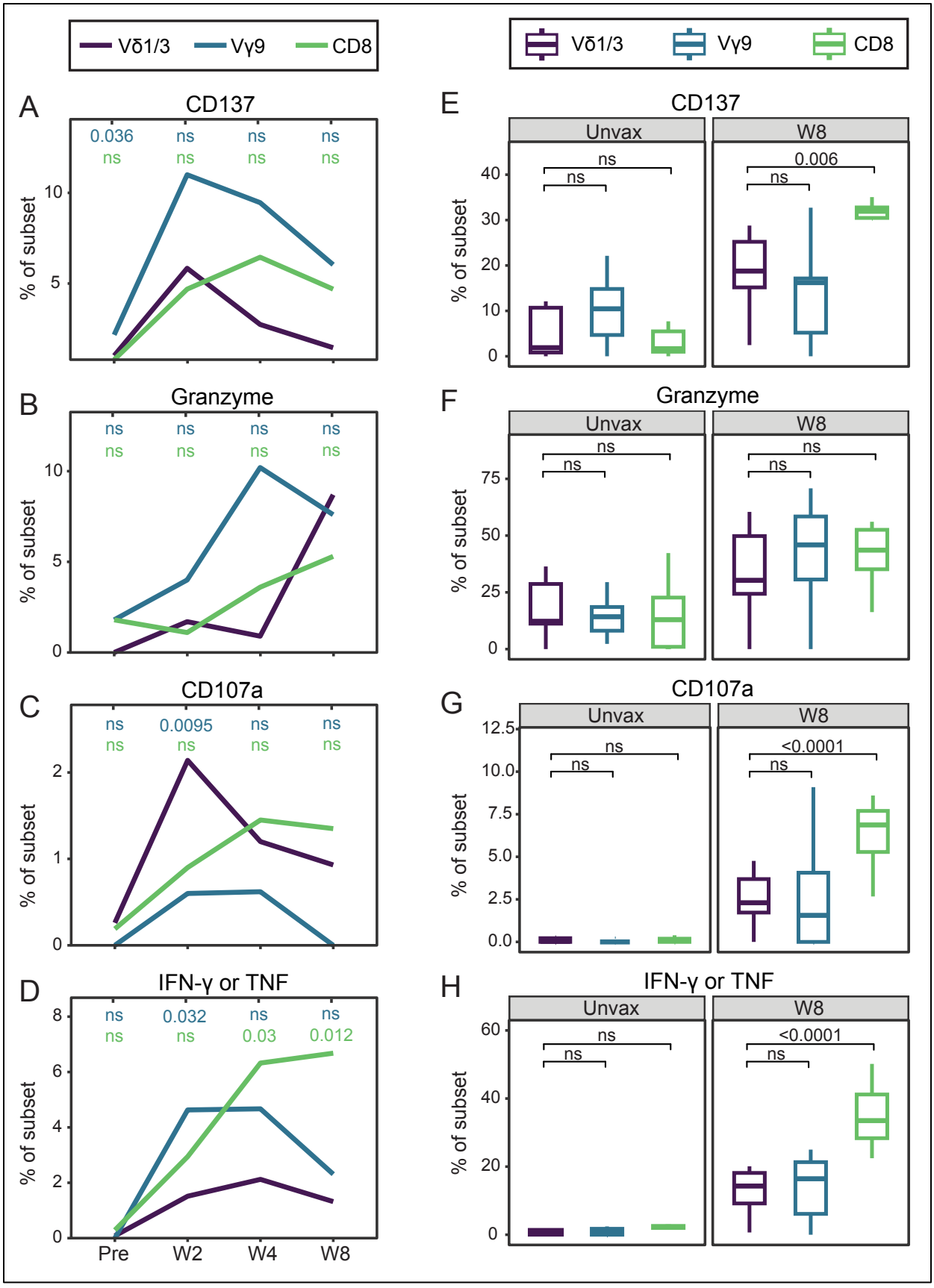
Vδ1/3
Vγ9
CD8
A
CD137
0.036
ns
ns
ns
ns
ns
ns
ns
ns
% of subset
10
5
B
Granzyme
ns
ns
ns
ns
ns
ns
ns
ns
% of subset
10
5
0
C
CD107a
ns
ns
0.0095
ns
ns
ns
ns
ns
% of subset
2
1
0
D
IFN-γ or TNF
ns
ns
0.032
ns
ns
0.03
ns
0.012
% of subset
8
6
4
2
0
Pre
W2
W4
W8
E
CD137
Unvax
W8
ns
ns
ns
0.006
% of subset
40
30
20
10
0
F
Granzyme
Unvax
W8
ns
ns
ns
ns
% of subset
75
50
25
0
G
CD107a
Unvax
W8
ns
ns
ns
<0.0001
% of subset
12.5
10.0
7.5
5.0
2.5
0.0
H
IFN-γ or TNF
Unvax
W8
ns
ns
ns
<0.0001
% of subset
60
40
20
0

Figure 2.8. Vδ1/3 T cells respond to IV-BCG earlier than CD8 T cells. Background-subtracted frequency of T cell subsets expressing cell surface and intracellular proteins after stimulation with Mtb whole cell lysate. Profiling was performed in T cells collected from IV-BCG vaccinated (n=16) and unvaccinated (n=9) rhesus macaques. Frequencies are shown pre-vaccination (Pre) and at week 2 (W2), week 4 (W4), and week 8 (W8) post IV-BCG in PBMC. Frequencies are shown in unvaccinated rhesus macaques (Unvax) and at week 8 (W8) post IV-BCG in BAL. **(A)** Median percentage of T cells expressing CD137 after stimulation with Mtb whole cell lysate in PBMC. Each T cell subset is shown in a separate line. The frequency among Vγ9+ γδ T cells or CD8 T cells is compared to the frequency among Vδ1/3 T cells at each time point. **(B)** Median percentage of T cells expressing Granzyme (granzyme B or granzyme K) after stimulation with Mtb whole cell lysate in PBMC. Each T cell subset is shown in a separate line. The frequency among Vγ9+ γδ T cells or CD8 T cells is compared to the frequency among Vδ1/3 T cells at each time point. **(C)** Median percentage of T cells expressing CD107a after stimulation with Mtb whole cell lysate in PBMC. Each T cell subset is shown in a separate line. The frequency among Vγ9+ γδ T cells or CD8 T cells is compared to the frequency among Vδ1/3 T cells at each time point. **(D)** Median percentage of T cells expressing Cytokine (IFN-γ or TNF) after stimulation with Mtb whole cell lysate in PBMC. Each T cell subset is shown in a separate line. The frequency among Vγ9+ γδ T cells or CD8 T cells is compared to the frequency among Vδ1/3 T cells at each time point. **(E)** Percentage of T cells expressing CD137 after stimulation with Mtb whole cell lysate in BAL. Boxplots indicate median and interquartile range. **(F)** Percentage of T cells expressing Granzyme (granzyme B or granzyme K) after stimulation with Mtb whole cell lysate in BAL. Boxplots indicate median and interquartile range. **(G)** Percentage of T cells expressing CD107a after stimulation with Mtb whole cell lysate in BAL. Boxplots indicate median and interquartile range. **(H)** Percentage of T cells expressing Cytokine (IFN-γ or TNF) after stimulation with Mtb whole cell lysate in BAL. Boxplots indicate median and interquartile range. Statistical testing was performed using a paired Wilcoxon signed-rank test. Unadjusted p-values are displayed.

for 3- to 5-fold lower expression of IFN-γ or TNF in week 4 and week 8 PBMC (**Figure 2.8A, 2.8B, 2.8C, and 2.8D**). Further, CD8 T cells expressing CD137 ($p=0.006$), CD107a ($p<0.0001$) and IFN-γ or TNF ($p<0.0001$) were 2- to 3-fold more frequent compared to Vδ1/3 T cells in the BAL of vaccinated animals (**Figure 2.8E, 2.8G, and 2.8H**). However, there was no significant difference in the expression of granzymes between CD8 T cells and Vδ1/3 T cells in BAL (**Figure 2.8F**). Vγ9+ T cells expressed higher levels of IFN-γ or TNF compared to Vδ1/3 T cells at week 2 in PBMC ($p=0.032$), but not at any other time point (**Figure 2.8D**). Additionally, CD137 expression was also

elevated in Vγ9+ T cells compared to Vδ1/3 T cells in PBMC from unvaccinated animals (p=0.036), consistent with an enhanced ability to recognize Mtb in an unprimed state (**Figure 2.8A**). Finally, Vδ1/3 T cells expressed 3-fold higher levels of CD107a compared to Vγ9+ γδ T cells in week 2 PBMC (p=0.0095) (**Figure 2.8C**). Our results suggest that Vδ1/3 T cells show peak functional responsiveness to IV-BCG at an earlier timepoint compared to CD8 T cells, yet the durability of these responses may be comparable to that seen in CD8 T cells. However, CD8 T cells may exert stronger pro-inflammatory activity in the blood and airway at late timepoints. Additionally, Vγ9+ γδ T cells in PBMC, but not BAL, may show more potent pro-inflammatory activity than Vδ1/3 T cells at early timepoints.

2.6 Vδ1/3 T cells in the airway correlate with protection against Mtb challenge

We next asked whether Vγ9-negative γδ T cells correlate with protection against Mtb challenge after IV BCG. We leveraged a published dataset examining BAL collected from 34 rhesus macaques who were vaccinated with a range of IV-BCG doses, resulting in variable degrees of protection against Mtb challenge (Darrah et al., 2023). In this study, Vγ9+ T cells were identified as an immune correlate of protection, but Vγ9-negative T cells were not analyzed (Darrah et al., 2023). We obtained the original FCS files and gated Vg9-negative cells, which we inferred to be 96% Vδ1/3+ T cells on the basis of paired-chain TCR sequencing (**Figure 2.9A, 2.9B, Appendix B.VI, and Appendix A.IV**). Per the published study, we defined 'protected' as <100 total thoracic

Mtb CFU enumerated at necropsy. Protected (n=18) and unprotected (n=16) animals showed similar distribution of sex and age at vaccination (**Appendix D.III**).

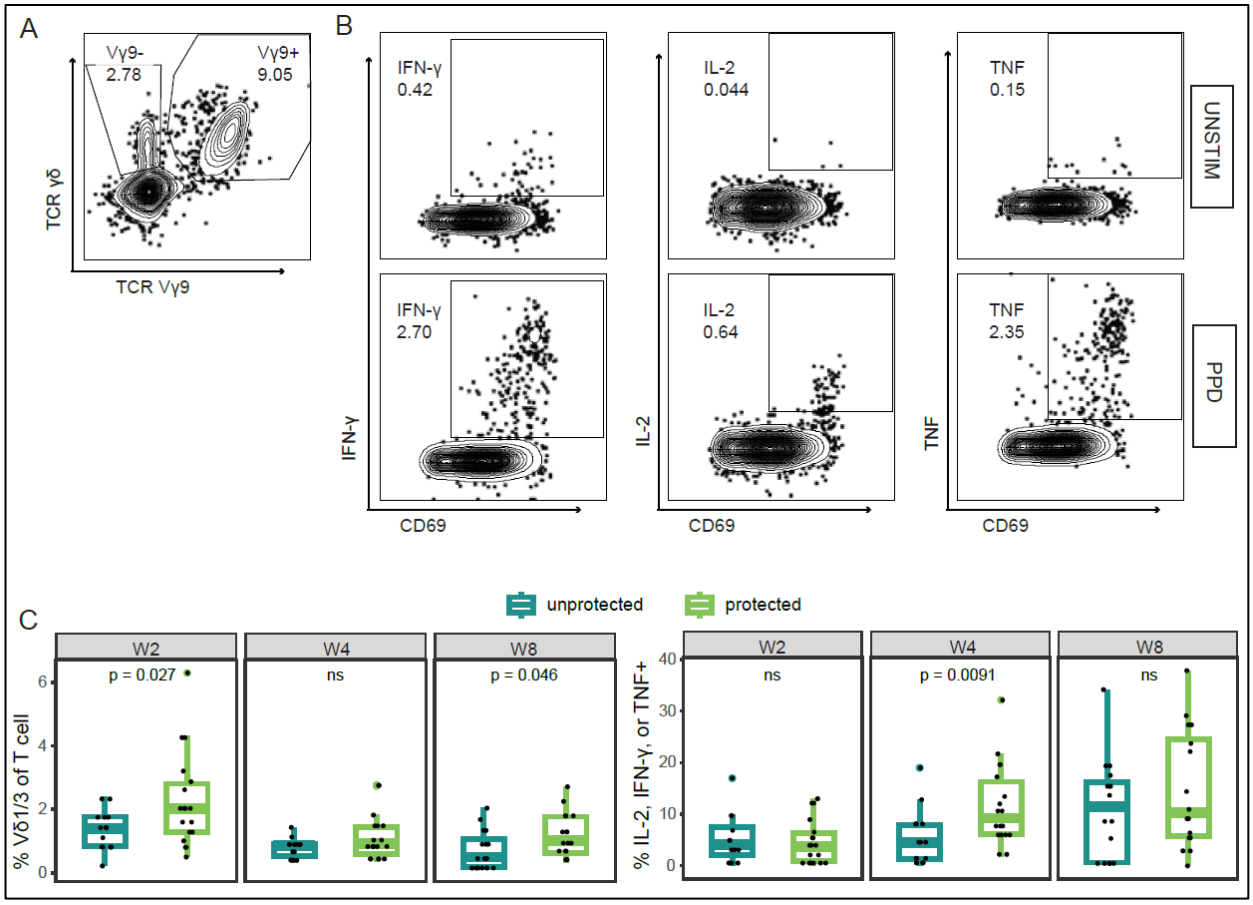

Figure 2.9. Vδ1/3 T cells in the airway correlate with protection against Mtb challenge. Published flow cytometry data from PMID: 37267955 were re-analyzed to examine associations between Vγ9-negative T cells and protection from Mtb challenge. **(A)** Representative bivariate plot showing the identification of Vγ9-negative γδ T cells, which were shown to express a Vδ1/3 TCR. **(B)** Representative bivariate plots showing the expression of cytokines (% positive) among Vδ1/3 T cells in response to stimulation with Mtb purified protein derivative (PPD). Background-subtracted frequencies are shown. **(C)** Box plots displaying the distribution of each feature in protected (<100 total thoracic CFU) or unprotected (≥100 total thoracic CFU) animals. Statistical testing was performed with a Welch's t-test. Unadjusted p-values are displayed.

Animals who were protected after challenge showed 1.5- to 2-fold higher frequency of Vγ9-negative γδ T cells in the BAL at week 2 (p=0.027) and week 8 (p=0.046) after vaccination compared to animals who were not protected (**Figure 2.9C**). At week 4, protected animals showed 2-fold higher frequency of Vγ9-negative γδ T cells producing IFN-γ, IL-2, or TNF in response to stimulation with PPD (p=0.0091) (**Figure 2.9C**). The frequency of cytokine-producing Vγ9-negative γδ T cells did not significantly differ between protected and unprotected animals at week 2 or week 8. Our results suggest that both the overall frequency of Vγ9-negative γδ T cells and the frequency of PPD-reactive Vγ9-negative γδ T cells in the lung after IV-BCG are associated with protection against Mtb.

2.7 Conclusion

Our results advance the field in at least three respects. First, we demonstrate that BCG-vaccinated human infants express a subset of cytotoxic Vδ1/3 T cells that express granzyme B and IFN-γ in response to stimulation with Mtb whole-cell lysate. These Mtb-responsive effector functions were not observed in cord blood, suggesting that they may be induced by BCG vaccination. Second, we report that IV-BCG increases the frequency of cytotoxic Vδ1/3 T cells in both the blood and the airway of macaques. It is notable that pro-inflammatory and cytotoxic Vδ1/3 T cells were observed in both human and NHPs in the context of BCG-mediated protection. Finally, we show that pro-inflammatory responses to mycobacterial antigens in macaque Vδ1/3 T cells correlate with protection against Mtb. Our findings suggest that Vδ1/3 T cells may contribute to Mtb control and define the T cell effector functions that may mediate protection.

CHAPTER 3: THE ROLE OF THE γδ T CELL RECEPTOR IN THE IMMUNE RESPONSE TO BCG

3.1 Introduction

Vδ1/3 T cells are known to be activated by TCR-dependent or TCR-independent signals, including NK receptor ligands, TLR ligands, and cytokines (Ribeiro et al., 2015). Although γδ T cells are frequently described as an innate-like immune cell subset, increasing evidence suggests that Vδ1/3 T cells may respond to disease in a TCR-dependent, adaptive-like manner. In Malian children, Vδ1 T cells clonally expand during episodes of febrile malaria, driving higher overall Vδ1 frequencies in geographic regions with seasonal malaria (von Borstel et al., 2021). Clonal expansions of Vδ1 T cells have also been observed during CMV infection, where the expanded clonotypes persisted for at least 1.5 years and displayed a more differentiated phenotype compared with Vδ1 T cells bearing unexpanded TCRs (Davey et al., 2017). Immune profiling within Merkel cell carcinoma tumors found that Vδ2-negative γδ T cells are highly expanded in a subset of patients (Gherardin et al., 2021). In one Merkel cell carcinoma tumor in which γδ T cells were strongly enriched, TCR sequencing revealed four hyperexpanded Vδ1+ clonotypes with a terminally differentiated and exhausted phenotype, consistent with chronic activation driven by tumor antigens (Gherardin et al., 2021). A separate study of six Merkel cell carcinoma patients described one patient in which tumor-infiltrating γδ T cells expanded nearly 10-fold following treatment with PD-1 blockade (Lien et al., 2024). Single-cell RNA sequencing and bulk TCR sequencing revealed that the expansion was driven by a single Vδ1+ clonotype which reacted to Merkel cancer cell lines but not ovarian cancer cell lines (Lien et al., 2024). Further, in patients

with colorectal cancer, a subgroup of Vδ1 T cells characterized by their expression of NKp46 was associated with increased cytotoxicity, antitumor activity and reduced risk of metastatic disease (Mikulak et al., 2019). TCR sequencing of NKp46+ and NKp46-negative Vδ1 T cells revealed non-overlapping clonotypes in these two subsets, with increased Vγ4 usage in the NKp46+ cells and increased Vγ9 usage in the NKp46-negative cells (Mikulak et al., 2019). Finally, an independent study in patients with colorectal cancer found that tumor-infiltrating γδ T cells preferentially used a Vγ4Vδ1 TCR and displayed a protumorigenic, Th17-like phenotype, while γδ T cells from neighboring healthy tissue were enriched in Vγ8Vδ3 TCRs and were more likely to show a cytotoxic phenotype (Reis et al., 2022). Considered together, these studies provide evidence that Vδ1 T cells identify and respond to pathogens and tumors in a TCR-dependent manner.

It remains unclear whether Vδ1/3 T cell responses to mycobacterial antigens are primarily mediated through TCR-dependent or TCR-independent modes. TCR deep-sequencing analysis of paired blood and lung samples from TB patients revealed several Vδ1+ and Vδ3+ clonotypes that were enriched by 10- to 2000-fold in the lungs compared to the blood, consistent with clonal expansion in response to Mtb infection (Ogongo et al., 2020). However, a recent study described Vδ1 T cells expanded in persistent Mtb infection that are refractory to TCR stimulation yet exert cytotoxic activity through CD16 (Chowdhury et al., 2023). It is unknown whether Vδ1/3 T cell responses to BCG vaccination are mediated through the TCR. Additionally, it is unclear whether the innate-like and adaptive-like functions of Vδ1/3 T cells differentially contribute to immune protection against Mtb. Here, we leveraged the experimental approaches outlined in Figure 2.2A

as well as functional analysis using a TCR inhibitor to explore whether Vδ1/3 T cell responses to BCG are mediated through the TCR.

3.2 Vδ1/3 T cells are clonally expanded in BCG-vaccinated human infants

We leveraged data described in Chapter 2.2 to explore whether distinct γδ T cell phenotypes were associated with specific TCR clonotypes, CDR3 motifs, or TCR gene usage. We used scRNA-seq and single-cell TCR sequencing to characterize unstimulated peripheral γδ T cells from ten-week-old South African infants (n=6) who received intradermal BCG at birth (Hawkridge et al., 2008). A total of 14,302 unstimulated γδ T cells were analyzed and nine distinct clusters of γδ T cells were defined based on their gene expression and expression of either a Vδ1/3+ or Vγ9Vδ2 TCR (**Figure 3.1A, 3.1B**).

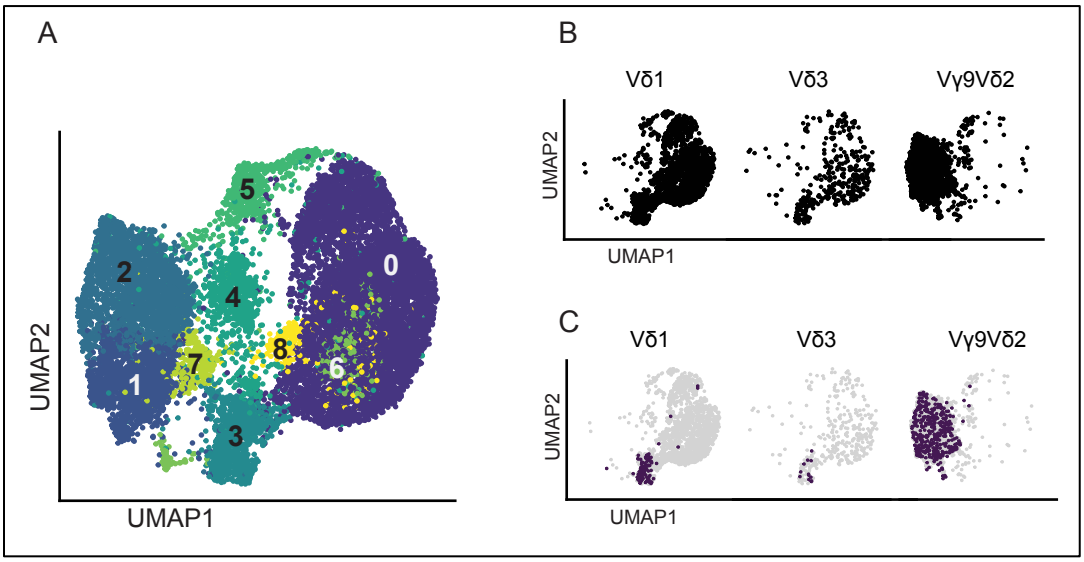

Figure 3.1. Single cell analysis of γδ T cells in BCG-vaccinated human infants reveals clonally expanded Vδ1/3 T cells expressing a cytotoxic effector phenotype. (A) UMAP displaying 14,302 γδ T cells from 10-week-old South African infants who were vaccinated with BCG at birth (n=6). Cells are clustered according to their gene expression. Each cell is color-coded according to its cluster assignment. **(B)** Cluster positions of cells expressing Vδ1+, Vδ3+, or Vγ9Vδ2 TCRs. **(C)** Cluster positions of cells expressing an expanded TCR (purple) or TCR that was only counted once per subject (grey).

We first identified TCR clonotypes that were counted only once (singlets) or at least twice (expanded) per sample donor. Overall, 8% of Vγ9Vδ2 clonotypes, 1.6% of Vδ1 clonotypes, and 1.2% of Vδ3 clonotypes were expanded (**Appendix A.II**). Expanded Vγ9Vδ2 clonotypes were distributed across multiple cell clusters, suggesting that clonal expansion was not associated with a particular transcriptional phenotype (**Figure 3.1C**). However, expanded Vδ1/3 clonotypes were strongly enriched in Cluster 3 (**Figure 3.1C).** In contrast with the majority of Vδ1/3 T cells, Cluster 3 was uniquely enriched in cells expressing low levels of naïve-like genes, high levels of cytotoxicity genes, high levels of genes associated with T cell activation (HLA-DPA1, HLA-DPB1, HLA-DRB1, and TIGIT), and high expression of TXB21, a master regulator of pro-inflammatory function in T cells (**Figure 2.1C**). These results suggest that clonally expanded Vδ1+ and Vδ3+ T cells express an activated cytotoxic effector phenotype in BCG-vaccinated infants.

Next, we applied the Clonotype Neighbor Graph Analysis (CoNGA) tool to this dataset to formally test associations between Vδ1/3 TCR sequence and gene expression programs in BCG-vaccinated infants (Schattgen et al., 2020). Briefly, Vδ1/3 T cells were first hierarchically clustered according to their gene expression. Next, Vδ1/3 TCRs were hierarchically clustered according to their paired CDR3-γ and CDR3-δ sequences, permitting the identification of Vδ1/3 clonotypes with biochemically similar TCRs. The two resulting distance matrices were visualized in two-dimensional space using UMAPs. CoNGA tests for correlations between gene expression and TCR by identifying T cell clonotypes with common ‘neighbors’ with respect to both gene expression and TCR sequence. Accordingly, if two clonotypes are adjacent in both the gene expression UMAP

and the TCR UMAP, this contributes to a higher 'CoNGA score'. Using the CoNGA tool, we identified 11 Vδ1/3 T cell clusters based on their gene expression (**Figure 3.2A**). Cluster 2 was strongly enriched in Vδ1/3 clonotypes with a high CoNGA score, indicating that Vδ1/3 T cells populating Cluster 2 were similar in terms of their TCR sequence as well as their transcriptional profiles. We next visualized the enriched genes and shared TCR sequences of the cells populating Cluster 2, revealing a group of 46 Vδ1/3 T cells expressing a Vδ1+ Vγ9+ TCR together with high levels of several genes associated with cytotoxic function (KLRB1, GZMK, NKG7, GZMA). In sum, our results provide evidence that Vδ1/3 T cells undergo clonal expansion and differentiation into a cytotoxic effector phenotype in BCG-vaccinated infants. Further, Vδ1 TCRs using a Vγ9 segment may show enhanced cytotoxic potential after neonatal BCG.

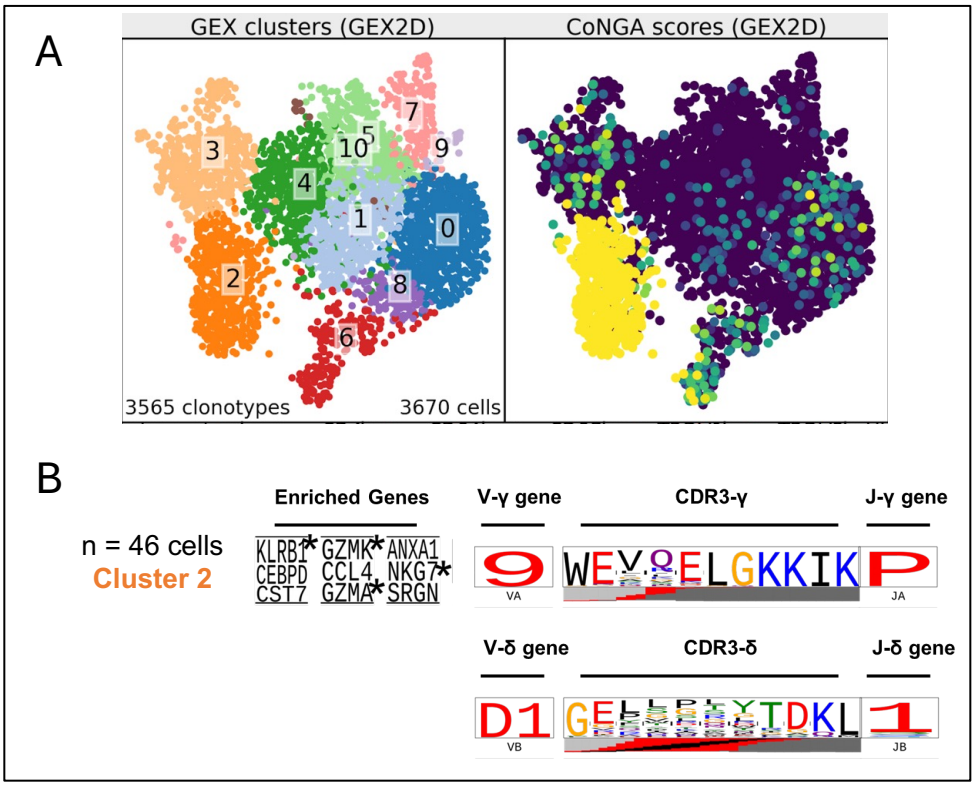

Figure 3.2. Expression of a Vγ9+ TCR is associated with increased expression of genes associated with cytotoxic function. (A) UMAP displaying 3,565 Vδ1/3 T cell clonotypes from 10-week-old South African infants who were vaccinated with BCG at birth (n=6) (left). Cell clonotypes are

clustered according to their gene expression. Each clonotype is color-coded according to its cluster assignment. UMAP displaying the CoNGA score calculated for each Vδ1/3 clonotype (right). An elevated CoNGA score (yellow) indicates a correlation between TCR sequence and gene expression. **(B)** Logo plots depict enriched genes, TCR gene usage, and CDR3 sequences of clonotypes enriched in Cluster 2. Cytotoxic genes are marked by an asterisk.

3.3 IV-BCG vaccination promotes clonal expansion of Vδ1/3 T cells

We next sought to assess to what extent the Vδ1/3 T cell response to Mtb lysate was mediated through the TCR. We used single-cell TCR sequencing to analyze γδ T cells collected from rhesus macaques (n=4) pre-vaccination and at four and eight weeks post-vaccination. (**Figure 2.2A**). We first analyzed the frequency of peripheral blood γδ T cell clonotypes pre- and post-IV-BCG and found 21 Vδ1/3-negative clonotypes and 19 Vδ1/3-negative clonotypes that were expanded at week 4 and week 8, respectively, compared to baseline (**Figure 3.3A, Appendix A.IV**). In some cases, clonotypes were absent from baseline samples but counted three or more times post-vaccination (**Figure 3.3A, 3.3B, Appendix A.IV**). In other cases, clonotypes were present at a low frequency at baseline but underwent further expansion after IV-BCG (**Figure 3.3A, 3.3B, Appendix A.IV**). On average, we identified 11 clonotypes within each IV-BCG recipient that were expanded after vaccination, together representing roughly 1% of the total Vδ1/3 clonotypes within each recipient (**Appendix A.IV).** Additionally, in all four of the animals analyzed, the proportion of the Vδ1/3 TCR repertoire represented by expanded clonotypes appeared to increase at week 4 compared to baseline (**Figure 3.3C**). Clonotypes were compartment-specific, with only 0.75% and 0.6% of clonotypes present in both PBMC and BAL at week 4 or week 8, respectively (**Appendix A.IV**). Surprisingly, none of the circulating Vδ1/3 clonotypes that were expanded compared to baseline were detectable in BAL at either timepoint (**Appendix A.IV**). Taken together, these data

suggest that IV-BCG leads to the expansion of mycobacteria-responsive Vδ1/3 T cells in which the TCR repertoire of responding T cells is distinct between the blood and lung.

We next asked whether clonotypes that expand in response to IV-BCG display distinct patterns of gene expression from clonotypes that did not expand in response to IV-BCG. We assigned each peripheral blood clonotype to one of three categories: 'Responding' clonotypes expanded at least two-fold after IV-BCG (ExpR), 'Expanded non-responding' clonotypes were counted at least three times in unvaccinated animals but did not expand at least two-fold after IV-BCG (ExpNR), and 'Unexpanded' clonotypes included any clonotype that did not fall into the previous two categories (UnExp) (**Figure 5D**). While UnExp clonotypes were predominantly located in Cluster 0 (Resting), Cluster 1 (Naïve-like), and Cluster 5 (Exhausted-like), ExpR and ExpNR clonotypes were preferentially distributed in Cluster 3 (Activated Granzyme K-high), Cluster 4 (Activated Granzyme A-high), and Cluster 7 (Cytotoxic MAMU-DRA-high) (**Figure 5E**). Additionally, ExpR clonotypes were enriched in Cluster 4, while ExpNR clonotypes were enriched in Cluster 7. (**Figure 5E**). Genes that were preferentially enriched among ExpR clonotypes compared to ExpNR clonotypes included *GZMB*, *GZMA*, and *FGFBP2*, characteristic of cytotoxic lymphocytes (**Figure 5F**). Taken together, these data suggest that Vδ1/3 T cells that undergo clonal expansion after IV-BCG preferentially express genes associated with cytotoxic function.

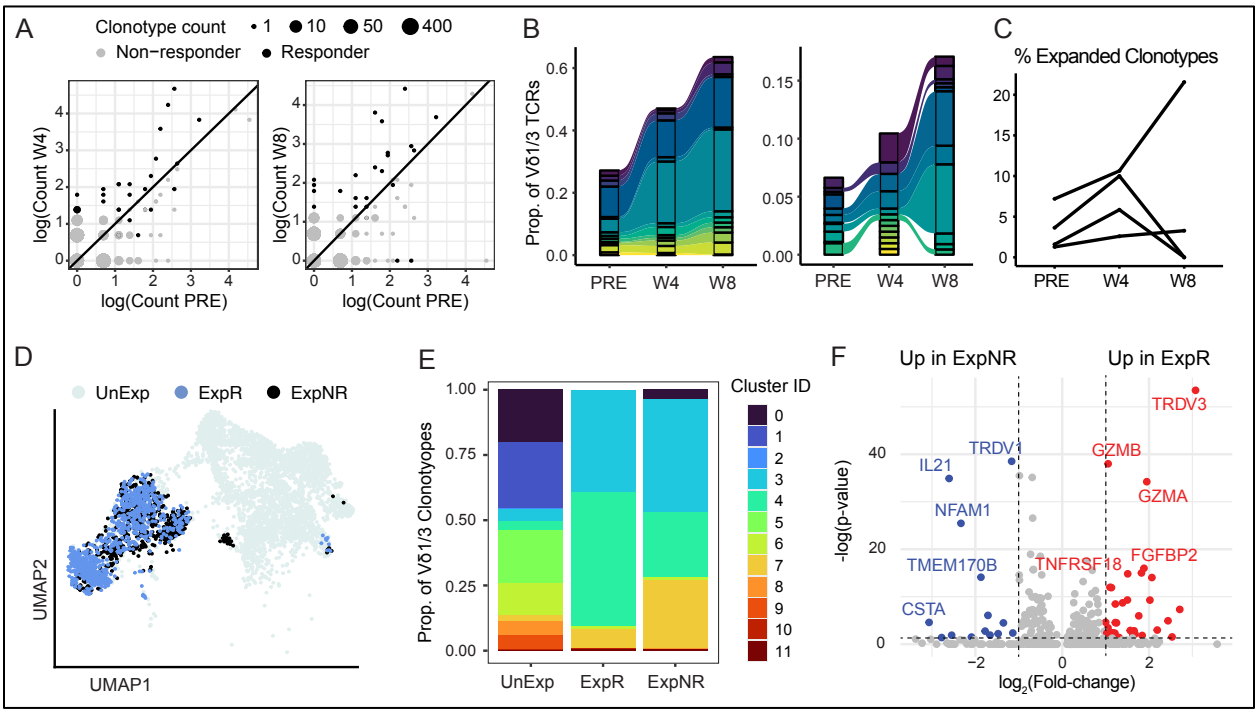

Figure 3.3. Vδ1/3 T cell responses to IV-BCG are mediated through the TCR. Analysis of the Vδ1/3 TCR repertoire IV-BCG vaccinated rhesus macaques (n=4) and the effect of TCR inhibition on Vδ1/3 effector functions (n=3-6). **(A)** Count of unique Vδ1/3 clonotypes in pre-vaccination (Pre) vs. week 4 (W4) and pre-vaccination (Pre) vs. week 8 (W8) PBMC. The size of each dot is proportional to the number of clonotypes plotted at each point. Clonotypes that are expanded at least two-fold compared to pre-vaccination are depicted in black. Count values were natural-log-transformed after adding one. **(B)** Proportion of the Vδ1/3 TCR repertoire occupied by the top 10 clonotypes at each time point in PBMC. Each clonotype is represented by a colored bar. Dynamics are shown in two representative subjects. Clonotype colors are not consistent between the two plots. **(C)** Frequency of expanded (non-singlet) clonotypes within the Vδ1/3 TCR repertoire at each time point in PBMC. Each sample donor (n=4) is shown in a separate line. **(D)** UMAP displaying the cluster position of clonotypes that are unexpanded (UnExp), clonotypes that expand at least two-fold post-vaccination ('Responding', ExpR), and clonotypes that are expanded pre-vaccination but do not further expand after IV-BCG ('Expanded non-responding', ExpNR). **(E)** Bar plot displaying the cluster distribution of cells in the UnExp, ExpR, and ExpNR categories. **(F)** Volcano plot depicting genes that are upregulated (red) or downregulated (blue) in ExpR clonotypes compared to ExpNR clonotypes. **(G)** Background-subtracted frequency of Vδ1/3 T cells expressing CD137 (left) or IFN-γ (right) after stimulation with Mtb whole cell lysate. Frequencies are shown pre-vaccination (Pre) and at week 2 (W2), week 4 (W4), and week 8 (W8) post IV-BCG. Cells were either left untreated or were treated with the TCR inhibitor cyclosporin A (CsA) prior to stimulation. Each sample donor is shown in a separate line. Median frequencies are shown in black.

3.4 Vγ9-negative T cell responses to mycobacteria are mediated through the TCR

Given this evidence of in vivo clonal expansion in response to IV-BCG vaccination, we next examined whether Vδ1/3 T cells respond to mycobacteria in a TCR-dependent manner. PBMCs collected from IV-BCG vaccinated rhesus macaques pre-vaccination and at week 2, week 4, and week 8 post-vaccination were stimulated with Mtb lysate in the presence or absence of cyclosporin A, an inhibitor of TCR signaling (Thomson & Webster, 1988). We confirmed that cyclosporin A does not reduce the viability of Vδ1 T cells after short-term stimulation (**Appendix B.VIII.A**). Consistent with our prior results, cells obtained post-vaccination were more responsive to Mtb lysate than cells obtained pre-vaccination (**Figure 2.6 and Figure 3.4A**). Treatment with cyclosporin A reduced both CD137 and IFN-γ expression in response to stimulation with Mtb lysate by approximately 90% at all post-vaccination timepoints (**Figure 3.4A**). In Vδ1/3 T cells stimulated with a cocktail of IL-12, IL-15, and IL-18, treatment with cyclosporin A reduced CD137 expression by approximately 50% but did not reduce IFN-γ expression (**Appendix B.VIII.B**). Therefore, the ablation of Vδ1/3 T cell responses to Mtb lysate in the presence of cyclosporin A cannot be explained by inhibited bystander responses to inflammatory cytokines. Notably, Vδ1/3 T cells were not more responsive to stimulation with PHA over time, suggesting that the increased responsiveness to Mtb lysate after IV-BCG is dependent on the presence of mycobacterial antigens (**Figure 3.4B**). In sum, our results suggest that IV-BCG leads to TCR-dependent activation and clonal expansion of mycobacteria-reactive Vδ1/3 T cells in the blood.

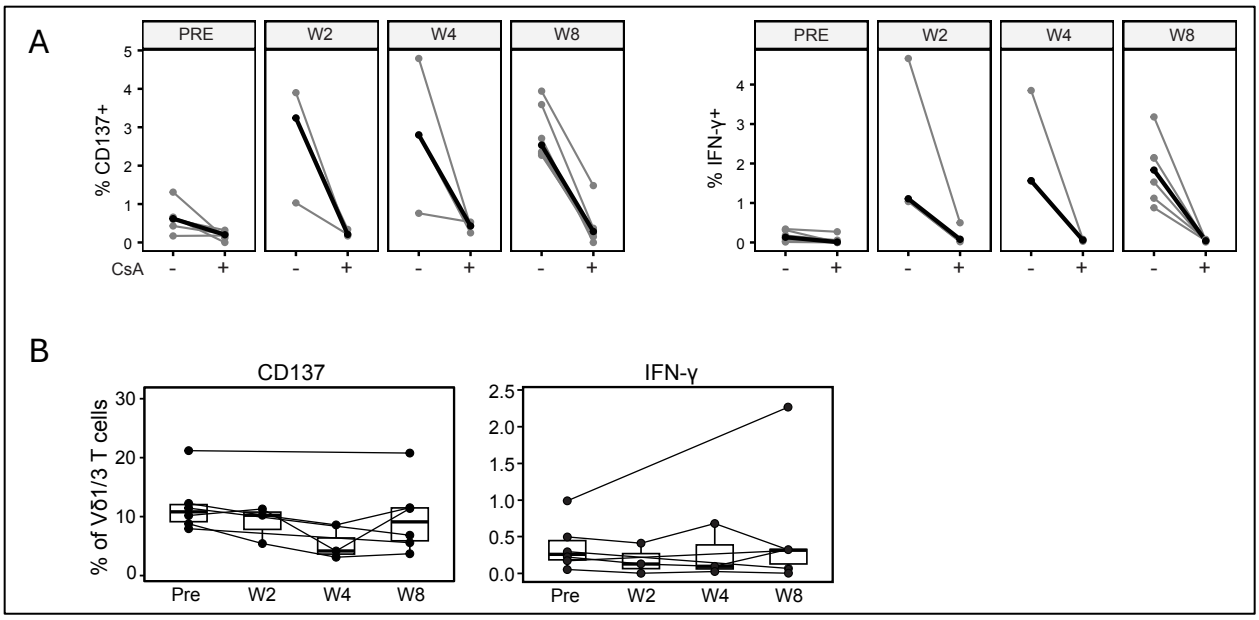

Figure 3.4. Vδ1/3 T cell responses to mycobacteria are mediated through the TCR. (A) Background-subtracted frequency of Vδ1/3 T cells expressing CD137 (left) or IFN-γ (right) after stimulation with Mtb whole cell lysate. Frequencies are shown pre-vaccination (Pre) and at week 2 (W2), week 4 (W4), and week 8 (W8) post IV-BCG. Cells were either left untreated or were treated with the TCR inhibitor cyclosporin A (CsA) prior to stimulation. Each sample donor is shown in a separate line. Median frequencies are shown in black. (**B)** Background-subtracted frequency of Vδ1/3 T cells expressing CD137 or IFN-γ in response to stimulation with PHA. Frequencies are shown pre-vaccination (Pre) and at week 2 (W2), week 4 (W4), and week 8 (W8) post IV-BCG in PBMC. Matched samples are indicated by a black line. Boxplots indicate median and interquartile range.

3.5 Conclusion

In sum, we report evidence of clonal expansion of Vδ1/3 T cells in both BCG-vaccinated human infants and in IV-BCG-vaccinated rhesus macaques. In both species, clonally expanded Vδ1/3 T cells expressed elevated levels of genes associated with cytotoxic effector function. In rhesus macaques, we demonstrate that production of IFN-γ by Vδ1/3 T cells after IV-BCG is almost entirely dependent on signaling through the TCR. Additionally, we show that Vδ1/3 T cells are not more responsive to non-specific TCR stimulation after IV-BCG, suggesting that the TCR-dependent

effector functions of Vδ1/3 T cells are specifically promoted by exposure to mycobacterial antigens. Notably, in Chapter 2 we showed that the production of IFN-γ by Vδ1/3 T cells correlates with protection against Mtb challenge. Therefore, our results support a role for an adaptive, pro-inflammatory Vδ1/3 T cell response in BCG-mediated protection.

CHAPTER 4: MATERIALS AND METHODS

4.1 Clinical Cohorts and Sample Collection

The BCG-vaccinated infant cohort has been previously described (**Appendix D.I**) (Soares et al., 2008). Briefly, HIV-uninfected infants in the Cape Town region of South Africa received routine intradermal vaccination with BCG (Statens Serum Institut, Copenhagen) at birth. Sodium heparinized blood was collected from each infant ten weeks after BCG vaccination. PBMC were isolated from whole blood using Ficoll-Paque PLUS gradient separation (GE Healthcare Biosciences) and cryopreserved in FBS containing 10% DMSO in liquid nitrogen until use.

Cord blood samples were collected from HIV-uninfected mothers enrolled in a previously published study conducted in the Cape Town region of South Africa (**Appendix D.I**) (Shey et al., 2014). Pregnant mothers with TB disease or exposure or who were undergoing treatment for any other disease were excluded from the study. Sodium heparinized cord blood samples were collected immediately after birth by Caesarian section. Samples were treated for 10 minutes with 2mM EDTA (Sigma Aldrich), washed, and treated again for 10 minutes with 2mM EDTA. Red blood cells were then lysed using red blood cell lysis buffer before washing and cryopreserving in fetal calf serum containing 10% DMSO in liquid nitrogen until use.

Details regarding the non-human primate cohorts have been previously published (**Appendix D.II**) (Darrah et al., 2023; Simonson et al., 2024). Briefly, Indian-origin rhesus macaques (*Macaca mulatta*) aged 3-5 years were vaccinated with $5x10^7$ colony forming units (CFU) of BCG Danish

Strain 1331 (Statens Serum Institut, Copenhagen, Denmark) into the saphenous vein. 6 months after vaccination, macaques were challenged intrabronchially with Mtb Erdman strain. All granulomas and other lung pathologies, all thoracic LNs, and peripheral LNs were collected for quantification of Mtb bacterial burden. CFUs were enumerated and summed to calculate the total thoracic bacterial burden for each macaque. Peripheral blood mononuclear cells (PBMCs) were isolated using Ficoll-Paque PLUS gradient separation (GE Healthcare Biosciences) as we have previously described (Simonson et al., 2024). Bronchoalveolar lavage (BAL) wash fluid (3 × 20 mL washes of PBS) was centrifuged and cells were combined before counting. Samples were cryopreserved in fetal bovine serum containing 10% dimethyl sulfoxide (DMSO) in liquid nitrogen until use.

4.2 Single-cell RNA sequencing

4.2.1 Sample preparation

Non-human primate samples:

PBMC and BAL samples were thawed in RPMI medium (Thermo Fisher Scientific) plus 10% fetal bovine serum (Atlas Biologicals) and cell counts and sample viabilities were measured using a hemocytometer. Three million viable cells from each sample were plated in a 96-well plate. The cells were then washed with PBS and stained using a LIVE/DEAD™ Fixable Green Dead Cell Stain Kit (Invitrogen) for 15 minutes at room temperature. Next, the cells were blocked using Fc Block (eBioscience) for 15 minutes at 4°C. Cells were then stained with an antibody cocktail containing fluorescent-tagged antibodies for cell sorting, hashtags to allow sample multiplexing, and

oligonucleotide-tagged antibodies for CITE-seq analysis (**Appendix A.V**). Cells were stained in the antibody cocktail for 30 minutes at 4°C. Next, live Vγ9+ γδ T cells (Live, CD3+, TCR γδ+, TCR Vγ9+) and live Vγ9-negative γδ T cells (Live, CD3+, TCR γδ+, TCR Vγ9-negative) were sorted using a FACSAria cell sorter (BD Biosciences). After sorting, cells were counted using a hemocytometer and up to 33,000 cells were loaded per well in a Chromium Chip G (10x Genomics).

Human infant samples:

PBMC samples were thawed in complete RPMI medium and cell counts and sample viabilities were measured using a hemocytometer. Three million viable cells from each sample were plated in a 96-well plate. The cells were then washed with PBS and stained using a LIVE/DEAD™ Fixable Green Dead Cell Stain Kit (Invitrogen) for 15 minutes at room temperature. Next, the cells were blocked using Fc Block (eBioscience) for 15 minutes at 4°C. Cells were then stained with an antibody cocktail containing fluorescent-tagged antibodies for cell sorting. Cells were stained in the antibody cocktail for 30 minutes at 4°C. Next, live γδ T cells (Live, CD3+, TCR γδ+) were sorted using a FACSAria cell sorter (BD Biosciences). After sorting, cells were counted using a hemocytometer and up to 33,000 cells were loaded per well in a Chromium Chip K (10x Genomics).

4.2.2 Developing a method for high-throughput γδ TCR sequencing

Reagents to generate γδ TCR libraries are not commercially available from 10x Genomics, so a protocol using custom reagents is required. Briefly, the steps to generate a TCR library using the 10x Genomics platform include single-cell partitioning and barcoding, reverse transcription and

cleanup, cDNA amplification, target enrichment, and library construction. The custom primers are used during Step 4: Target Enrichment to amplify TCR-γ- and TCR-δ-encoding transcripts within bulk cDNA and to add adaptor sequences that are required in the following library construction steps. Using custom primers (**Appendix A.VI**), we adapted the 10x TCR library synthesis protocol to enrich human and rhesus macaque γδ TCR transcripts from total cDNA and prepare them for library construction (Mimitou et al., 2019).

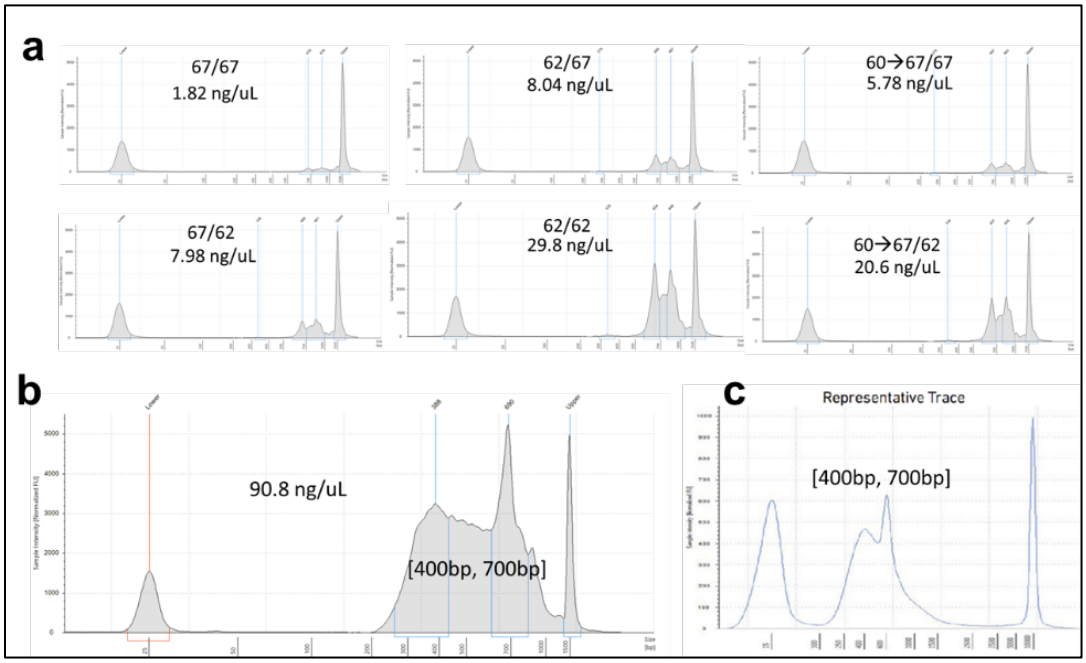

Figure 4.1. Synthesis of γδ TCR libraries. (A) TapeStation traces showing band size and intensity within the Target Enrichment product. The annealing temperature was set at either 62°C, 67°C, or a ramp-up from 60°C to 67°C for the first nested PCR and at either 62°C or 67°C for the second nested PCR, for a total of six combinations. The annealing temperatures and DNA concentration are shown on each trace. **(B)** TapeStation trace for the final product of γδ TCR library synthesis, with DNA concentration and approximate sizes of the two major bands shown on the plot. **(C)** Representative Bioanalyzer trace from the 10x Genomics manual showing the expected band sizes for an αβ TCR library product.

Barcoded cDNA was generated from γδ T cells according to the Chromium Next GEM Single Cell V(D)J v1.1 user manual with minor adjustments. Different annealing temperatures for each

nested PCR were tested to determine the optimal conditions required for the custom γδ TCR primers **(Figure 4.1A)**. We considered the optimal conditions for the nested PCR to be the annealing temperatures at which we observed two strong peaks between 600-900 base pairs, the expected size for enriched TCR templates according to the 10x Genomics manual, together with minimal off-target amplification. According to these criteria, we determined the optimal annealing temperatures for each nested PCR to be 62°C. The resulting target enrichment product was carried through Step 5, Library Construction, with no alterations to the published 10x Genomics protocol. When analyzed using a TapeStation electrophoresis system (Agilent), the final γδ TCR library product showed a high DNA concentration and strong bands at the expected size **(Figure 4.1B and 4.1C)**. The resulting library was sequenced to a depth of approximately 50,000 reads per cell using the NextSeq 2000 system (Illumina). We next validated the quality and accuracy of the targeted γδ TCR sequences. Of the cell barcodes that passed our gene expression QC steps (n= 17,267), 93% were assigned a TCR sequence, showing that cells which produced high-quality gene expression data also yielded a TCR sequence. Additionally, TRDV2 genes were paired almost exclusively with TRGV9 genes, in agreement with prior analysis of human γδ T cells. The same optimization and validation method was used to generate γδ TCR libraries from NHP samples **(data not shown).**

4.2.3 Library preparation

Non-human primate samples:

The Chromium Next GEM Single Cell 5' Reagent kit (v2, 10x Genomics) was used to prepare mRNA, TCR, and surface protein libraries. γδ TCR libraries were prepared using custom primers

(**Appendix A.VI**). cDNA amplification and target enrichment were quantified using a Qubit 3 Fluorometer (Invitrogen) and assessed for quality using a 4200 TapeStation System (Agilent). Libraries were constructed and sequenced to a depth of approximately 40,000 reads per cell using the NextSeq 500/550 system (Illumina).

Human infant samples:

The Chromium Next GEM Single Cell V(D)J Reagent kit (v1.1, 10x Genomics) was used to prepare mRNA, TCR, and surface protein libraries. γδ TCR libraries were prepared using custom primers (**Appendix A.VI**). cDNA amplification and target enrichment were quantified using a Qubit 3 Fluorometer (Invitrogen) and assessed for quality using a 4200 TapeStation System (Agilent). Libraries were constructed and sequenced to a depth of approximately 50,000 reads per cell using the NextSeq 2000 system (Illumina).

4.2.4 Data preprocessing

Non-human primate samples:

The Cell Ranger Multi pipeline (10x Genomics) was used to conduct alignment and feature expression quantification of the single-cell sequencing data and to generate custom *Macaca mulatta* references. We generated a custom reference transcriptome using Ensembl genome assembly Mmul_10 (GCA_003339765.3). We included protein coding, lncRNA, antisense, immunoglobulin, T-cell receptor, and mitochondrial genes. Additionally, we created a custom V(D)J reference using the Rhesus macaque reference sequences from IMGT (Lefranc, 2014). Constant regions that were not in IMGT were included from the reference Mmul_10

transcriptome. Hashtag oligo (HTO) and antibody-derived tag (ADT) reads were aligned to a feature reference containing the relevant barcode sequences.

Quality control and analysis of the single-cell mRNA and surface protein expression data were performed using the R package Seurat (Hao et al., 2021). First, we excluded HTOs that did not appear in at least 50 cells as well as cells with fewer than three HTO counts. Next, we excluded cells with fewer than 200 feature counts, greater than 4000 feature counts, fewer than 500 RNA counts, greater than 15,000 RNA counts, or greater than 10% mitochondrial reads. Next, HTO data were normalized using a centered log-ratio transformation and samples were demultiplexed based on HTO enrichment using the MULTIseqDemux function, which demultiplexes samples based on the classification method from MULTI-seq (McGinnis et al., 2019). We then removed cell barcodes that could not be assigned to a single HTO.

Next, the ADT counts were normalized using a centered log-ratio transformation and visualized using the RidgePlot function. Antibodies with counts that did not exceed the expression level of respective mouse IgG isotype controls were excluded. Next, for each cell barcode, the mRNA count data were log-normalized. For each sample donor, cells were then clustered according to their gene expression. Non-T-cell clusters were then excluded based on low *CD3E* RNA expression combined with high RNA expression of *MS4A1* or *CD14* and high ADT expression of CD20 or CD14.

Finally, we quality checked our TCR libraries. We first excluded TCR sequences from any cell barcodes that were excluded based on the criteria above. Next, we excluded any TCR sequences

that failed to meet the following criteria: 1. The arrangement is productive, 2. The TCR is amplified from at least three templates corresponding to three unique molecular identifiers, and 3. The TCR includes at least 20 reads. We next used the scRepertoire package to identify the single most highly expressed TCR clonotype for every cell barcode (Borcherding et al., 2020). Cell barcodes expressing at least one quality-checked γδ TCR chain were annotated as γδ T cells. γδ T cells were further stratified into Vδ1, Vδ3, Vγ9^{neg}Vδ2, and Vγ9+Vδ2 subsets according to their TCR expression.

Human infant samples:

The Cell Ranger Multi pipeline (10x Genomics) was used to conduct alignment and feature expression quantification of the single-cell sequencing data. We used data analysis services provided by Azenta Life Sciences (Burlington, MA) to align mRNA reads to the GRCh38 human reference genome and V(D)J reads to a custom reference using the human γδ TCR reference sequences from IMGT (Lefranc, 2014).

Quality control and analysis of the single-cell mRNA expression data were performed using the R package Seurat (Hao et al., 2021). We first excluded cell barcodes with fewer than 200 feature counts, greater than 3500 feature counts, fewer than 500 RNA counts, greater than 15,000 RNA counts, or greater than 10% mitochondrial reads. Next, for each cell barcode, the mRNA count data were log-normalized. We then clustered all cell barcodes according to their gene expression using a principal component analysis reduction including the first 10 principal components. The Seurat FindAllMarkers function was used to identify differentially expressed genes across cell

clusters. One cell cluster was excluded due to low expression of *CD3E* and high expression of *MS4A1*.

We then quality checked our TCR libraries. We first excluded TCR sequences from any cell barcodes that were excluded based on the criteria above. We next used the scRepertoire package to identify the single most highly expressed TCR clonotype for every cell barcode (Borcherding et al., 2020). Finally, γδ T cells were stratified into Vδ1, Vδ3, Vγ9^{neg}Vδ2, and Vγ9+Vδ2 subsets according to their TCR expression.

4.2.5 Data Analysis

Non-human primate samples

We applied the Seurat Integration procedure to combine the cell barcodes from all four sample donors and used differential gene expression analysis to verify that sample integration did not weaken the major biological axes of variation, such as tissue or origin and sample timepoint (Hao et al., 2021). Next, we clustered the integrated data based on gene expression using a principal component analysis reduction including the first 12 principal components. The Seurat FindAllMarkers function was used to identify differentially expressed genes across cell clusters, sample tissues, and timepoints. Cell clusters were annotated according to differential expression of key T cell related genes and ADTs.

Next, we analyzed our TCR libraries to define γδ T cell clonotypes that were expanded in response to vaccination. Expanded clonotypes were defined as clonotypes that were counted at least three

times at week 4 or week 8 and were expanded at least two-fold relative to pre-vaccination. Additionally, clonotypes that were absent pre-vaccination but were counted at least three times post-vaccination were considered expanded. We also identified clonotypes that were counted at least twice in pre-vaccination samples but did not expand at least two-fold after vaccination. Finally, unexpanded clonotypes included any clonotype that did not align with either of these criteria. The scRepertoire function compareClonotypes was used to visualize changes in frequency among the most highly expressed TCR-δ clonotypes at each timepoint. Plots were generated using the ggplot2 R package (Wickham, 2016).

Human infant samples:

After excluding one cell cluster with low *CD3E* expression and high *MS4A1* expression consistent with B cells, we re-clustered the remaining cells according to their mRNA expression. Cell clusters were defined after principal component analysis reduction using the first 10 principal components. The FindAllMarkers function was used to distinguish genes that were differentially expressed across the resulting cell clusters. Relative expression of key T cell related genes was used to determine cell cluster identities. Plots were generated using the ggplot2 R package (Wickham, 2016).

4.3 Cell processing and stimulation

Cryopreserved PBMC were thawed in sterile-filtered RPMI 1640 (Thermo Fisher Scientific) with 10% FBS (Hyclone) and 0.2% Benzonase (MilliporeSigma) and then centrifuged at 500 relative centrifugal force for 5 minutes at room temperature. Cells were washed using PBS and

centrifuged at 500 RCF for an additional 5 minutes at room temperature and were then rested for two hours at a density of 1-4 million cells/mL. Viable cells were counted using the Guava easyCyte (MilliporeSigma) with guavaSoft 2.6 software. After resting, up to 3 million cells were plated in a 96-well plate. Next, cells were stimulated with 100 ug/mL *Mycobacterium tuberculosis* whole-cell lysate (strain H37Rv, BEI Resources). After 12 hours of stimulation, cells were treated with 1.4 ug/mL GolgiStop (BD Biosciences) and 10 ug/mL Brefeldin A (Sigma Aldrich) and stained with anti-CD107a antibody (**Appendix B.IV**) for the remaining 6 hours.

For TCR inhibition assays, cells were thawed, counted, and plated as described above. Cells were then treated with 1.6 ug/mL Cyclosporin A for one hour prior to stimulation. Next, cells were treated with 5 ug/mL Phytohemagglutinin (Sigma Aldrich), or *Mycobacterium tuberculosis* whole-cell lysate (strain H37Rv, BEI Resources). After 12 hours of stimulation, cells were treated with 1.4 ug/mL GolgiStop (BD Biosciences) and 10 ug/mL Brefeldin A (Sigma Aldrich) and stained with anti-CD107a antibody (**Appendix B.IV**) for the remaining 6 hours.

4.4 Mass cytometry

Metal-labelled antibodies were either obtained from Standard BioTools or were conjugated in-house by labelling purified antibodies using the Maxpar Antibody Labelling kit (Standard BioTools). Immediately following stimulation, cells were washed twice with PBS before viability staining with Cisplatin for 5 minutes at room temperature. Cells were then washed twice in FACS buffer before staining with MR1-5-OPRU-APC tetramer (NIH Tetramer Core Facility) for 60 minutes at room temperature. Next, cells were washed three times with cell staining buffer

(Standard BioTools) before staining with a surface antibody cocktail for 30 minutes at room temperature (**Appendix C.II).** Cells were then treated with Fix 1 Buffer (Standard BioTools) for 20 minutes at room temperature. Next, cells were washed three times with Perm-S buffer before staining with an intracellular antibody cocktail for 30 minutes at room temperature (**Appendix C.II**). Stained cells were then washed three times in Perm-S buffer and fixed using a 1% paraformaldehyde solution for 15 minutes at 4°C. Cells were held in a DNA-intercalator stain at 4°C for up to 7 days until sample acquisition. Immediately before acquisition, cells were washed three times with UltraPure water (ThermoFisher) and were resuspended in UltraPure water with 1:5 EQ calibration beads (Standard BioTools). Cells were then filtered into cell strainer cap tubes (Fisher Scientific). Data were acquired on a Helios (Fluidigm) at up to 500 cells per second. The resulting FCS files were normalized using EQ™ Four Element Calibration Beads (Fluidigm), as previously described (Finck et al., 2013). Data were analyzed using FlowJo v10 software (Tree Star).

4.5 Flow cytometry

Immediately following stimulation, cells were washed twice with PBS and then stained with Zombie Yellow fixable viability dye (Biolegend) for 15 minutes at room temperature. Samples were then washed twice using FACS buffer and incubated in Fc Block according to the manufacturer's instructions (eBiosciences). Next, samples were washed once with FACS buffer and stained with a cell surface antibody cocktail for 30 minutes at 4°C (**Appendix B.IV**). After the incubation period, samples were washed twice with FACS buffer and fixed using CytoFix Fixation buffer (BD Biosciences) according to the manufacturer's instructions. Next, samples were washed

twice with Perm/Wash buffer (BD Biosciences) and stained with an intracellular antibody cocktail for 30 minutes at 4°C (**Appendix B.IV**). Finally, cells were washed twice with PBS, fixed in a 1% paraformaldehyde solution, and held in 2mM EDTA at 4C for up to 36 hours prior to sample acquisition. Cells were acquired on a BD LSRFortessa (BD Biosciences, San Jose, CA) equipped with a high-throughput sampler and configured with blue (488 nm), green (532 nm), red (628 nm), violet (405 nm), and ultraviolet (355 nm) lasers using standardized good clinical laboratory practice procedures to minimize variability of data generated. For all flow cytometry experiments, study groups were evenly distributed to avoid batch effects and operators were not blinded to study group assignments. Data were analyzed using FlowJo v10 software (Tree Star).

CHAPTER 5: CONCLUSIONS AND FUTURE DIRECTIONS

5.1 Summary

Identifying mechanistic immune correlates of protection against Mtb has been a long-standing goal for the field (Nemes et al., 2022). While the importance of T cell immunity has been broadly established, several questions remain, including the specific antigens targeted by protective T cells as well as their functions. We focused on understanding how γδ T cells might be important for protection by studying their phenotypes and functions among infants and macaques and examining whether there were consistent findings across species. Our results advance the field in at least three respects. First, we report that IV-BCG increases the frequency of cytotoxic Vδ1/3 T cells in both the blood and the lung of macaques. Second, we show that that BCG promotes pro-inflammatory responses to mycobacterial antigens in both human infant and macaque Vδ1/3 T cells, which correlate with protection against Mtb. In macaques, these enhanced pro-inflammatory functions are almost entirely driven by signaling through the TCR. Third, Mtb-reactive Vδ1/3 T cells are clonally expanded in the airway by week 8 after IV-BCG, reflecting either expansion of tissue-resident cells or trafficking of circulating Vδ1/3 T cells to the lung. Our findings suggest that Vδ1/3 T cells may contribute to Mtb control and define the T cell effector functions that may mediate protection.

5.2 Implications for γδ T cell biology

A strength of our study is demonstrating how the Vδ1/3 TCR repertoire is modulated by BCG vaccination. We report evidence of clonally expanded Vδ1/3 T cells in BCG-vaccinated infants and

non-human primates which express genes associated with TCR activation and cytotoxic activity. These changes in transcription were validated through functional analyses. Treatment with cyclosporin A virtually eliminated Vδ1/3 T cell effector function after Mtb lysate stimulation, suggesting activation through the TCR is required. Clonal expansion of Vδ1/3 T cells has been observed in diverse human disease settings, including Merkel cell carcinoma tumors, colorectal tumors, CMV infection, and febrile malaria, consistent with an adaptive-like immune role (Davey et al., 2017; Gherardin et al., 2021; Reis et al., 2022; von Borstel et al., 2021). Notably, the Vδ1/3 TCR ligands identified thus far include several human proteins that are regulated by cellular stress, such as CD1b, CD1c, MR1, MHC class I chain-related proteins A and B, endothelial protein C receptor, and annexin A2 (Chancellor et al., 2022; Groh et al., 1999; Le Nours et al., 2019; Marlin et al., 2017; D. Morita et al., 2013; Rice et al., 2021; Willcox et al., 2012). While the specific ligands promoting the TCR-dependent Vδ1/3 T cell response to BCG vaccination remain to be defined, we speculate that stress-regulated, endogenous human proteins are a likely target. It is also probable that Vδ1/3+ T cells are recognizing mycobacterial lipid antigens complexed with CD1 molecules (Reijneveld et al., 2020; S. Roy et al., 2016).

Our results contrast with a recent report describing circulating Vδ1 T cells expanded in persistent Mtb infection that are refractory to TCR stimulation yet exert cytotoxic activity through CD16 (Chowdhury et al., 2023). Chowdhury et al hypothesize that innate-like Vδ1 T cells may be a feature of chronic inflammation, while our study has characterized Vδ1/3 T cells in a setting of acute infection, potentially explaining the differential role of TCR-dependent effector functions in these two contexts. Our results are consistent with other studies describing circulating Vδ1/3 T

cells as a largely adaptive immune subset that follow a naïve to effector differentiation pathway mirroring that of conventional CD8 T cells (McMurray et al., 2022). Therefore, the role of innate-like vs. adaptive-like effector functions of Vδ1/3 T cells may be context-dependent.

There are several limitations to our study. First, we were unable to analyze BAL samples collected at week 2 after vaccination, potentially precluding us from studying γδ T cells at the timepoint of peak responsiveness in the airway (Darrah et al., 2020). Additionally, our analysis only includes samples collected until eight weeks after vaccination, so we were unable to study the durability of Vδ1/3 T cell responses to IV-BCG. We have previously shown that circulating Vδ2 clonotypes are expanded up to one year after BCG vaccination in humans (James et al., 2022). Additionally, prior analysis of Vδ1 T cell clonotypes that are expanded after CMV infection have demonstrated that these clonotypes persist in circulation for at least 18 months, but whether similar durability is observed after mycobacterial infection is unknown (Davey et al., 2017). Future studies may seek to elucidate whether the long-term durability of the Vδ1/3 T cell immune response is comparable to that of conventional T cells, which has implications for vaccination strategies targeting Vδ1/3 T cells.

Since BCG is routinely delivered at birth to infants in TB endemic areas, our experiments lacked a control group of unvaccinated ten-week-old South African infants. However, the concordant findings of clonal expansion and cytotoxic effector functions in Vδ1/3 T cells across species suggest that at least some of the effects we observed among infants were due to BCG. Additionally, expression of IFN-γ and granzyme B in response to Mtb lysate was elevated in Vδ1/3

T cells derived from infants compared to cord blood, suggesting that such responses are induced after birth, rather than innately programmed. Nonetheless, an aim of future experiments may be to determine whether BCG is directly associated with the population of clonally expanded cytotoxic Vδ1/3 T cells we observed in BCG-vaccinated infants.

5.3 Implications for design of tuberculosis vaccines

Our findings have direct implications for the design of new vaccines for TB which are largely focused on boosting CD4 T cell responses to mycobacterial protein antigens (Lai et al., 2023). γδ T cells are not directly targeted by these products but may be activated indirectly by adjuvants or signals from other immune cells (Rezende et al., 2018). The demonstration that boosting Vγ9Vδ2 T cell responses via a modified Listeria vaccine protects against TB in macaques provides proof-of-concept for products focused on this T cell subset (L. Shen et al., 2019). Vδ1/3 T cells are not activated by the phosphoantigens that stimulate Vγ9Vδ2 T cells, but our data suggest they may also be important to mediating protection. Whole cell mycobacterial vaccines currently in Phase 3 clinical trials, such as VPM001 and MTBVAC, may be able to engage Vδ1/3 T cells through both TCR-dependent and TCR-independent mechanisms (Joosten et al., 2019).

Although the protective role of IFN-γ, TNF, and IL-2 produced by CD4 T cells has been well-established, the contribution of cytotoxic immune cells such as CD8 T cells, NK cells, MAIT cells, and γδ T cells is less understood (Ruibal et al., 2021). Our results align with recent evidence that cytotoxic T cells may have a previously unappreciated role in TB immunity. In a dose-ranging study of IV-BCG, NK cells, Vγ9+ T cells, MAIT cells, and CD8 T cells were among the immune subsets

correlated with protection against Mtb challenge after IV-BCG (Darrah et al., 2023). Additionally, GZMB^{high} CD4 T cells in the lungs and a blood transcriptional module enriched in NK cell pathways were associated with protection against Mtb after IV-BCG (Liu et al., 2023; Peters et al., 2023). Granzyme K was found to be enriched in innate-like immune populations compared to conventional T cells and decreased after TCR stimulation, consistent with a role in pre-programmed antimicrobial responses (Duquette et al., 2023). By contrast, granzyme A binds directly to Mtb bacilli to promote phagocytosis independent of its enzymatic activity (Rasi et al., 2023). Consistent with this, we show that expression of granzyme A, B, and K transcripts and expression of granzyme B and K proteins were increased in Vδ1/3 T cells following IV-BCG. Additionally, we noted that IV-BCG led to the expansion of two distinct populations of cytotoxic Vδ1/3 T cells, one expressing high levels of granzyme K and granzyme M, and the other expressing high granzyme A. Induction of cytotoxic effector functions is not typically a criterion for evaluating the immunogenicity of candidate vaccines, but our data add to an emerging body of literature suggesting that this could be a key feature of a protective immune response to TB.

REFERENCES

Adams, E. J., Chien, Y.-H., & Garcia, K. C. (2005). Structure of a gammadelta T cell receptor in complex with the nonclassical MHC T22. *Science (New York, N.Y.)*, *308*(5719), 227–231. https://doi.org/10.1126/science.1106885

Adams, E. J., Strop, P., Shin, S., Chien, Y.-H., & Garcia, K. C. (2008). An autonomous CDR3delta is sufficient for recognition of the nonclassical MHC class I molecules T10 and T22 by gammadelta T cells. *Nature Immunology*, *9*(7), 777–784. https://doi.org/10.1038/ni.1620

Alcaïs, A., Fieschi, C., Abel, L., & Casanova, J.-L. (2005). Tuberculosis in children and adults. *The Journal of Experimental Medicine*, *202*(12), 1617–1621. https://doi.org/10.1084/jem.20052302

Bagchi, S., Genardi, S., & Wang, C.-R. (2018). Linking CD1-Restricted T Cells With Autoimmunity and Dyslipidemia: Lipid Levels Matter. *Frontiers in Immunology*, *9*. https://www.frontiersin.org/articles/10.3389/fimmu.2018.01616

Barclay, W. R., Anacker, R. L., Brehmer, W., Leif, W., & Ribi, E. (1970). Aerosol-Induced Tuberculosis in Subhuman Primates and the Course of the Disease After Intravenous BCG Vaccination. *Infection and Immunity*, *2*(5), 574–582. https://doi.org/10.1128/iai.2.5.574-582.1970

BCG vaccines: WHO position paper – February 2018. (2018). *Releve Epidemiologique Hebdomadaire*, *93*(8), 73–96.

Beckman, E. M., Porcelli, S. A., Morita, C. T., Behar, S. M., Furlong, S. T., & Brenner, M. B. (1994). Recognition of a lipid antigen by CD1-restricted alpha beta+ T cells. *Nature*, *372*(6507), 691–694. https://doi.org/10.1038/372691a0

Bhatt, K., Verma, S., Ellner, J. J., & Salgame, P. (2015). Quest for Correlates of Protection against Tuberculosis. *Clinical and Vaccine Immunology*, *22*(3), 258–266. https://doi.org/10.1128/CVI.00721-14

Borcherding, N., Bormann, N. L., & Kraus, G. (2020). scRepertoire: An R-based toolkit for single-cell immune receptor analysis. *F1000Research*, *9*, 47. https://doi.org/10.12688/f1000research.22139.2

Chancellor, A., Vacchini, A., & De Libero, G. (2022). MR1, an immunological periscope of cellular metabolism. *International Immunology*, *34*(3), 141–147. https://doi.org/10.1093/intimm/dxab101

Chen, C. Y., Huang, D., Wang, R. C., Shen, L., Zeng, G., Yao, S., Shen, Y., Halliday, L., Fortman, J., McAllister, M., Estep, J., Hunt, R., Vasconcelos, D., Du, G., Porcelli, S. A., Larsen, M. H., Jr, W. R. J., Haynes, B. F., Letvin, N. L., & Chen, Z. W. (2009). A Critical Role for CD8 T Cells in a Nonhuman Primate Model of Tuberculosis. *PLOS Pathogens*, *5*(4), e1000392. https://doi.org/10.1371/journal.ppat.1000392

Cheung, K. L., Jarrett, R., Subramaniam, S., Salimi, M., Gutowska-Owsiak, D., Chen, Y.-L., Hardman, C., Xue, L., Cerundolo, V., & Ogg, G. (2016). Psoriatic T cells recognize neolipid antigens generated by mast cell phospholipase delivered by exosomes and presented by CD1a. *The Journal of Experimental Medicine*, *213*(11), 2399–2412. https://doi.org/10.1084/jem.20160258

Chien, Y., Meyer, C., & Bonneville, M. (2014). γδ T Cells: First Line of Defense and Beyond. *Annual Review of Immunology*, *32*(1), 121–155. https://doi.org/10.1146/annurev-immunol-032713-120216

Cho, S., Mehra, V., Thoma-Uszynski, S., Stenger, S., Serbina, N., Mazzaccaro, R. J., Flynn, J. L., Barnes, P. F., Southwood, S., Celis, E., Bloom, B. R., Modlin, R. L., & Sette, A. (2000). Antimicrobial activity of MHC class I-restricted CD8+ T cells in human tuberculosis. *Proceedings of the National Academy of Sciences of the United States of America*, *97*(22), 12210–12215. https://doi.org/10.1073/pnas.210391497

Chowdhury, R. R., Valainis, J. R., Dubey, M., von Boehmer, L., Sola, E., Wilhelmy, J., Guo, J., Kask, O., Ohanyan, M., Sun, M., Huang, H., Huang, X., Nguyen, P. K., Scriba, T. J., Davis, M. M., Bendall, S. C., & Chien, Y. (2023). NK-like CD8+ γδ T cells are expanded in persistent Mycobacterium tuberculosis infection and chronic inflammation. *Science Immunology*, *8*(81), eade3525. https://doi.org/10.1126/sciimmunol.ade3525

Cooper, A. M., Dalton, D. K., Stewart, T. A., Griffin, J. P., Russell, D. G., & Orme, I. M. (1993). Disseminated tuberculosis in interferon gamma gene-disrupted mice. *Journal of Experimental Medicine*, *178*(6), 2243–2247. https://doi.org/10.1084/jem.178.6.2243

Cotton, R. N., Cheng, T.-Y., Wegrecki, M., Nours, J. L., Orgill, D. P., Pomahac, B., Talbot, S. G., Willis, R. A., Altman, J. D., Jong, A. de, Ogg, G., Rhijn, I. V., Rossjohn, J., Clark, R. A., & Moody, D. B. (2021). Human skin is colonized by T cells that recognize CD1a independently of lipid. *The Journal of Clinical Investigation*, *131*(1). https://doi.org/10.1172/JCI140706

Darrah, P. A., Zeppa, J. J., Maiello, P., Hackney, J. A., Wadsworth, M. H., Hughes, T. K., Pokkali, S., Swanson, P. A., Grant, N. L., Rodgers, M. A., Kamath, M., Causgrove, C. M., Laddy, D. J., Bonavia, A., Casimiro, D., Lin, P. L., Klein, E., White, A. G., Scanga, C. A., … Seder, R. A. (2020). Prevention of tuberculosis in macaques after intravenous BCG immunization. *Nature*, *577*(7788), Article 7788. https://doi.org/10.1038/s41586-019-1817-8

Darrah, P. A., Zeppa, J. J., Wang, C., Irvine, E. B., Bucsan, A. N., Rodgers, M. A., Pokkali, S., Hackney, J. A., Kamath, M., White, A. G., Borish, H. J., Frye, L. J., Tomko, J., Kracinovsky, K., Lin, P. L., Klein, E., Scanga, C. A., Alter, G., Fortune, S. M., … Roederer, M. (2023). Airway T cells are a correlate of i.v. Bacille Calmette-Guerin-mediated protection against tuberculosis in rhesus macaques. *Cell Host & Microbe*, *31*(6), 962-977.e8. https://doi.org/10.1016/j.chom.2023.05.006

Davey, M. S., Willcox, C. R., Hunter, S., Kasatskaya, S. A., Remmerswaal, E. B. M., Salim, M., Mohammed, F., Bemelman, F. J., Chudakov, D. M., Oo, Y. H., & Willcox, B. E. (2018). The human Vδ2+ T-cell compartment comprises distinct innate-like Vγ9+ and adaptive Vγ9- subsets. *Nature Communications*, *9*(1), Article 1. https://doi.org/10.1038/s41467-018-04076-0

Davey, M. S., Willcox, C. R., Joyce, S. P., Ladell, K., Kasatskaya, S. A., McLaren, J. E., Hunter, S., Salim, M., Mohammed, F., Price, D. A., Chudakov, D. M., & Willcox, B. E. (2017). Clonal selection in the human Vδ1 T cell repertoire indicates γδ TCR-dependent adaptive immune surveillance. *Nature Communications*, *8*(1), Article 1. https://doi.org/10.1038/ncomms14760

de Jong, A., & Ogg, G. (2021). CD1a function in human skin disease. *Molecular Immunology*, *130*, 14–19. https://doi.org/10.1016/j.molimm.2020.12.006

de Jong, A., Peña-Cruz, V., Cheng, T.-Y., Clark, R. A., Van Rhijn, I., & Moody, D. B. (2010). CD1a-autoreactive T cells are a normal component of the human αβ T cell repertoire. *Nature Immunology*, *11*(12), Article 12. https://doi.org/10.1038/ni.1956

Deseke, M., Rampoldi, F., Sandrock, I., Borst, E., Böning, H., Ssebyatika, G. L., Jürgens, C., Plückebaum, N., Beck, M., Hassan, A., Tan, L., Demera, A., Janssen, A., Steinberger, P., Koenecke, C., Viejo-Borbolla, A., Messerle, M., Krey, T., & Prinz, I. (2022). A CMV-induced adaptive human Vδ1+ γδ T cell clone recognizes HLA-DR. *The Journal of Experimental Medicine*, *219*(9), e20212525. https://doi.org/10.1084/jem.20212525

Deusch, K., Lüling, F., Reich, K., Classen, M., Wagner, H., & Pfeffer, K. (1991). A major fraction of human intraepithelial lymphocytes simultaneously expresses the γ/δ T cell receptor, the CD8 accessory molecule and preferentially uses the Vδ1 gene segment. *European Journal of Immunology*, *21*(4), 1053–1059. https://doi.org/10.1002/eji.1830210429

Di Marco Barros, R., Roberts, N. A., Dart, R. J., Vantourout, P., Jandke, A., Nussbaumer, O., Deban, L., Cipolat, S., Hart, R., Iannitto, M. L., Laing, A., Spencer-Dene, B., East, P., Gibbons, D., Irving, P. M., Pereira, P., Steinhoff, U., & Hayday, A. (2016). Epithelia Use Butyrophilin-like Molecules to Shape Organ-Specific γδ T Cell Compartments. *Cell*, *167*(1), 203-218.e17. https://doi.org/10.1016/j.cell.2016.08.030

Donald, P. R., Diacon, A. H., Lange, C., Demers, A.-M., von Groote-Bidlingmaier, F., & Nardell, E. (2018). Droplets, dust and guinea pigs: An historical review of tuberculosis transmission research, 1878-1940. *The International Journal of Tuberculosis and Lung Disease: The Official Journal of the International Union Against Tuberculosis and Lung Disease*, *22*(9), 972–982. https://doi.org/10.5588/ijtld.18.0173

Du Bruyn, E., Ruzive, S., Lindestam Arlehamn, C. S., Sette, A., Sher, A., Barber, D. L., Wilkinson, R. J., & Riou, C. (2021). Mycobacterium tuberculosis -specific CD4 T cells expressing CD153 inversely associate with bacterial load and disease severity in human tuberculosis. *Mucosal Immunology*, *14*(2), Article 2. https://doi.org/10.1038/s41385-020-0322-6

Duquette, D., Harmon, C., Zaborowski, A., Michelet, X., O'Farrelly, C., Winter, D., Koay, H.-F., & Lynch, L. (2023). Human Granzyme K Is a Feature of Innate T Cells in Blood, Tissues, and Tumors, Responding to Cytokines Rather than TCR Stimulation. *The Journal of Immunology*, *211*(4), 633–647. https://doi.org/10.4049/jimmunol.2300083

Eckhardt, E., & Bastian, M. (2021). Animal models for human group 1 CD1 protein function. *Molecular Immunology*, *130*, 159–163. https://doi.org/10.1016/j.molimm.2020.12.018

Eggesbø, L. M., Risnes, L. F., Neumann, R. S., Lundin, K. E. A., Christophersen, A., & Sollid, L. M. (2020). Single-cell TCR sequencing of gut intraepithelial γδ T cells reveals a vast and diverse repertoire in celiac disease. *Mucosal Immunology*, *13*(2), Article 2. https://doi.org/10.1038/s41385-019-0222-9

Fichtner, A. S., Ravens, S., & Prinz, I. (2020). Human γδ TCR Repertoires in Health and Disease. *Cells*, *9*(4), Article 4. https://doi.org/10.3390/cells9040800

Finck, R., Simonds, E. F., Jager, A., Krishnaswamy, S., Sachs, K., Fantl, W., Pe'er, D., Nolan, G. P., & Bendall, S. C. (2013). Normalization of mass cytometry data with bead standards. *Cytometry. Part A: The Journal of the International Society for Analytical Cytology*, *83*(5), 483–494. https://doi.org/10.1002/cyto.a.22271

Fine, P. E. (1995). Variation in protection by BCG: Implications of and for heterologous immunity. *Lancet (London, England)*, *346*(8986), 1339–1345. https://doi.org/10.1016/s0140-6736(95)92348-9

Fletcher, H. A., Snowden, M. A., Landry, B., Rida, W., Satti, I., Harris, S. A., Matsumiya, M., Tanner, R., O'Shea, M. K., Dheenadhayalan, V., Bogardus, L., Stockdale, L., Marsay, L., Chomka, A., Harrington-Kandt, R., Manjaly-Thomas, Z.-R., Naranbhai, V., Stylianou, E., Darboe, F., … McShane, H. (2016). T-cell activation is an immune correlate of risk in BCG vaccinated infants. *Nature Communications*, *7*(1), Article 1. https://doi.org/10.1038/ncomms11290

Flynn, J. L., Chan, J., Triebold, K. J., Dalton, D. K., Stewart, T. A., & Bloom, B. R. (1993). An essential role for interferon gamma in resistance to Mycobacterium tuberculosis infection. *The Journal of Experimental Medicine*, *178*(6), 2249–2254. https://doi.org/10.1084/jem.178.6.2249

Flynn, J. L., Goldstein, M. M., Chan, J., Triebold, K. J., Pfeffer, K., Lowenstein, C. J., Schreiber, R., Mak, T. W., & Bloom, B. R. (1995). Tumor necrosis factor-alpha is required in the protective immune response against Mycobacterium tuberculosis in mice. *Immunity*, *2*(6), 561–572. https://doi.org/10.1016/1074-7613(95)90001-2

Fu, S., He, K., Tian, C., Sun, H., Zhu, C., Bai, S., Liu, J., Wu, Q., Xie, D., Yue, T., Shen, Z., Dai, Q., Yu, X., Zhu, S., Liu, G., Zhou, R., Duan, S., Tian, Z., Xu, T., … Bai, L. (2020). Impaired lipid biosynthesis hinders anti-tumor efficacy of intratumoral iNKT cells. *Nature Communications*, *11*(1), Article 1. https://doi.org/10.1038/s41467-020-14332-x

Gallegos, A. M., Pamer, E. G., & Glickman, M. S. (2008). Delayed protection by ESAT-6-specific effector CD4+ T cells after airborne M. tuberculosis infection. *The Journal of Experimental Medicine*, *205*(10), 2359–2368. https://doi.org/10.1084/jem.20080353

Gela, A., Murphy, M., Hadley, K., Hanekom, W., Boom, H., Johnson, J., Hoft, D., Joosten, S., Ottenhoff, T., Suliman, S., Moody, B., Lewinsohn, D., Hatherill, M., Seshadri, C., Nemes, E., & Scriba, T. (2021). Effects of BCG vaccination on donor unrestricted T cells in humans. *bioRxiv*, 2021.04.29.441927. https://doi.org/10.1101/2021.04.29.441927

Gela, A., Murphy, M., Rodo, M., Hadley, K., Hanekom, W. A., Boom, W. H., Johnson, J. L., Hoft, D. F., Joosten, S. A., Ottenhoff, T. H. M., Suliman, S., Moody, D. B., Lewinsohn, D. M., Hatherill, M., Seshadri, C., Nemes, E., Scriba, T. J., Briel, L., Veldtsman, H., … Delayed BCG Study Team. (2022). Effects of BCG vaccination on donor unrestricted T cells in two prospective cohort studies. *EBioMedicine*, *76*, 103839. https://doi.org/10.1016/j.ebiom.2022.103839

Geneva: World Health Organization. (2023). *Global Tuberculosis Report 2023*.

Geneva: World Health Organization. (2024). *Global Tuberculosis Report 2024*.

Gherardin, N. A., Souter, M. N., Koay, H.-F., Mangas, K. M., Seemann, T., Stinear, T. P., Eckle, S. B., Berzins, S. P., d'Udekem, Y., Konstantinov, I. E., Fairlie, D. P., Ritchie, D. S.,

Neeson, P. J., Pellicci, D. G., Uldrich, A. P., McCluskey, J., & Godfrey, D. I. (2018). Human blood MAIT cell subsets defined using MR1 tetramers. *Immunology and Cell Biology*, *96*(5), 507–525. https://doi.org/10.1111/imcb.12021

Gherardin, N. A., Waldeck, K., Caneborg, A., Martelotto, L. G., Balachander, S., Zethoven, M., Petrone, P. M., Pattison, A., Wilmott, J. S., Quiñones-Parra, S. M., Rossello, F., Posner, A., Wong, A., Weppler, A. M., Shannon, K. F., Hong, A., Ferguson, P. M., Jakrot, V., Raleigh, J., … Tothill, R. W. (2021). Γδ T Cells in Merkel Cell Carcinomas Have a Proinflammatory Profile Prognostic of Patient Survival. *Cancer Immunology Research*. https://doi.org/10.1158/2326-6066.CIR-20-0817

Gideon, H. P., Hughes, T. K., Wadsworth, M. H., Tu, A. A., Gierahn, T. M., Peters, J. M., Hopkins, F. F., Wei, J.-R., Kummerlowe, C., Grant, N. L., Nargan, K., Phuah, J., Borish, H. J., Maiello, P., White, A. G., Winchell, C. G., Nyquist, S. K., Ganchua, S. K. C., Myers, A., … Shalek, A. K. (2020). *Multimodal profiling of lung granulomas reveals cellular correlates of tuberculosis control* [Preprint]. Immunology. https://doi.org/10.1101/2020.10.24.352492

Godfrey, D. I., Uldrich, A. P., McCluskey, J., Rossjohn, J., & Moody, D. B. (2015). The burgeoning family of unconventional T cells. *Nature Immunology*, *16*(11), 1114–1123. https://doi.org/10.1038/ni.3298

Groh, V., Bahram, S., Bauer, S., Herman, A., Beauchamp, M., & Spies, T. (1996). Cell stress-regulated human major histocompatibility complex class I gene expressed in gastrointestinal epithelium. *Proceedings of the National Academy of Sciences of the United States of America*, *93*(22), 12445–12450. https://doi.org/10.1073/pnas.93.22.12445

Groh, V., Rhinehart, R., Secrist, H., Bauer, S., Grabstein, K. H., & Spies, T. (1999). Broad tumor-associated expression and recognition by tumor-derived γδ T cells of MICA and MICB. *Proceedings of the National Academy of Sciences of the United States of America*, *96*(12), 6879–6884.

Groh, V., Steinle, A., Bauer, S., & Spies, T. (1998). Recognition of Stress-Induced MHC Molecules by Intestinal Epithelial γδ T Cells. *Science*, *279*(5357), 1737–1740. https://doi.org/10.1126/science.279.5357.1737

Gutierrez-Arcelus, M., Teslovich, N., Mola, A. R., Polidoro, R. B., Nathan, A., Kim, H., Hannes, S., Slowikowski, K., Watts, G. F. M., Korsunsky, I., Brenner, M. B., Raychaudhuri, S., & Brennan, P. J. (2019). Lymphocyte innateness defined by transcriptional states reflects a balance between proliferation and effector functions. *Nature Communications*, *10*(1), Article 1. https://doi.org/10.1038/s41467-019-08604-4

Hao, Y., Hao, S., Andersen-Nissen, E., Mauck, W. M., Zheng, S., Butler, A., Lee, M. J., Wilk, A. J., Darby, C., Zager, M., Hoffman, P., Stoeckius, M., Papalexi, E., Mimitou, E. P., Jain, J., Srivastava, A., Stuart, T., Fleming, L. M., Yeung, B., … Satija, R. (2021). Integrated analysis of multimodal single-cell data. *Cell*, *184*(13), 3573-3587.e29. https://doi.org/10.1016/j.cell.2021.04.048

Hawkridge, A., Hatherill, M., Little, F., Goetz, M. A., Barker, L., Mahomed, H., Sadoff, J., Hanekom, W., Geiter, L., & Hussey, G. (2008). Efficacy of percutaneous versus

intradermal BCG in the prevention of tuberculosis in South African infants: Randomised trial. *BMJ*, *337*, a2052. https://doi.org/10.1136/bmj.a2052

Hayday, A. C. (2000). γδ Cells: A Right Time and a Right Place for a Conserved Third Way of Protection. *Annual Review of Immunology*, *18*(1), 975–1026. https://doi.org/10.1146/annurev.immunol.18.1.975

Hayday, A. C. (2009). Gammadelta T cells and the lymphoid stress-surveillance response. *Immunity*, *31*(2), 184–196. https://doi.org/10.1016/j.immuni.2009.08.006

Hinks, T. S. C., & Zhang, X.-W. (2020). MAIT Cell Activation and Functions. *Frontiers in Immunology*, *11*, 1014. https://doi.org/10.3389/fimmu.2020.01014

Hu, Y., Hu, Q., Li, Y., Lu, L., Xiang, Z., Yin, Z., Kabelitz, D., & Wu, Y. (2023). γδ T cells: Origin and fate, subsets, diseases and immunotherapy. *Signal Transduction and Targeted Therapy*, *8*(1), 434. https://doi.org/10.1038/s41392-023-01653-8

Hviid, L., Akanmori, B. D., Loizon, S., Kurtzhals, J. A. L., Ricke, C. H., Lim, A., Koram, K. A., Nkrumah, F. K., Mercereau-Puijalon, O., & Behr, C. (2000). High frequency of circulating γδ T cells with dominance of the Vδ1 subset in a healthy population. *International Immunology*, *12*(6), 797–805. https://doi.org/10.1093/intimm/12.6.797

Ismail, A. S., Severson, K. M., Vaishnava, S., Behrendt, C. L., Yu, X., Benjamin, J. L., Ruhn, K. A., Hou, B., DeFranco, A. L., Yarovinsky, F., & Hooper, L. V. (2011). Gammadelta intraepithelial lymphocytes are essential mediators of host-microbial homeostasis at the intestinal mucosal surface. *Proceedings of the National Academy of Sciences of the United States of America*, *108*(21), 8743–8748. https://doi.org/10.1073/pnas.1019574108

Iwasaki, A., & Medzhitov, R. (2015). Control of adaptive immunity by the innate immune system. *Nature Immunology*, *16*(4), Article 4. https://doi.org/10.1038/ni.3123

James, C. A., Yu, K. K. Q., Mayer-Blackwell, K., Fiore-Gartland, A., Smith, M. T., Layton, E. D., Johnson, J. L., Hanekom, W. A., Scriba, T. J., & Seshadri, C. (2022). Durable Expansion of TCR-δ Meta-Clonotypes After BCG Revaccination in Humans. *Frontiers in Immunology*, *13*, 834757. https://doi.org/10.3389/fimmu.2022.834757

Ji, X., Huang, G., Peng, Y., Wang, J., Cai, X., Yang, E., Zhu, L., Wu, Y., Sha, W., Wang, F., Shen, L., & Shen, H. (2024). CD137 expression and signal function drive pleiotropic γδ T-cell effector functions that inhibit intracellular *M. tuberculosis* growth. *Clinical Immunology*, *266*, 110331. https://doi.org/10.1016/j.clim.2024.110331

Joosten, S. A., Ottenhoff, T. H. M., Lewinsohn, D. M., Hoft, D. F., Moody, D. B., & Seshadri, C. (2019). Harnessing donor unrestricted T-cells for new vaccines against tuberculosis. *Vaccine*, *37*(23), 3022–3030. https://doi.org/10.1016/j.vaccine.2019.04.050

Kagina, B. M. N., Abel, B., Scriba, T. J., Hughes, E. J., Keyser, A., Soares, A., Gamieldien, H., Sidibana, M., Hatherill, M., Gelderbloem, S., Mahomed, H., Hawkridge, A., Hussey, G., Kaplan, G., & Hanekom, W. A. (2010). Specific T Cell Frequency and Cytokine Expression Profile Do Not Correlate with Protection against Tuberculosis after Bacillus Calmette-Guérin Vaccination of Newborns. *American Journal of Respiratory and Critical Care Medicine*, *182*(8), 1073–1079. https://doi.org/10.1164/rccm.201003-0334OC

Karunakaran, M. M., Willcox, C. R., Salim, M., Paletta, D., Fichtner, A. S., Noll, A., Starick, L., Nöhren, A., Begley, C. R., Berwick, K. A., Chaleil, R. A. G., Pitard, V., Déchanet-

Merville, J., Bates, P. A., Kimmel, B., Knowles, T. J., Kunzmann, V., Walter, L., Jeeves, M., … Herrmann, T. (2020). Butyrophilin-2A1 Directly Binds Germline-Encoded Regions of the Vγ9Vδ2 TCR and Is Essential for Phosphoantigen Sensing. *Immunity*, *52*(3), 487-498.e6. https://doi.org/10.1016/j.immuni.2020.02.014

Keane, J., Gershon, S., Wise, R. P., Mirabile-Levens, E., Kasznica, J., Schwieterman, W. D., Siegel, J. N., & Braun, M. M. (2001). Tuberculosis associated with infliximab, a tumor necrosis factor alpha-neutralizing agent. *The New England Journal of Medicine*, *345*(15), 1098–1104. https://doi.org/10.1056/NEJMoa011110

Kim, P. S., & Swaminathan, S. (2021). Ending TB: The world's oldest pandemic. *Journal of the International AIDS Society*, *24*(3), e25698. https://doi.org/10.1002/jia2.25698

Kjer-Nielsen, L., Patel, O., Corbett, A. J., Le Nours, J., Meehan, B., Liu, L., Bhati, M., Chen, Z., Kostenko, L., Reantragoon, R., Williamson, N. A., Purcell, A. W., Dudek, N. L., McConville, M. J., O'Hair, R. A. J., Khairallah, G. N., Godfrey, D. I., Fairlie, D. P., Rossjohn, J., & McCluskey, J. (2012). MR1 presents microbial vitamin B metabolites to MAIT cells. *Nature*, *491*(7426), 717–723. https://doi.org/10.1038/nature11605

Kulicke, C., Karamooz, E., Lewinsohn, D., & Harriff, M. (2020). Covering All the Bases: Complementary MR1 Antigen Presentation Pathways Sample Diverse Antigens and Intracellular Compartments. *Frontiers in Immunology*, *11*. https://www.frontiersin.org/articles/10.3389/fimmu.2020.02034

Lai, R., Ogunsola, A. F., Rakib, T., & Behar, S. M. (2023). Key advances in vaccine development for tuberculosis-success and challenges. *NPJ Vaccines*, *8*(1), 158. https://doi.org/10.1038/s41541-023-00750-7

Layton, E. D., Barman, S., Wilburn, D. B., Yu, K. K. Q., Smith, M. T., Altman, J. D., Scriba, T. J., Tahiri, N., Minnaard, A. J., Roederer, M., Seder, R. A., Darrah, P. A., & Seshadri, C. (2021). T Cells Specific for a Mycobacterial Glycolipid Expand after Intravenous Bacillus Calmette–Guérin Vaccination. *The Journal of Immunology*, *206*(6), 1240–1250. https://doi.org/10.4049/jimmunol.2001065

Le Nours, J., Gherardin, N. A., Ramarathinam, S. H., Awad, W., Wiede, F., Gully, B. S., Khandokar, Y., Praveena, T., Wubben, J. M., Sandow, J. J., Webb, A. I., Borstel, A. von, Rice, M. T., Redmond, S. J., Seneviratna, R., Sandoval-Romero, M. L., Li, S., Souter, M. N. T., Eckle, S. B. G., … Rossjohn, J. (2019). A class of γδ T cell receptors recognize the underside of the antigen-presenting molecule MR1. *Science*, *366*(6472), 1522–1527. https://doi.org/10.1126/science.aav3900

Lefranc, M.-P. (2014). Immunoglobulin and T Cell Receptor Genes: IMGT(®) and the Birth and Rise of Immunoinformatics. *Frontiers in Immunology*, *5*, 22. https://doi.org/10.3389/fimmu.2014.00022

Lepore, M., Kalinichenko, A., Calogero, S., Kumar, P., Paleja, B., Schmaler, M., Narang, V., Zolezzi, F., Poidinger, M., Mori, L., & De Libero, G. (2017). Functionally diverse human T cells recognize non-microbial antigens presented by MR1. *eLife*, *6*, e24476. https://doi.org/10.7554/eLife.24476

Lien, S. C., Ly, D., Yang, S. Y. C., Wang, B. X., Clouthier, D. L., St. Paul, M., Gadalla, R., Noamani, B., Garcia-Batres, C. R., Boross-Harmer, S., Bedard, P. L., Pugh, T. J., Spreafico, A., Hirano, N., Razak, A. R. A., & Ohashi, P. S. (2024). Tumor reactive γδ T cells contribute to a complete response to PD-1 blockade in a Merkel cell

carcinoma patient. *Nature Communications*, *15*, 1094. https://doi.org/10.1038/s41467-024-45449-y

Lin, P. L., Pawar, S., Myers, A., Pegu, A., Fuhrman, C., Reinhart, T. A., Capuano, S. V., Klein, E., & Flynn, J. L. (2006). Early Events in Mycobacterium tuberculosis Infection in Cynomolgus Macaques. *Infection and Immunity*, *74*(7), 3790–3803. https://doi.org/10.1128/IAI.00064-06

Liu, Y. E., Darrah, P. A., Zeppa, J. J., Kamath, M., Laboune, F., Douek, D. C., Maiello, P., Roederer, M., Flynn, J. L., Seder, R. A., & Khatri, P. (2023). Blood transcriptional correlates of BCG-induced protection against tuberculosis in rhesus macaques. *Cell Reports Medicine*, *4*(7), 101096. https://doi.org/10.1016/j.xcrm.2023.101096

Lopez, K., Iwany, S. K., Suliman, S., Reijneveld, J. F., Ocampo, T. A., Jimenez, J., Calderon, R., Lecca, L., Murray, M. B., Moody, D. B., & Van Rhijn, I. (2020). CD1b Tetramers Broadly Detect T Cells That Correlate With Mycobacterial Exposure but Not Tuberculosis Disease State. *Frontiers in Immunology*, *11*. https://doi.org/10.3389/fimmu.2020.00199

López-Sagaseta, J., Dulberger, C. L., Crooks, J. E., Parks, C. D., Luoma, A. M., McFedries, A., Van Rhijn, I., Saghatelian, A., & Adams, E. J. (2013). The molecular basis for Mucosal-Associated Invariant T cell recognition of MR1 proteins. *Proceedings of the National Academy of Sciences*, *110*(19), E1771–E1778. https://doi.org/10.1073/pnas.1222678110

Luoma, A. M., Castro, C. D., Mayassi, T., Bembinster, L. A., Bai, L., Picard, D., Anderson, B., Scharf, L., Kung, J. E., Sibener, L. V., Savage, P. B., Jabri, B., Bendelac, A., & Adams, E. J. (2013). Crystal structure of Vδ1 T cell receptor in complex with CD1d-sulfatide shows MHC-like recognition of a self-lipid by human γδ T cells. *Immunity*, *39*(6), 1032–1042. https://doi.org/10.1016/j.immuni.2013.11.001

Maerz, M. D., Cross, D. L., & Seshadri, C. (2024). Functional and biological implications of clonotypic diversity among human donor-unrestricted T cells. *Immunology and Cell Biology*, *102*(6), 474–486. https://doi.org/10.1111/imcb.12751

Magalhaes, I., Solders, M., & Kaipe, H. (2020). MAIT Cells in Health and Disease. *Methods in Molecular Biology (Clifton, N.J.)*, *2098*, 3–21. https://doi.org/10.1007/978-1-0716-0207-2_1

Makatsa, M. S., Kus, A., Wiedeman, A., Long, S. A., & Seshadri, C. (2024). *42-parameter mass cytometry panel to assess cellular and functional phenotypes of leukocytes in bronchoalveolar lavage of Rhesus macaque* (p. 2024.09.19.613973). bioRxiv. https://doi.org/10.1101/2024.09.19.613973

Marlin, R., Pappalardo, A., Kaminski, H., Willcox, C. R., Pitard, V., Netzer, S., Khairallah, C., Lomenech, A.-M., Harly, C., Bonneville, M., Moreau, J.-F., Scotet, E., Willcox, B. E., Faustin, B., & Déchanet-Merville, J. (2017). Sensing of cell stress by human γδ TCR-dependent recognition of annexin A2. *Proceedings of the National Academy of Sciences of the United States of America*, *114*(12), 3163–3168. https://doi.org/10.1073/pnas.1621052114

McCaffrey, E. F., Donato, M., Keren, L., Chen, Z., Delmastro, A., Fitzpatrick, M. B., Gupta, S., Greenwald, N. F., Baranski, A., Graf, W., Kumar, R., Bosse, M., Fullaway, C. C., Ramdial, P. K., Forgó, E., Jojic, V., Van Valen, D., Mehra, S., Khader, S. A., … Angelo,

M. (2022). The immunoregulatory landscape of human tuberculosis granulomas. *Nature Immunology*, *23*(2), 318–329. https://doi.org/10.1038/s41590-021-01121-x

McGinnis, C. S., Patterson, D. M., Winkler, J., Conrad, D. N., Hein, M. Y., Srivastava, V., Hu, J. L., Murrow, L. M., Weissman, J. S., Werb, Z., Chow, E. D., & Gartner, Z. J. (2019). MULTI-seq: Sample multiplexing for single-cell RNA sequencing using lipid-tagged indices. *Nature Methods*, *16*(7), 619–626. https://doi.org/10.1038/s41592-019-0433-8

McMurray, J. L., von Borstel, A., Taher, T. E., Syrimi, E., Taylor, G. S., Sharif, M., Rossjohn, J., Remmerswaal, E. B. M., Bemelman, F. J., Braga, F. A. V., Chen, X., Teichmann, S. A., Mohammed, F., Berry, A. A., Lyke, K. E., Williamson, K. C., Stubbington, M. J. T., Davey, M. S., Willcox, C. R., & Willcox, B. E. (2022). Transcriptional profiling of human Vδ1 T cells reveals a pathogen-driven adaptive differentiation program. *Cell Reports*, *39*(8), 110858. https://doi.org/10.1016/j.celrep.2022.110858

Meermeier, E. W., Laugel, B. F., Sewell, A. K., Corbett, A. J., Rossjohn, J., McCluskey, J., Harriff, M. J., Franks, T., Gold, M. C., & Lewinsohn, D. M. (2016). Human TRAV1-2-negative MR1-restricted T cells detect S. pyogenes and alternatives to MAIT riboflavin-based antigens. *Nature Communications*, *7*(1), Article 1. https://doi.org/10.1038/ncomms12506

Mikulak, J., Oriolo, F., Bruni, E., Roberto, A., Colombo, F. S., Villa, A., Bosticardo, M., Bortolomai, I., Lo Presti, E., Meraviglia, S., Dieli, F., Vetrano, S., Danese, S., Della Bella, S., Carvello, M. M., Sacchi, M., Cugini, G., Colombo, G., Klinger, M., … Mavilio, D. (2019). NKp46-expressing human gut-resident intraepithelial Vδ1 T cell subpopulation exhibits high antitumor activity against colorectal cancer. *JCI Insight*, *4*(24). https://doi.org/10.1172/jci.insight.125884

Miller, L. G., Asch, S. M., Yu, E. I., Knowles, L., Gelberg, L., & Davidson, P. (2000). A Population-Based Survey of Tuberculosis Symptoms: How Atypical Are Atypical Presentations? *Clinical Infectious Diseases*, *30*(2), 293–299. https://doi.org/10.1086/313651

Mimitou, E. P., Cheng, A., Montalbano, A., Hao, S., Stoeckius, M., Legut, M., Roush, T., Herrera, A., Papalexi, E., Ouyang, Z., Satija, R., Sanjana, N. E., Koralov, S. B., & Smibert, P. (2019). Multiplexed detection of proteins, transcriptomes, clonotypes and CRISPR perturbations in single cells. *Nature Methods*, *16*(5), Article 5. https://doi.org/10.1038/s41592-019-0392-0

Morita, C. T., Mariuzza, R. A., & Brenner, M. B. (2000). Antigen recognition by human γδ T cells: Pattern recognition by the adaptive immune system. *Springer Seminars in Immunopathology*, *22*(3), 191–217. https://doi.org/10.1007/s002810000042

Morita, D., Hattori, Y., Nakamura, T., Igarashi, T., Harashima, H., & Sugita, M. (2013). Major T Cell Response to a Mycolyl Glycolipid Is Mediated by CD1c Molecules in Rhesus Macaques. *Infection and Immunity*, *81*(1), 311–316. https://doi.org/10.1128/iai.00871-12

Müller, I., Cobbold, S. P., Waldmann, H., & Kaufmann, S. H. (1987). Impaired resistance to Mycobacterium tuberculosis infection after selective in vivo depletion of L3T4+ and Lyt-2+ T cells. *Infection and Immunity*, *55*(9), 2037–2041. https://doi.org/10.1128/iai.55.9.2037-2041.1987

Nel, I., Bertrand, L., Toubal, A., & Lehuen, A. (2021). MAIT cells, guardians of skin and mucosa? *Mucosal Immunology*, *14*(4), Article 4. https://doi.org/10.1038/s41385-021-00391-w

Nemes, E., Fiore-Gartland, A., Boggiano, C., Coccia, M., D'Souza, P., Gilbert, P., Ginsberg, A., Hyrien, O., Laddy, D., Makar, K., McElrath, M. J., Ramachandra, L., Schmidt, A. C., Shororbani, S., Sunshine, J., Tomaras, G., Yu, W.-H., Scriba, T. J., Frahm, N., & BCG Correlates PIs Study Team, M72 Correlates PIs Study Team. (2022). The quest for vaccine-induced immune correlates of protection against tuberculosis. *Vaccine Insights*, *1*(3), 165–181. https://doi.org/10.18609/vac/2022.027

Nicolai, S., Wegrecki, M., Cheng, T.-Y., Bourgeois, E. A., Cotton, R. N., Mayfield, J. A., Monnot, G. C., Le Nours, J., Van Rhijn, I., Rossjohn, J., Moody, D. B., & de Jong, A. (2020). Human T cell response to CD1a and contact dermatitis allergens in botanical extracts and commercial skin care products. *Science Immunology*, *5*(43), eaax5430. https://doi.org/10.1126/sciimmunol.aax5430

Nielsen, M. M., Witherden, D. A., & Havran, W. L. (2017). Γδ T cells in homeostasis and host defence of epithelial barrier tissues. *Nature Reviews. Immunology*, *17*(12), 733–745. https://doi.org/10.1038/nri.2017.101

Ogongo, P., Steyn, A. J. C., Karim, F., Dullabh, K. J., Awala, I., Madansein, R., Leslie, A., & Behar, S. M. (2020, January 2). *Differential skewing of donor-unrestricted and γδ T cell repertoires in tuberculosis-infected human lungs*. American Society for Clinical Investigation. https://doi.org/10.1172/JCI130711

Orme, I. M., & Collins, F. M. (1983). Protection against Mycobacterium tuberculosis infection by adoptive immunotherapy. Requirement for T cell-deficient recipients. *The Journal of Experimental Medicine*, *158*(1), 74–83. https://doi.org/10.1084/jem.158.1.74

Orme, I. M., & Collins, F. M. (1984). Adoptive protection of the Mycobacterium tuberculosis-infected lung. Dissociation between cells that passively transfer protective immunity and those that transfer delayed-type hypersensitivity to tuberculin. *Cellular Immunology*, *84*(1), 113–120. https://doi.org/10.1016/0008-8749(84)90082-0

Ottenhoff, T. H. M., de Boer, T., Verhagen, C. E., Verreck, F. A. W., & van Dissel, J. T. (2000). Human deficiencies in type 1 cytokine receptors reveal the essential role of type 1 cytokines in immunity to intracellular bacteria. *Microbes and Infection*, *2*(13), 1559–1566. https://doi.org/10.1016/S1286-4579(00)01312-5

Pai, M., Behr, M. A., Dowdy, D., Dheda, K., Divangahi, M., Boehme, C. C., Ginsberg, A., Swaminathan, S., Spigelman, M., Getahun, H., Menzies, D., & Raviglione, M. (2016). Tuberculosis. *Nature Reviews. Disease Primers*, *2*, 16076. https://doi.org/10.1038/nrdp.2016.76

Parker, C. M., Groh, V., Band, H., Porcelli, S. A., Morita, C., Fabbi, M., Glass, D., Strominger, J. L., & Brenner, M. B. (1990). Evidence for extrathymic changes in the T cell receptor gamma/delta repertoire. *Journal of Experimental Medicine*, *171*(5), 1597–1612. https://doi.org/10.1084/jem.171.5.1597

Pei, Y., Wen, K., Xiang, Z., Huang, C., Wang, X., Mu, X., Wen, L., Liu, Y., & Tu, W. (2020). CD137 costimulation enhances the antiviral activity of Vγ9Vδ2-T cells against

influenza virus. *Signal Transduction and Targeted Therapy*, *5*(1), 74. https://doi.org/10.1038/s41392-020-0174-2

Peters, J. M., Irvine, E. B., Rosenberg, J. M., Wadsworth, M. H., Hughes, T. K., Sutton, M., Nyquist, S. K., Bromley, J. D., Mondal, R., Roederer, M., Seder, R. A., Darrah, P. A., Alter, G., Flynn, J. L., Shalek, A. K., Fortune, S. M., & Bryson, B. D. (2023). Protective intravenous BCG vaccination induces enhanced immune signaling in the airways. *bioRxiv: The Preprint Server for Biology*, 2023.07.16.549208. https://doi.org/10.1101/2023.07.16.549208

Pizzolato, G., Kaminski, H., Tosolini, M., Franchini, D.-M., Pont, F., Martins, F., Valle, C., Labourdette, D., Cadot, S., Quillet-Mary, A., Poupot, M., Laurent, C., Ysebaert, L., Meraviglia, S., Dieli, F., Merville, P., Milpied, P., Déchanet-Merville, J., & Fournié, J.-J. (2019). Single-cell RNA sequencing unveils the shared and the distinct cytotoxic hallmarks of human TCRVδ1 and TCRVδ2 γδ T lymphocytes. *Proceedings of the National Academy of Sciences*, *116*(24), 11906–11915. https://doi.org/10.1073/pnas.1818488116

Porcelli, S., Morita, C. T., & Brenner, M. B. (1992). CD1b restricts the response of human CD4-8- T lymphocytes to a microbial antigen. *Nature*, *360*(6404), 593–597. https://doi.org/10.1038/360593a0

Qaqish, A., Huang, D., Chen, C. Y., Zhang, Z., Wang, R., Li, S., Yang, E., Lu, Y., Larsen, M. H., Jacobs, W. R., Qian, L., Frencher, J., Shen, L., & Chen, Z. W. (2017). Adoptive Transfer of Phosphoantigen-Specific γδ T Cell Subset Attenuates Mycobacterium tuberculosis Infection in Nonhuman Primates. *The Journal of Immunology*, *198*(12), 4753–4763. https://doi.org/10.4049/jimmunol.1602019

Rasi, V., Phelps, K. R., Paulson, K. R., Eickhoff, C. S., Chinnaraj, M., Pozzi, N., Di Gioia, M., Zanoni, I., Shakya, S., Carlson, H. L., Ford, D. A., Kolar, G. R., & Hoft, D. F. (2023). Homodimeric Granzyme A Opsonizes Mycobacterium tuberculosis and Inhibits Its Intracellular Growth in Human Monocytes via Toll-Like Receptor 4 and CD14. *The Journal of Infectious Diseases*, *229*(3), 876–887. https://doi.org/10.1093/infdis/jiad378

Rast, J. P., Anderson, M. K., Strong, S. J., Luer, C., Litman, R. T., & Litman, G. W. (1997). α, β, γ, and δ T Cell Antigen Receptor Genes Arose Early in Vertebrate Phylogeny. *Immunity*, *6*(1), 1–11. https://doi.org/10.1016/S1074-7613(00)80237-X

Reantragoon, R., Corbett, A. J., Sakala, I. G., Gherardin, N. A., Furness, J. B., Chen, Z., Eckle, S. B. G., Uldrich, A. P., Birkinshaw, R. W., Patel, O., Kostenko, L., Meehan, B., Kedzierska, K., Liu, L., Fairlie, D. P., Hansen, T. H., Godfrey, D. I., Rossjohn, J., McCluskey, J., & Kjer-Nielsen, L. (2013). Antigen-loaded MR1 tetramers define T cell receptor heterogeneity in mucosal-associated invariant T cells. *The Journal of Experimental Medicine*, *210*(11), 2305–2320. https://doi.org/10.1084/jem.20130958

Reijneveld, J. F., Ocampo, T. A., Shahine, A., Gully, B. S., Vantourout, P., Hayday, A. C., Rossjohn, J., Moody, D. B., & Van Rhijn, I. (2020). Human γδ T cells recognize CD1b by two distinct mechanisms. *Proceedings of the National Academy of Sciences*, *117*(37), 22944–22952. https://doi.org/10.1073/pnas.2010545117

Reiley, W. W., Calayag, M. D., Wittmer, S. T., Huntington, J. L., Pearl, J. E., Fountain, J. J., Martino, C. A., Roberts, A. D., Cooper, A. M., Winslow, G. M., & Woodland, D. L.

(2008). ESAT-6-specific CD4 T cell responses to aerosol Mycobacterium tuberculosis infection are initiated in the mediastinal lymph nodes. *Proceedings of the National Academy of Sciences of the United States of America*, *105*(31), 10961–10966. https://doi.org/10.1073/pnas.0801496105

Reis, B. S., Darcy, P. W., Khan, I. Z., Moon, C. S., Kornberg, A. E., Schneider, V. S., Alvarez, Y., Eleso, O., Zhu, C., Schernthanner, M., Lockhart, A., Reed, A., Bortolatto, J., Castro, T. B. R., Bilate, A. M., Grivennikov, S., Han, A. S., & Mucida, D. (2022). TCR-Vγδ usage distinguishes protumor from antitumor intestinal γδ T cell subsets. *Science*, *377*(6603), 276–284. https://doi.org/10.1126/science.abj8695

Rezende, R. M., Lanser, A. J., Rubino, S., Kuhn, C., Skillin, N., Moreira, T. G., Liu, S., Gabriely, G., David, B. A., Menezes, G. B., & Weiner, H. L. (2018). Γδ T cells control humoral immune response by inducing T follicular helper cell differentiation. *Nature Communications*, *9*(1), 3151. https://doi.org/10.1038/s41467-018-05487-9

Ribeiro, S. T., Ribot, J. C., & Silva-Santos, B. (2015). Five layers of receptor signalling in γδ T cell differentiation and activation. *Frontiers in Immunology*, *6*. https://doi.org/10.3389/fimmu.2015.00015

Rice, M. T., von Borstel, A., Chevour, P., Awad, W., Howson, L. J., Littler, D. R., Gherardin, N. A., Le Nours, J., Giles, E. M., Berry, R., Godfrey, D. I., Davey, M. S., Rossjohn, J., & Gully, B. S. (2021). Recognition of the antigen-presenting molecule MR1 by a Vδ3+ γδ T cell receptor. *Proceedings of the National Academy of Sciences*, *118*(49), e2110288118. https://doi.org/10.1073/pnas.2110288118

Rigau, M., Ostrouska, S., Fulford, T. S., Johnson, D. N., Woods, K., Ruan, Z., McWilliam, H. E. G., Hudson, C., Tutuka, C., Wheatley, A. K., Kent, S. J., Villadangos, J. A., Pal, B., Kurts, C., Simmonds, J., Pelzing, M., Nash, A. D., Hammet, A., Verhagen, A. M., … Uldrich, A. P. (2020). Butyrophilin 2A1 is essential for phosphoantigen reactivity by γδ T cells. *Science (New York, N.Y.)*, *367*(6478), eaay5516. https://doi.org/10.1126/science.aay5516

Roy, A., Eisenhut, M., Harris, R. J., Rodrigues, L. C., Sridhar, S., Habermann, S., Snell, L., Mangtani, P., Adetifa, I., Lalvani, A., & Abubakar, I. (2014). Effect of BCG vaccination against Mycobacterium tuberculosis infection in children: Systematic review and meta-analysis. *BMJ*, *349*, g4643. https://doi.org/10.1136/bmj.g4643

Roy, S., Ly, D., Castro, C. D., Li, N.-S., Hawk, A. J., Altman, J. D., Meredith, S. C., Piccirilli, J. A., Moody, D. B., & Adams, E. J. (2016). Molecular analysis of lipid reactive Vδ1 γδ T cells identified by CD1c tetramers. *Journal of Immunology (Baltimore, Md. : 1950)*, *196*(4), 1933–1942. https://doi.org/10.4049/jimmunol.1502202

Ruibal, P., Voogd, L., Joosten, S. A., & Ottenhoff, T. H. M. (2021). The role of donor-unrestricted T-cells, innate lymphoid cells, and NK cells in anti-mycobacterial immunity. *Immunological Reviews*, *301*(1), 30–47. https://doi.org/10.1111/imr.12948

Sáez de Guinoa, J., Jimeno, R., Gaya, M., Kipling, D., Garzón, M. J., Dunn-Walters, D., Ubeda, C., & Barral, P. (2018). CD1d-mediated lipid presentation by CD11c+ cells regulates intestinal homeostasis. *The EMBO Journal*, *37*(5), e97537. https://doi.org/10.15252/embj.201797537

Sallin, M. A., Kauffman, K. D., Riou, C., Du Bruyn, E., Foreman, T. W., Sakai, S., Hoft, S. G., Myers, T. G., Gardina, P. J., Sher, A., Moore, R., Wilder-Kofie, T., Moore, I. N., Sette, A., Lindestam Arlehamn, C. S., Wilkinson, R. J., & Barber, D. L. (2018). Host resistance to pulmonary Mycobacterium tuberculosis infection requires CD153 expression. *Nature Microbiology*, *3*(11), 1198–1205. https://doi.org/10.1038/s41564-018-0231-6

Salou, M., Legoux, F., Gilet, J., Darbois, A., du Halgouet, A., Alonso, R., Richer, W., Goubet, A.-G., Daviaud, C., Menger, L., Procopio, E., Premel, V., & Lantz, O. (2019). A common transcriptomic program acquired in the thymus defines tissue residency of MAIT and NKT subsets. *The Journal of Experimental Medicine*, *216*(1), 133–151. https://doi.org/10.1084/jem.20181483

Sandstrom, A., Peigné, C.-M., Léger, A., Crooks, J. E., Konczak, F., Gesnel, M.-C., Breathnach, R., Bonneville, M., Scotet, E., & Adams, E. J. (2014). The intracellular B30.2 domain of Butyrophilin 3A1 binds phosphoantigens to mediate activation of human Vγ9Vδ2 T cells. *Immunity*, *40*(4), 490–500. https://doi.org/10.1016/j.immuni.2014.03.003

Sanz, M., Mann, B. T., Ryan, P. L., Bosque, A., Pennington, D. J., Hackstein, H., & Soriano-Sarabia, N. (2023). Deep characterization of human γδ T cell subsets defines shared and lineage-specific traits. *Frontiers in Immunology*, *14*. https://doi.org/10.3389/fimmu.2023.1148988

Schattgen, S. A., Guion, K., Crawford, J. C., Souquette, A., Barrio, A. M., Stubbington, M. J. T., Thomas, P. G., & Bradley, P. (2020). Linking T cell receptor sequence to transcriptional profiles with clonotype neighbor graph analysis (CoNGA). *bioRxiv*, 2020.06.04.134536. https://doi.org/10.1101/2020.06.04.134536

Selwyn, P. A., Hartel, D., Lewis, V. A., Schoenbaum, E. E., Vermund, S. H., Klein, R. S., Walker, A. T., & Friedland, G. H. (1989). A prospective study of the risk of tuberculosis among intravenous drug users with human immunodeficiency virus infection. *The New England Journal of Medicine*, *320*(9), 545–550. https://doi.org/10.1056/NEJM198903023200901

Serbina, N. V., & Flynn, J. L. (1999). Early Emergence of CD8+ T Cells Primed for Production of Type 1 Cytokines in the Lungs of Mycobacterium tuberculosis-Infected Mice. *Infection and Immunity*, *67*(8), 3980–3988.

Seshadri, C., Sedaghat, N., Campo, M., Peterson, G., Wells, R. D., Olson, G. S., Sherman, D. R., Stein, C. M., Mayanja-Kizza, H., Shojaie, A., Boom, W. H., Hawn, T. R., & Unit (TBRU), on behalf of the T. R. (2017). Transcriptional networks are associated with resistance to Mycobacterium tuberculosis infection. *PLOS ONE*, *12*(4), e0175844. https://doi.org/10.1371/journal.pone.0175844

Seshadri, C., Shenoy, M., Wells, R. D., Hensley-McBain, T., Andersen-Nissen, E., McElrath, M. J., Cheng, T.-Y., Moody, D. B., & Hawn, T. R. (2013). Human CD1a deficiency is common and genetically regulated. *Journal of Immunology (Baltimore, Md.: 1950)*, *191*(4), 1586–1593. https://doi.org/10.4049/jimmunol.1300575

Seshadri, C., Thuong, N. T. T., Yen, N. T. B., Bang, N. D., Chau, T. T. H., Thwaites, G. E., Dunstan, S. J., & Hawn, T. R. (2014). A polymorphism in human CD1A is associated with susceptibility to tuberculosis. *Genes & Immunity*, *15*(3), Article 3. https://doi.org/10.1038/gene.2014.5

Shen, L., Frencher, J., Huang, D., Wang, W., Yang, E., Chen, C. Y., Zhang, Z., Wang, R., Qaqish, A., Larsen, M. H., Shen, H., Porcelli, S. A., Jacobs, W. R., & Chen, Z. W. (2019). Immunization of Vγ2Vδ2 T cells programs sustained effector memory responses that control tuberculosis in nonhuman primates. *Proceedings of the National Academy of Sciences*, *116*(13), 6371–6378. https://doi.org/10.1073/pnas.1811380116

Shen, Y., Zhou, D., Qiu, L., Lai, X., Simon, M., Shen, L., Kou, Z., Wang, Q., Jiang, L., Estep, J., Hunt, R., Clagett, M., Sehgal, P. K., Li, Y., Zeng, X., Morita, C. T., Brenner, M. B., Letvin, N. L., & Chen, Z. W. (2002). Adaptive Immune Response of Vγ2Vδ2+ T Cells During Mycobacterial Infections. *Science (New York, N.Y.)*, *295*(5563), 2255–2258. https://doi.org/10.1126/science.1068819

Shey, M. S., Nemes, E., Whatney, W., De Kock, M., Africa, H., Barnard, C., Van Rooyen, M., Stone, L., Riou, C., Kollmann, T., Hawn, T. R., Scriba, T. J., & Hanekom, W. A. (2014). Maturation of Innate Responses to Mycobacteria over the First Nine Months of Life. *The Journal of Immunology*, *192*(10), 4833–4843. https://doi.org/10.4049/jimmunol.1400062

Siddiqui, S., Visvabharathy, L., & Wang, C.-R. (2015). Role of Group 1 CD1-Restricted T Cells in Infectious Disease. *Frontiers in Immunology*, *6*, 337. https://doi.org/10.3389/fimmu.2015.00337

Simonson, A. W., Zeppa, J. J., Bucsan, A. N., Chao, M. C., Pokkali, S., Hopkins, F., Chase, M. R., Vickers, A. J., Sutton, M. S., Winchell, C. G., Myers, A. J., Ameel, C. L., Kelly, R., Krouse, B., Hood, L. E., Li, J., Lehman, C. C., Kamath, M., Tomko, J., … Flynn, J. L. (2024). CD4 T cells and CD8α+ lymphocytes are necessary for intravenous BCG-induced protection against tuberculosis in macaques. *bioRxiv: The Preprint Server for Biology*, 2024.05.14.594183. https://doi.org/10.1101/2024.05.14.594183

Soares, A. P., Kwong Chung, C. K. C., Choice, T., Hughes, E. J., Jacobs, G., van Rensburg, E. J., Khomba, G., de Kock, M., Lerumo, L., Makhethe, L., Maneli, M. H., Pienaar, B., Smit, E., Tena-Coki, N. G., van Wyk, L., Boom, W. H., Kaplan, G., Scriba, T. J., & Hanekom, W. A. (2013). Longitudinal changes in CD4(+) T-cell memory responses induced by BCG vaccination of newborns. *The Journal of Infectious Diseases*, *207*(7), 1084–1094. https://doi.org/10.1093/infdis/jis941

Soares, A. P., Scriba, T. J., Joseph, S., Harbacheuski, R., Murray, R. A., Gelderbloem, S. J., Hawkridge, A., Hussey, G. D., Maecker, H., Kaplan, G., & Hanekom, W. A. (2008). Bacillus Calmette-Guérin Vaccination of Human Newborns Induces T Cells with Complex Cytokine and Phenotypic Profiles. *The Journal of Immunology*, *180*(5), 3569–3577. https://doi.org/10.4049/jimmunol.180.5.3569

Song, Z., Henze, L., Casar, C., Schwinge, D., Schramm, C., Fuss, J., Tan, L., & Prinz, I. (2023). Human γδ T cell identification from single-cell RNA sequencing datasets by modular TCR expression. *Journal of Leukocyte Biology*, *114*(6), 630–638. https://doi.org/10.1093/jleuko/qiad069

Stein, C. M., Zalwango, S., Malone, L. L., Won, S., Mayanja-Kizza, H., Mugerwa, R. D., Leontiev, D. V., Thompson, C. L., Cartier, K. C., Elston, R. C., Iyengar, S. K., Boom, W. H., & Whalen, C. C. (2008). Genome scan of M. tuberculosis infection and disease in Ugandans. *PloS One*, *3*(12), e4094. https://doi.org/10.1371/journal.pone.0004094

Stenger, S., Hanson, D. A., Teitelbaum, R., Dewan, P., Niazi, K. R., Froelich, C. J., Ganz, T., Thoma-Uszynski, S., Melián, A., Bogdan, C., Porcelli, S. A., Bloom, B. R., Krensky, A. M., & Modlin, R. L. (1998). An antimicrobial activity of cytolytic T cells mediated by granulysin. *Science (New York, N.Y.)*, *282*(5386), 121–125. https://doi.org/10.1126/science.282.5386.121

Stenger, S., Mazzaccaro, R. J., Uyemura, K., Cho, S., Barnes, P. F., Rosat, J. P., Sette, A., Brenner, M. B., Porcelli, S. A., Bloom, B. R., & Modlin, R. L. (1997). Differential effects of cytolytic T cell subsets on intracellular infection. *Science (New York, N.Y.)*, *276*(5319), 1684–1687. https://doi.org/10.1126/science.276.5319.1684

Sun, M., Phan, J. M., Kieswetter, N. S., Huang, H., Yu, K. K. Q., Smith, M. T., Liu, Y. E., Wang, C., Gupta, S., Obermoser, G., Maecker, H. T., Krishnan, A., Suresh, S., Gupta, N., Rieck, M., Acs, P., Ghanizada, M., Chiou, S.-H., Khatri, P., … Seshadri, C. (2024). Specific CD4+ T cell phenotypes associate with bacterial control in people who 'resist' infection with Mycobacterium tuberculosis. *Nature Immunology*, *25*(8), 1411–1421. https://doi.org/10.1038/s41590-024-01897-8

Tameris, M. D., Hatherill, M., Landry, B. S., Scriba, T. J., Snowden, M. A., Lockhart, S., Shea, J. E., McClain, J. B., Hussey, G. D., Hanekom, W. A., Mahomed, H., & McShane, H. (2013). Safety and efficacy of MVA85A, a new tuberculosis vaccine, in infants previously vaccinated with BCG: A randomised, placebo-controlled phase 2b trial. *The Lancet*, *381*(9871), 1021–1028. https://doi.org/10.1016/S0140-6736(13)60177-4

Thomson, A. W., & Webster, L. M. (1988). The influence of cyclosporin A on cell-mediated immunity. *Clinical and Experimental Immunology*, *71*(3), 369–376.

Uldrich, A. P., Le Nours, J., Pellicci, D. G., Gherardin, N. A., McPherson, K. G., Lim, R. T., Patel, O., Beddoe, T., Gras, S., Rossjohn, J., & Godfrey, D. I. (2013). CD1d-lipid antigen recognition by the γδ TCR. *Nature Immunology*, *14*(11), Article 11. https://doi.org/10.1038/ni.2713

Ussher, J. E., Klenerman, P., & Willberg, C. B. (2014). Mucosal-Associated Invariant T-Cells: New Players in Anti-Bacterial Immunity. *Frontiers in Immunology*, *5*, 450. https://doi.org/10.3389/fimmu.2014.00450

van Pinxteren, L. A. H., Cassidy, J. P., Smedegaard, B. H. C., Agger, E. M., & Andersen, P. (2000). Control of latent Mycobacterium tuberculosis infection is dependent on CD8 T cells. *European Journal of Immunology*, *30*(12), 3689–3698. https://doi.org/10.1002/1521-4141(200012)30:12<3689::AID-IMMU3689>3.0.CO;2-4

Van Rhijn, I., Ly, D., & Moody, D. B. (2013). CD1a, CD1b, and CD1c in immunity against mycobacteria. *Advances in Experimental Medicine and Biology*, *783*, 181–197. https://doi.org/10.1007/978-1-4614-6111-1_10

Van Rhijn, I., & Moody, D. B. (2015). Donor Unrestricted T cells: A shared human T cell response. *Journal of Immunology (Baltimore, Md. : 1950)*, *195*(5), 1927–1932. https://doi.org/10.4049/jimmunol.1500943

Vermijlen, D., Brouwer, M., Donner, C., Liesnard, C., Tackoen, M., Van Rysselberge, M., Twité, N., Goldman, M., Marchant, A., & Willems, F. (2010). Human cytomegalovirus elicits fetal γδ T cell responses in utero. *Journal of Experimental Medicine*, *207*(4), 807–821. https://doi.org/10.1084/jem.20090348

von Borstel, A., Chevour, P., Arsovski, D., Krol, J. M. M., Howson, L. J., Berry, A. A., Day, C. L., Ogongo, P., Ernst, J. D., Nomicos, E. Y. H., Boddey, J. A., Giles, E. M., Rossjohn, J., Traore, B., Lyke, K. E., Williamson, K. C., Crompton, P. D., & Davey, M. S. (2021). Repeated Plasmodium falciparum infection in humans drives the clonal expansion of an adaptive γδ T cell repertoire. *Science Translational Medicine*, *13*(622), eabe7430. https://doi.org/10.1126/scitranslmed.abe7430

Wegrecki, M., Ocampo, T. A., Gunasinghe, S. D., von Borstel, A., Tin, S. Y., Reijneveld, J. F., Cao, T.-P., Gully, B. S., Le Nours, J., Moody, D. B., Van Rhijn, I., & Rossjohn, J. (2022). Atypical sideways recognition of CD1a by autoreactive γδ T cell receptors. *Nature Communications*, *13*(1), Article 1. https://doi.org/10.1038/s41467-022-31443-9

Wencker, M., Turchinovich, G., Di Marco Barros, R., Deban, L., Jandke, A., Cope, A., & Hayday, A. C. (2014). Innate-like T cells straddle innate and adaptive immunity by revising antigen-receptor responsiveness. *Nature Immunology*, *15*(1), 80–87. https://doi.org/10.1038/ni.2773

Wickham, H. (2016). *ggplot2: Elegant Graphics for Data Analysis*. Springer-Verlag New York. https://ggplot2.tidyverse.org

Willcox, C. R., Davey, M. S., & Willcox, B. E. (2018). Development and Selection of the Human Vγ9Vδ2+ T-Cell Repertoire. *Frontiers in Immunology*, *9*. https://www.frontiersin.org/articles/10.3389/fimmu.2018.01501

Willcox, C. R., Pitard, V., Netzer, S., Couzi, L., Salim, M., Silberzahn, T., Moreau, J.-F., Hayday, A. C., Willcox, B. E., & Déchanet-Merville, J. (2012). Cytomegalovirus and tumor stress surveillance by binding of a human γδ T cell antigen receptor to endothelial protein C receptor. *Nature Immunology*, *13*(9), 872–879. https://doi.org/10.1038/ni.2394

Willcox, C. R., Vantourout, P., Salim, M., Zlatareva, I., Melandri, D., Zanardo, L., George, R., Kjaer, S., Jeeves, M., Mohammed, F., Hayday, A. C., & Willcox, B. E. (2019). Butyrophilin-like 3 Directly Binds a Human Vγ4+ T Cell Receptor Using a Modality Distinct from Clonally-Restricted Antigen. *Immunity*, *51*(5), 813-825.e4. https://doi.org/10.1016/j.immuni.2019.09.006

Wolf, A. J., Desvignes, L., Linas, B., Banaiee, N., Tamura, T., Takatsu, K., & Ernst, J. D. (2008). Initiation of the adaptive immune response to Mycobacterium tuberculosis depends on antigen production in the local lymph node, not the lungs. *The Journal of Experimental Medicine*, *205*(1), 105–115. https://doi.org/10.1084/jem.20071367

Young, D. B., Gideon, H. P., & Wilkinson, R. J. (2009). Eliminating latent tuberculosis. *Trends in Microbiology*, *17*(5), 183–188. https://doi.org/10.1016/j.tim.2009.02.005

Zufferey, C., Germano, S., Dutta, B., Ritz, N., & Curtis, N. (2013). The Contribution of Non-Conventional T Cells and NK Cells in the Mycobacterial-Specific IFNγ Response in Bacille Calmette-Guérin (BCG)-Immunized Infants. *PLoS ONE*, *8*(10). https://doi.org/10.1371/journal.pone.0077334

Appendix A. Single-cell RNA Sequencing.

Appendix A.I. Quality checks applied to single-cell RNA sequencing of infant γδ T cells.

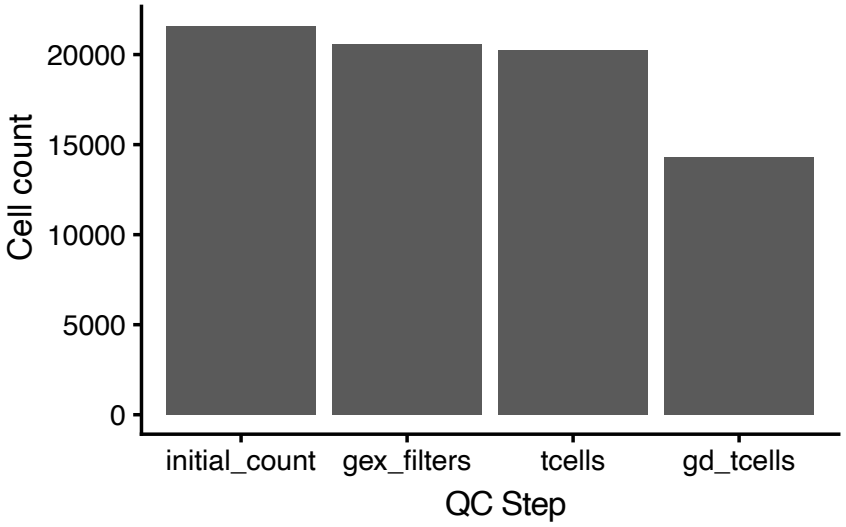

Quality checks applied to single-cell RNA sequencing of infant γδ T cells. Stacked bar plots depicting the cell counts at each of the quality checks applied to the single-cell RNA sequencing data. 'Initial_count' = initial cell barcode count before quality checks are applied; 'gex_filters' = cell barcodes with between 200 and 3500 unique genes expressed, between 500 and 15000 gene counts, and less than 10% mitochondrial DNA; 't_cells' = cell barcodes identified as T cells on the basis of CD3, CD14, and CD19 gene expression; 'gd_tcells' = cell barcodes identified as γδ T cells through the expression of at least one productive TCR-γ or TCR-δ chain.

Appendix A.II. Table of infant γδ TCR sequences.

All TCR sequences generated for this analysis are available under Zenodo under the citation below:

Maerz, M. (2025). BCG vaccination induces TCR-dependent effector functions among Vδ1/3 T cells that are associated with protection against tuberculosis [Data set]. Zenodo. https://doi.org/10.5281/zenodo.14583675

Appendix A.III. Quality checks applied to single-cell RNA sequencing of rhesus macaque γδ T cells.

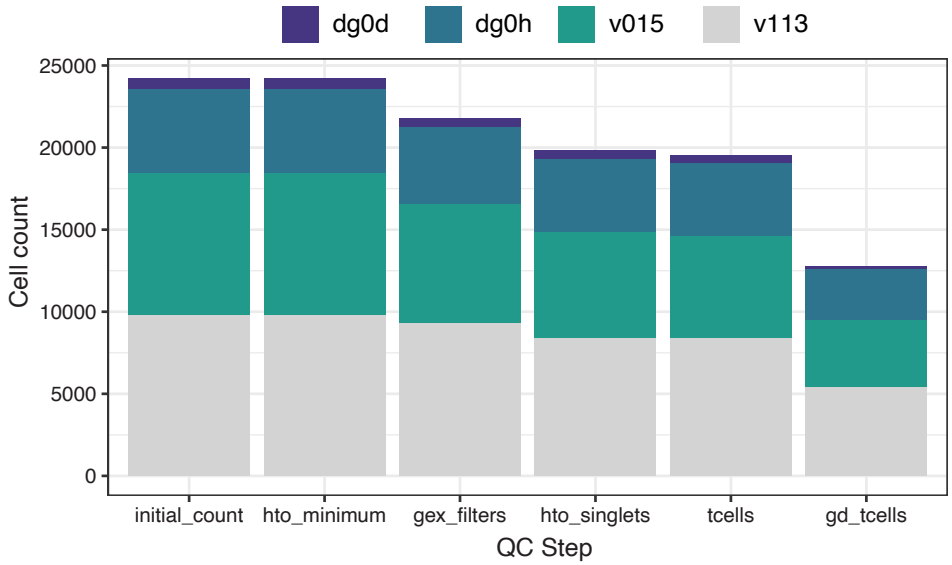

Quality checks applied to single-cell RNA sequencing of rhesus macaque γδ T cells. Stacked bar plots depicting the cell counts at each of the applied quality checks. Each sample donor is depicted in a different color. 'Initial_count' = initial cell barcode count before quality checks are applied; 'hto_minimum' = cell barcodes expressing hashtag oligos appearing in at least 50 cells and expressing at least 3 hashtag oligo counts; 'gex_filters' = cell barcodes with between 200 and 4000 unique genes expressed, between 500 and 15000 gene counts, and less than 10% mitochondrial DNA; 't_cells' = cell barcodes identified as T cells on the basis of CD3, CD14, and CD19 gene expression and CD14 or CD20 protein expression; 'gd_tcells' = cell barcodes identified as γδ T cells through the expression of at least one productive TCR-γ or TCR-δ chain.

Appendix A.IV. Table of rhesus macaque γδ TCR sequences.

All TCR sequences generated for this analysis are available under Zenodo under the citation below:

Maerz, M. (2025). BCG vaccination induces TCR-dependent effector functions among Vδ1/3 T cells that are associated with protection against tuberculosis [Data set]. Zenodo. https://doi.org/10.5281/zenodo.14583675

Appendix A.V. Panel of CITE-seq and cell sorting antibodies.

Antibody	Clone	Manufacturer	Catalog Number	DNA Barcode
Live/Dead Fixable Green	NA	ThermoFisher	L23101	NA
CD3 – BV421	SP34-2	BD Biosciences	562877	NA
TCR γδ – PE-Dazzle	B1	BioLegend	331225	NA
TCR Vγ9 – APC	B3	BioLegend	331309	NA
CD8b	SIDI8BEE	eBiosciences	14-5273-82	TCCTTTCCTGATAGG
CD86	IT2.2	BioLegend	305447	GTCTTTGTCAGTGCA
CD4	SK3	BioLegend	344651	GAGGTTAGTGATGGA
Mouse IgG1 Isotype Control	MOPC-21	BioLegend	400187	GCCGGACGACATTAA
Mouse IgG2a Isotype Control	MOPC-173	BioLegend	400293	CTCCTACCTAAACTG
Mouse IgG2b Isotype Control	MPC-11	BioLegend	400381	ATATGTATCACGCGA
CD20	2H7	BioLegend	302363	TTCTGGGTCCCTAGA
CD163	GHI/61	BioLegend	333637	GCTTCTCCTTCCTTA
CD25	BC96	BioLegend	302649	TTTGTCCTGTACGCC
CXCR3	G025H7	BioLegend	353747	GCGATGGTAGATTAT
CCR6	G034E3	BioLegend	353440	GATCCCTTTGTCACT
CD69	FN50	BioLegend	310951	GTCTCTTGGCTTAAA
CCR7	G043H7	BioLegend	353251	AGTTCAGTCAACCGA
CD161	HP-3G10	BioLegend	339945	GTACGCAGTCCTTCT
CD28	CD28.2	BioLegend	302963	TGAGAACGACCCTAA
CD127/IL-7R	A019D5	BioLegend	351356	GTGTGTTGTCCTATG
Hashtag 1	LNH-94 ; 2M2	BioLegend	394661	GTCAACTCTTTAGCG
Hashtag 2	LNH-94 ; 2M2	BioLegend	394603	TGATGGCCTATTGGG
Hashtag 6	LNH-94 ; 2M2	BioLegend	394671	GGTTGCCAGATGTCA
Hashtag 7	LNH-94 ; 2M2	BioLegend	394673	TGTCTTTCCTGCCAG
Hashtag 8	LNH-94 ; 2M2	BioLegend	394675	CTCCTCTGCAATTAC
PD-L1	29E.2A3	BioLegend	329751	GTTGTCCGACAATAC
CD11c	S-HCL-3	BioLegend	371521	TACGCCTATAACTTG
CD8a	RPA-T8	BioLegend	301071	GCTGCGCTTTCCATT
CD14	M5E2	BioLegend	301859	TCTCAGACCTCCGTA
CD16	3G8	BioLegend	302065	AAGTTCACTCTTTGC
CD95	DX2	BioLegend	305651	CCAGCTCATTAGAGC
HLA-DR	L243	BioLegend	307663	AATAGCGAGCAAGTA
CD11b	1CRF44	BioLegend	301359	GACAAGTGATCTGCA

Appendix A.VI. Custom primers for single-cell sequencing of γδ TCRs.

Primer Name	Sequence
10X_Outer-F	AAT GAT ACG GCG ACC ACC GAG ATC TAC ACT CTT TCC CTA CAC GAC GCT C
Illumina_P5_Inner-F	AAT GAT ACG GCG ACC ACC GAG ATC TAC AC
Human_TRDC_Outer-R	AGC TTG ACA GCA TTG TAC TTC C
Human_TRGC_Outer-R	TGT GTC GTT AGT CTT CAT GGT GTT CC
Human_TRDC_Inner-R	TCC TTC ACC AGA CAA GCG AC
Human_TRGC_Inner-R	GAT CCC AGA ATC GTG TTG CTC
Rhesus_TRDC_Outer-R	TGC ATA TTG ACC AAG CTT GAC AGC
Rhesus_TRGC_Outer-R	TCA TGT CTG ACG ATA CAT CTG TGC
rTRD_inner	GGG AGA GAC GAC AAT AGC AGG A
rTRG_inner	GTG ACT TTT CTG GCA CCG TT

Appendix B. Flow Cytometry.

Appendix B.I. Gating scheme for human samples.

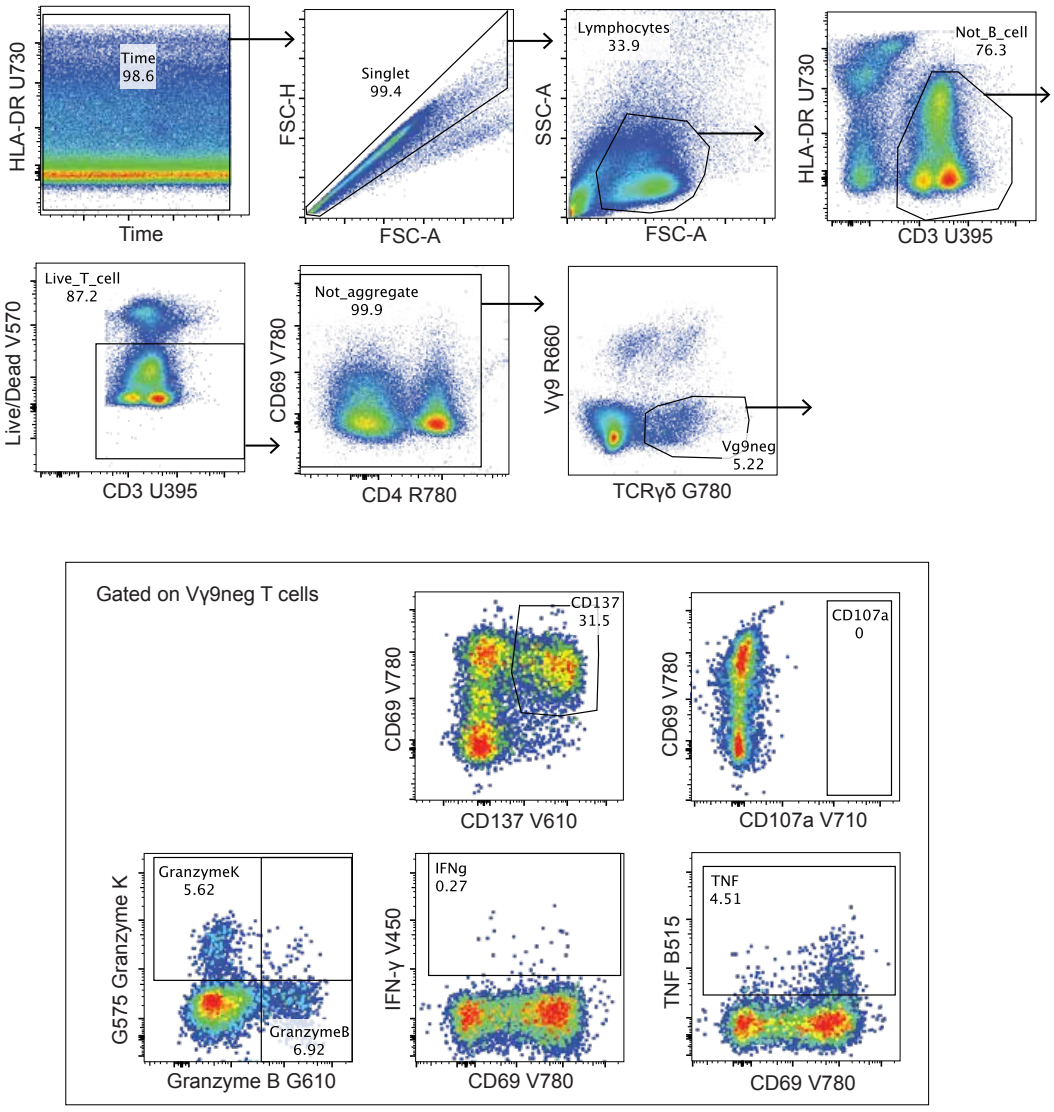

Gating scheme applied to human samples. Bivariate plots depicting the gating strategy for all human γδ T cells analyzed using flow cytometry.

Appendix B.II. Gating scheme for intracellular staining of IV-BCG-vaccinated rhesus macaques.

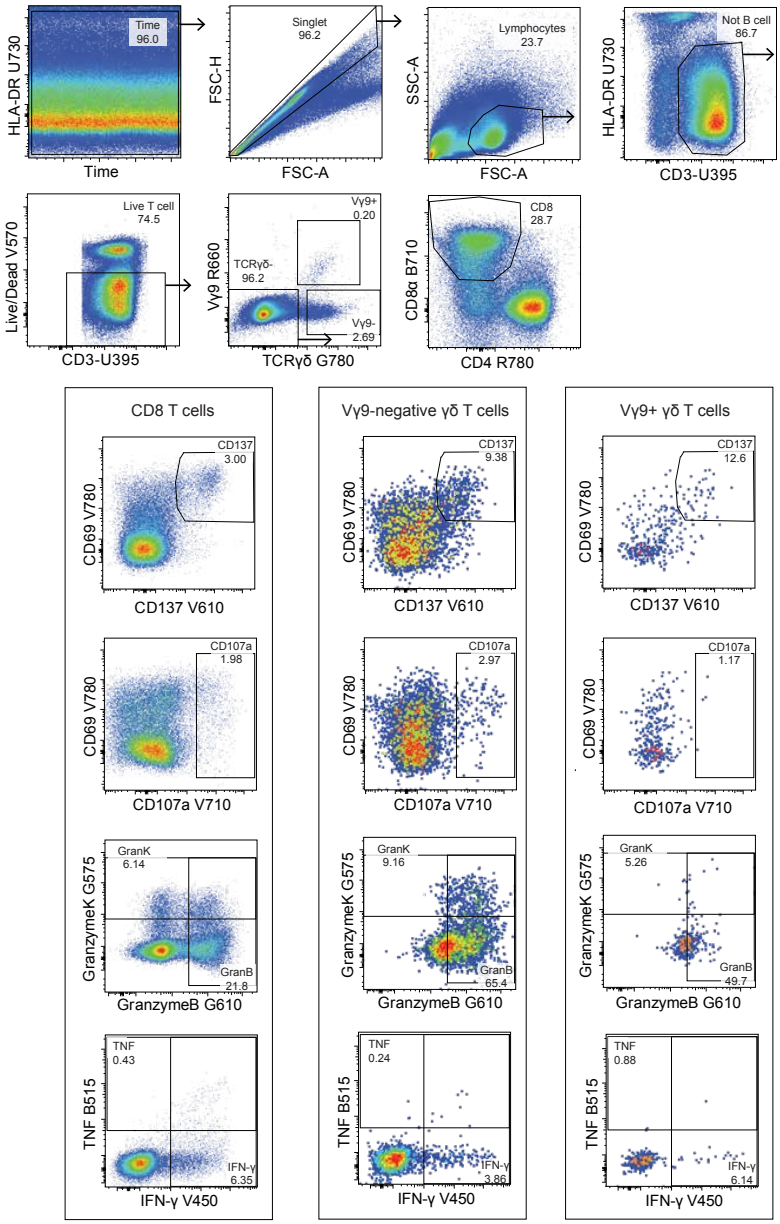

Gating scheme applied to rhesus macaque samples. Bivariate plots depicting the gating strategy used for all rhesus macaque samples analyzed using intracellular cytokine staining.

Appendix B.III. Frequency of Vγ9-negative γδ T cells in NHP samples analyzed using scRNA-seq.

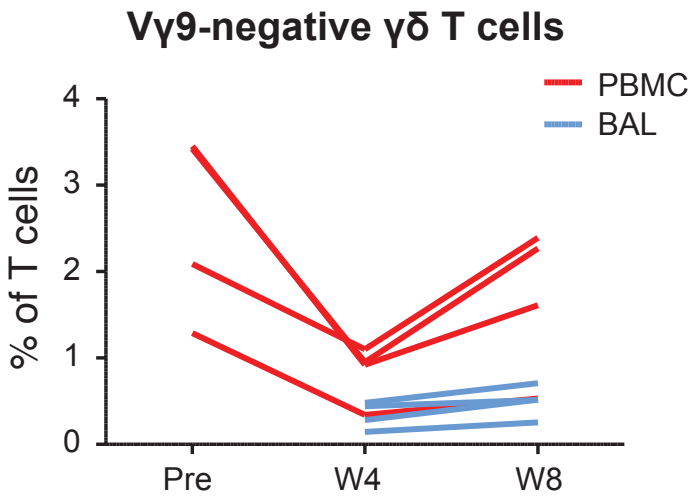

Frequency of Vγ9-negative γδ T cells in NHP samples analyzed using scRNA-seq. Frequency of Vγ9-negative γδ T cells in each of the samples analyzed using scRNA-seq. Frequencies were recorded while γδ T cells were sorted prior to single-cell processing.

Appendix B.IV. Flow cytometry panel applied to human and NHP samples.

Fluorochrome	Specificity	Antibody clone	Company	Catalog Number	Staining
FITC	TNF	Mab11	BD Biosciences	554512	Intracellular
BB700	CD8	RPA-T8	BD Biosciences	566452	Surface
PE	Granzyme K	GM26E7	BioLegend	370512	Intracellular
PE-CF594	Granzyme B	GB11	BD Biosciences	562462	Intracellular
PE-Cy7	TCRgd	B1	BioLegend	331222	Surface
APC	Vg9	B3	BioLegend	331310	Surface
APC-H7	CD4	L200	BD Biosciences	560837	Surface
V450	IFN-g	B27	BD Biosciences	560371	Intracellular
BV570	L/D		BioLegend	423103	
BV605	CD137	4B4-1	BioLegend	309822	Intracellular
BV711	CD107a	H4A3	BioLegend	328639	Surface
BV785	CD69	FN50	BioLegend	310932	Surface
BUV395	CD3	SP34-2	BD Biosciences	564117	Surface
BUV737	HLA-DR	LN3	ThermoFisher	367-9956-42	Surface

Appendix B.V. Comparison of T cell subsets in IV-BCG-vaccinated rhesus macaques.

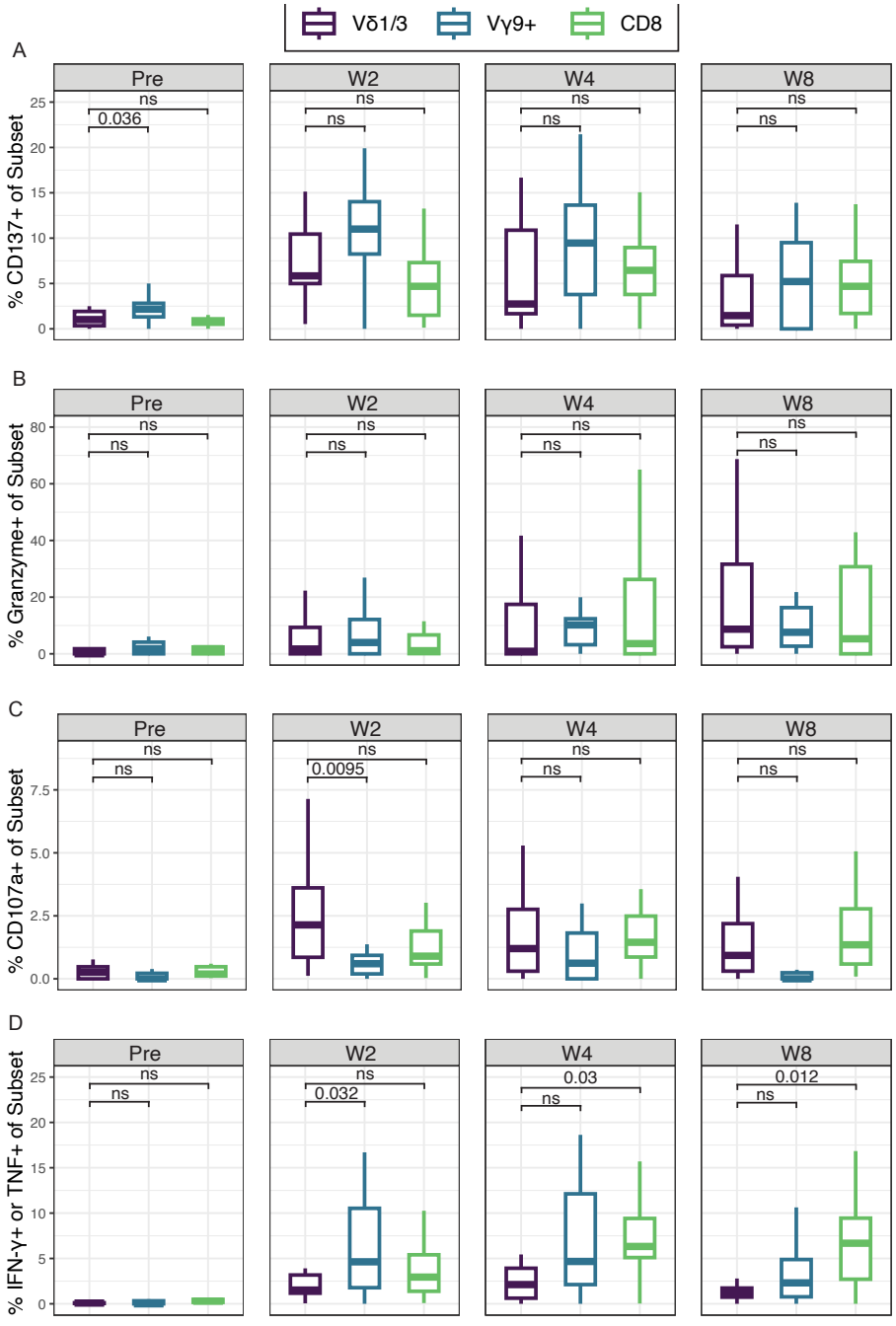

Comparison of functional responses among Vδ1/3 T cells, Vγ9+ T cells, and CD8 T cells. Background-subtracted frequency of T cell subsets expressing cell surface and intracellular proteins after stimulation with Mtb whole cell lysate. Frequencies are shown pre-vaccination (Pre) and at week 2 (W2), week 4 (W4), and week 8 (W8) post IV-BCG in PBMC. **(A)** Median

percentage of T cells expressing CD137 after stimulation with Mtb whole cell lysate in PBMC. The frequency among Vγ9+ γδ T cells or CD8 T cells is compared to the frequency among Vδ1/3 T cells at each time point. Paired Wilcoxon signed-rank test. **(B)** Median percentage of T cells expressing Granzyme (granzyme B or granzyme K) after stimulation with Mtb whole cell lysate in PBMC. The frequency among Vγ9+ γδ T cells or CD8 T cells is compared to the frequency among Vδ1/3 T cells at each time point. Paired Wilcoxon signed-rank test. **(C)** Median percentage of T cells expressing CD107a after stimulation with Mtb whole cell lysate in PBMC. The frequency among Vγ9+ γδ T cells or CD8 T cells is compared to the frequency among Vδ1/3 T cells at each time point. Paired Wilcoxon signed-rank test. **(D)** Median percentage of T cells expressing Cytokine (IFN-γ or TNF) after stimulation with Mtb whole cell lysate in PBMC. The frequency among Vγ9+ γδ T cells or CD8 T cells is compared to the frequency among Vδ1/3 T cells at each time point. Paired Wilcoxon signed-rank test.

Appendix B.VI. Gating scheme for correlations with protection in IV-BCG-vaccinated rhesus macaques.

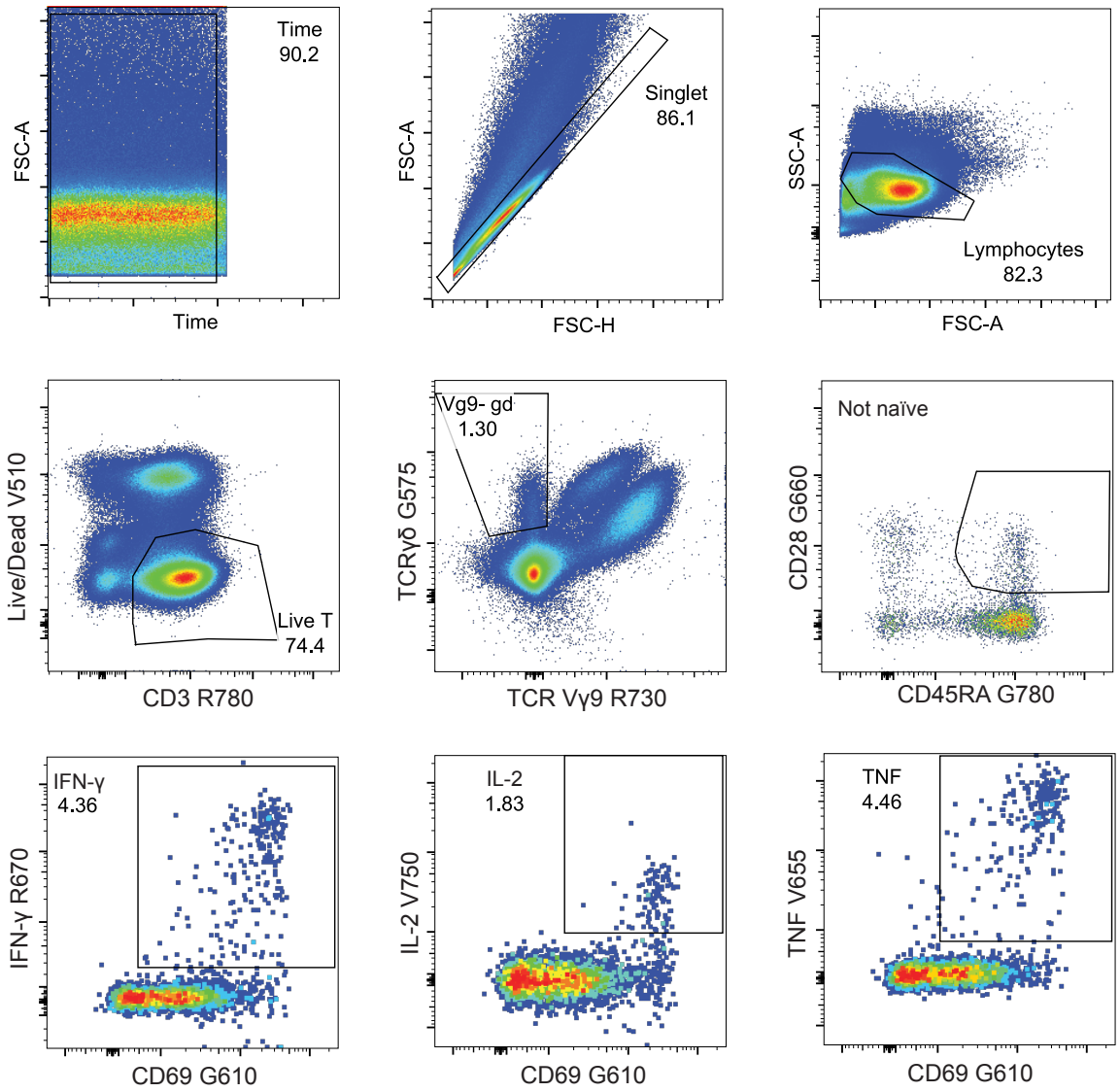

Gating strategy for correlations with protection. Bivariate plots depicting the gating strategy used for all rhesus macaque samples analyzed for immune correlates of protection.

Appendix B.VII. Frequency of γδ T cells in NHP samples analyzed using flow cytometry.

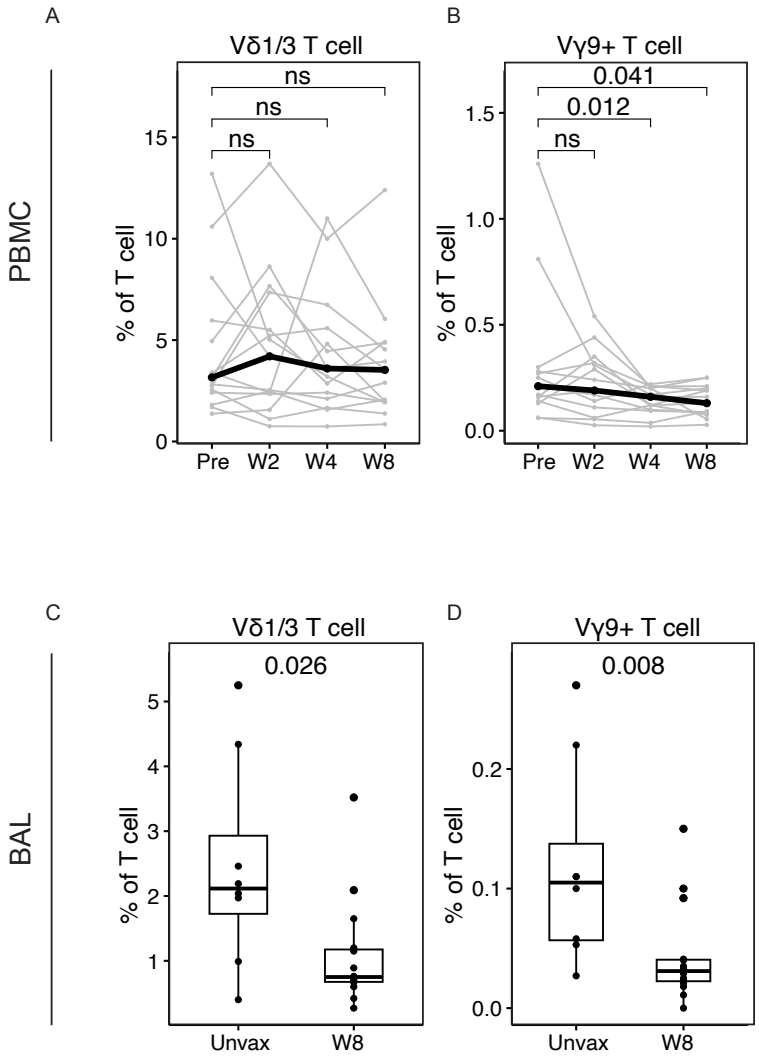

γδ T cell frequencies measured using flow cytometry. (A) The frequency of Vδ1/3 T cells is depicted in PBMC at each timepoint. Median frequencies are depicted in black. Paired Wilcoxon signed-rank test. (B) The frequency of Vγ9+ T cells is depicted in PBMC at each timepoint. Median frequencies are depicted in black. Paired Wilcoxon signed-rank test. (C) The frequency of Vδ1/3 T cells is depicted in BAL in vaccinated and unvaccinated animals. Median frequencies are depicted in black. Unpaired Wilcoxon signed-rank test. (D) The frequency of Vγ9+ T cells is depicted in BAL in vaccinated and unvaccinated animals. Median frequencies are depicted in black. Unpaired Wilcoxon signed-rank test.

Appendix B.VIII. Effect of cyclosporin A on viability and responses to cytokines.

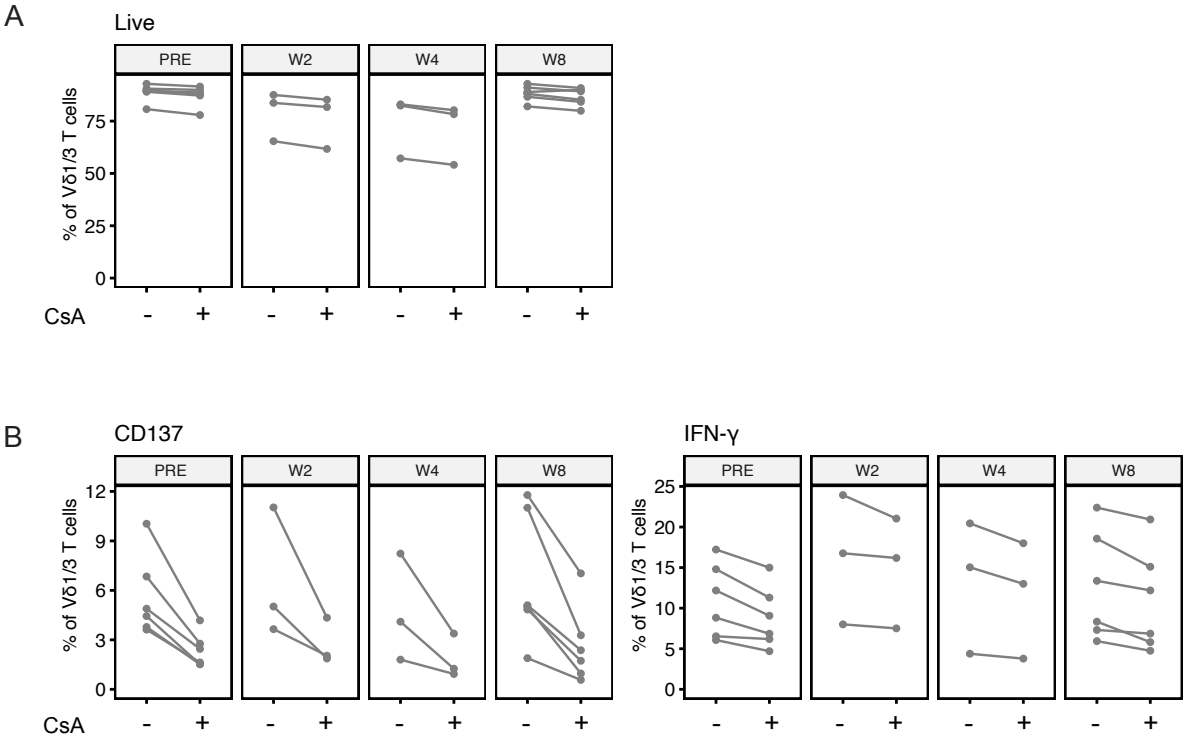

Effect of cyclosporin A on viability and response to cytokines in Vδ1/3 T cells. Frequencies are shown pre-vaccination (Pre) and at week 2 (W2), week 4 (W4), and week 8 (W8) post IV-BCG. Cells were either left untreated or were treated with the TCR inhibitor cyclosporin A (CsA) prior to stimulation. Each sample donor is shown in a separate line. **(A)** Frequency of live Vδ1/3 T cells. **(B)** Background-subtracted frequency of Vδ1/3 T cells expressing CD137 (left) or IFN-γ (right) in response to stimulation with IL-12, IL-15, and IL-18 cocktail.

Appendix C. Mass Cytometry.

Appendix C.I. Gating scheme for mass cytometry analysis.

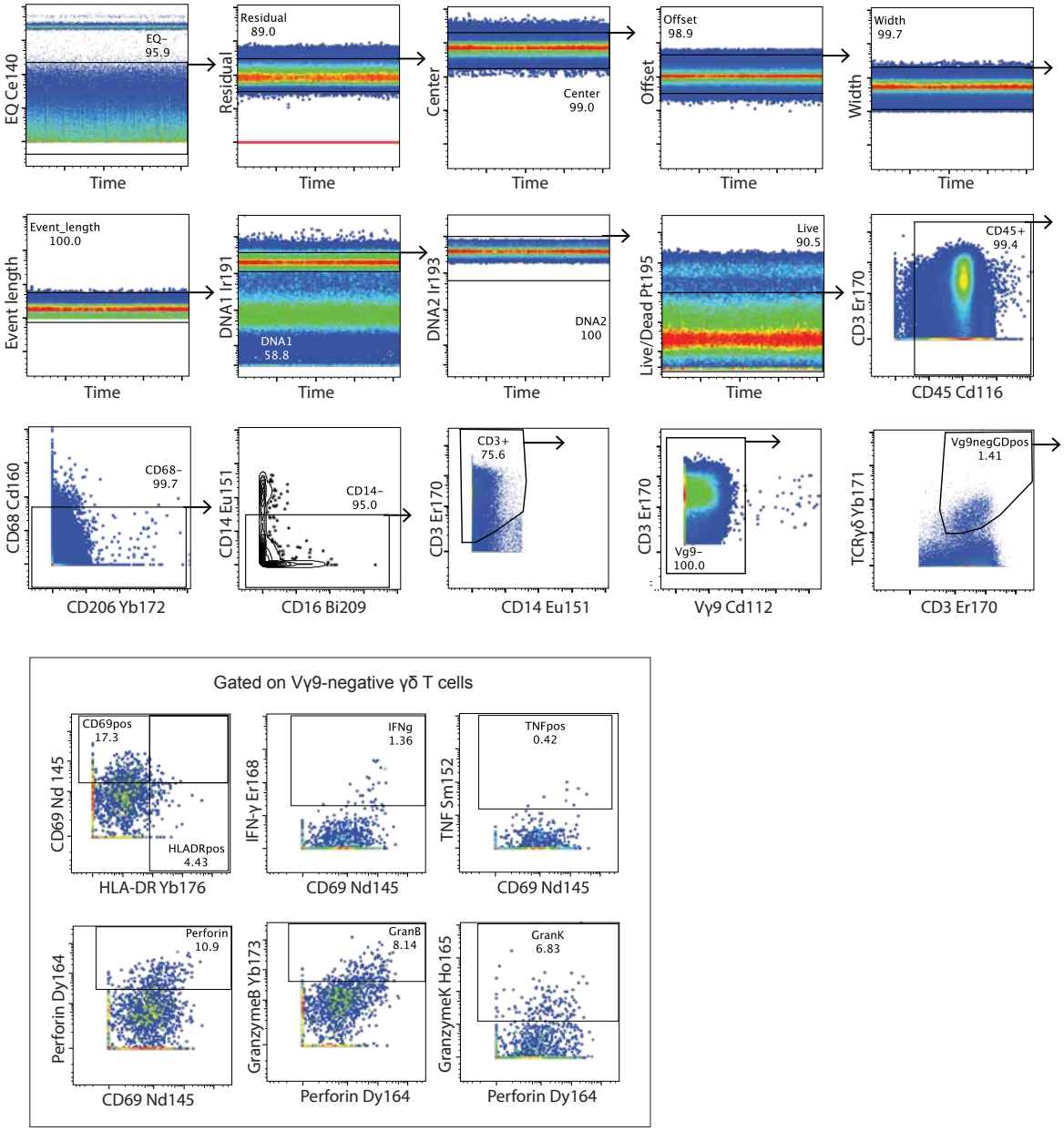

Supplementary Figure 3. CyTOF gating strategy. Bivariate plots depicting the gating strategy used for all samples analyzed using CyTOF.

Appendix C.II. Mass cytometry panel.

Mass and tag	Specificity	Antibody clone	Company	Catalog Number	Staining
116Cd	CD45	D058-1283	BD Biosciences	552566	Surface
106Cd	CD68	KP1	BioLegend	916104	Surface
172Yb	CD206	19,2	BD Biosciences	555953	Surface
154Sm	CD163	GHI/61	Fluidigm	3154007B	Surface
151Eu	CD14	M5E2	Fluidigm	3151009B	Surface
144Nd	CD11b (Mac-1)	ICRF44	Fluidigm	3144001B	Surface
209Bi	CD16	3G8	Fluidigm	3209002B	Surface
146Nd	CD11c	3,9	Fluidigm	3146014B	Surface
161Dy	CD123	6H6	BioLegend	306002	Surface
176Yb	HLA-DR	LN3	BioLegend	327002	Surface
169Tm	NKG2A	Z199	Fluidigm	3169013B	Surface
147Sm	CD20	2H7	Fluidigm	3147001B	Surface
153Eu	IgD	Polyclonal	Southern Biotech	2030-01	Surface
170Er	CD3	SP34-2	Fluidigm	3170007B	Intracellular
APC	MR1 5-OP-RU		NIH Tetramer Core		
163Dy	anti-APC		Fluidigm	3163001B	Surface
171Yb	TCRγδ	B1	BioLegend	331202	Surface
160Gd	CD161	HP-3G10	BioLegend	339902	Surface
111Cd	CD8α	RPA-T8	BioLegend	301053	Surface
113Cd	CD8β	2ST8.5H7	Novus Biologicals	NB100-65928	Surface
114Cd	CD4	L200	BD Biosciences	550625	Surface
174Yb	CD45RA	5H9	BD Biosciences	556625	Surface
175Lu	CD28	CD28.2	BioLegend	302902	Surface
159Tb	CCR7	G043H7	Fluidigm	3159003A	Surface
156Gd	CXCR3	G025H7	Fluidigm	3156004B	Surface
145Nd	CD69	FN50	BioLegend	310902	Surface
173Yb	Granzyme B	GB11	Fluidigm	3173006B	Intracellular
165Ho	Granzyme K	GM26E7	BioLegend	370502	Intracellular
164Dy	Perforin	Pf-80/164	Mabtech	3465-3-250	Intracellular
143Nd	CD107a	H4A3	BioLegend	328601	
162Dy	CD154	24-31	BioLegend	310802	Intracellular
152Sm	TNF	Mab11	Fluidigm	3152002B	Intracellular
168Er	IFN-g	B27	Fluidigm	3168005B	Intracellular
158Gd	IL-2	MQ1-17H12	Fluidigm	3158007B	Intracellular
148Nd	IL-17A	BL168	Fluidigm	3148008B	Intracellular
191Ir/193Ir	DNA (Cell ID)		Fluidigm	201192A	
196Pt	Cisplatin (Viability)		Fluidigm	201064	

Appendix D: Study Cohorts.

Appendix D.I. Human cohort.

RNAseq	ICS	Tissue	Sample ID	Sex	Ethnicity	HIV status	Household TB contact	Vax Route
X		PBMC	T14679	M	Coloured	Neg	Neg	intraderm
X	X	PBMC	T11434	M	Unknown	Neg	Neg	intraderm
X	X	PBMC	T13007	M	White	Neg	Neg	percut
X	X	PBMC	T13935	F	Black	Neg	Neg	percut
X	X	PBMC	T14668	F	Coloured	Neg	Neg	percut
X	X	PBMC	T14680	F	Coloured	Neg	Neg	percut
	X	PBMC	T13395	M	Black	Neg	Neg	intraderm
	X	PBMC	T13651	M	Coloured	Neg	Neg	percut
	X	PBMC	T14481	F	Coloured	Neg	Neg	percut
	X	PBMC	T14613	F	Black	Neg	Neg	percut
	X	PBMC	T14617	M	Coloured	Neg	Neg	percut
	X	PBMC	T14724	F	Coloured	Neg	Neg	percut
	X	PBMC	T14750	F	Coloured	Neg	Neg	percut
	X	PBMC	T14885	F	Coloured	Neg	Neg	intraderm
	X	PBMC	T14931	M	Coloured	Neg	Neg	percut
	X	PBMC	T15360	M	Coloured	Neg	Neg	intraderm
	X	PBMC	T15382	F	Coloured	Neg	Neg	intraderm
	X	PBMC	T15743	M	Coloured	Neg	Neg	intraderm
	X	PBMC	T15833	M	Coloured	Neg	Neg	percut
	X	PBMC	T16083	F	Coloured	Neg	Neg	percut
	X	PBMC	T16137	F	Black	Neg	Neg	intraderm
	X	PBMC	T16196	M	Coloured	Neg	Neg	percut
	X	PBMC	T16340	M	Coloured	Neg	Neg	intraderm
	X	PBMC	T16756	F	Black	Neg	Neg	intraderm
	X	PBMC	T17040	F	Coloured	Neg	Neg	intraderm
	X	PBMC	T17065	M	Coloured	Neg	Neg	percut
	X	CBMC	Ps18-1271C	F	White	Neg	Unknown	NA
	X	CBMC	Ps18-1275C	F	White	Neg	Unknown	NA
	X	CBMC	Ps18-1277C	M	Coloured	Neg	Unknown	NA
	X	CBMC	Ps18-1280C	F	Coloured	Neg	Unknown	NA
	X	CBMC	Ps18-1281C	M	White	Neg	Unknown	NA
	X	CBMC	Ps18-1282C	F	White	Neg	Unknown	NA

	X	CBMC	Ps18-1285C	M	Black	Neg	Unknown	NA
	X	CBMC	Ps18-1286C	F	Coloured	Neg	Unknown	NA
	X	CBMC	Ps18-1287C	M	Coloured	Neg	Unknown	NA
	X	CBMC	Ps18-1289C	F	White	Neg	Unknown	NA
	X	CBMC	Ps18-1290C	M	White	Neg	Unknown	NA
	X	CBMC	Ps18-1293C	M	Coloured	Neg	Unknown	NA
	X	CBMC	Ps18-1295C	M	Coloured	Neg	Unknown	NA
	X	CBMC	Ps18-1296C	M	White	Neg	Unknown	NA
	X	CBMC	Ps18-1299C	F	White	Neg	Unknown	NA
	X	CBMC	Ps18-1300C	M	White	Neg	Unknown	NA
	X	CBMC	Ps18-1301C	M	Coloured	Neg	Unknown	NA
	X	CBMC	Ps18-1302C	F	White	Neg	Unknown	NA
	X	CBMC	Ps18-1303C	F	White	Neg	Unknown	NA
	X	CBMC	Ps18-1304C	M	Coloured	Neg	Unknown	NA
	X	CBMC	Ps18-1306C	F	Coloured	Neg	Unknown	NA

Appendix D.II. Non-human primate cohort.

RNAseq	ICS	TCR Inhib.	Correlations	Animal ID	Age at Vax	Sex	BCG Dose (CFU)	Mtb at Necropsy (CFU)
X				DG0D			50000000	NA
X				DG0H			50000000	NA
X				A14V015			50000000	NA
X				A14V113			50000000	NA
	X			36327			50000000	NA
	X			DF4P			50000000	NA
	X			D12L			50000000	NA
	X			MC30			50000000	NA
	X			DF2C			50000000	NA
	X			A14V139			50000000	NA
	X			DIC4			50000000	NA
	X			17C231			50000000	NA
	X			MF46			50000000	NA
	X			HRP			50000000	NA
	X			DGKM			50000000	NA
	X			O8M			50000000	NA
	X			P599			50000000	NA
	X			18C062			50000000	NA
	X			36852			50000000	NA
	X			DF1R			50000000	NA
	X			DGPR			50000000	NA
	X			O4A			50000000	NA
	X			DHZI			50000000	NA
	X			16C192			50000000	NA
	X			DGHL			50000000	NA
	X			DGFM			50000000	NA
	X			OCC			50000000	NA
	X			DIAV			50000000	NA
	X			DI4R			50000000	NA
		X		36818			50000000	NA
		X		MI12			50000000	NA
		X		MB92			50000000	NA
		X	X	2618	5.3	F	6960000	182028
		X	X	2718	5.6	F	6960000	2970
		X	X	2818	4.4	M	24900000	40
			X	2918	3.9	M	461000	0
			X	3018	4.3	F	202000	651031
			X	3118	5.5	F	202000	0

			X	3218	4.4	F	2470000	0
			X	3318	4.3	F	461000	0
			X	3418	5.6	F	38800	0
			X	3518	4.6	M	6960000	0
			X	3618	4.6	F	2470000	0
			X	3718	2.9	M	38800	44635
			X	3818	2.9	M	2470000	329996
			X	3918	2.9	M	24900000	0
			X	4018	5.5	F	38800	96612
			X	4118	5.6	F	24900000	0
			X	4218	4.4	M	2470000	0
			X	4318	5.6	F	461000	0
			X	4418	5.6	F	2470000	8545
			X	4518	3.9	M	6960000	0
			X	4618	6.4	F	24900000	0
			X	4718	8.3	F	6960000	0
			X	4818	4.9	F	6960000	0
			X	4918	5.6	F	2470000	0
			X	5018	3.5	M	202000	0
			X	17819	5.1	M	423000	169720
			X	17919	5.1	M	137000	20030
			X	18019	4.1	M	137000	40082
			X	18119	4.1	M	311000	9118
			X	18219	4.1	M	311000	1625
			X	18419	3.8	M	311000	5205545
			X	18519	3.9	M	311000	243454
			X	18619	4.1	F	311000	669933
			X	18719	4.1	F	137000	2775